. .



g70219

ABSTRACT

APPLICATIONS OF CYCLIC VOLTAMMETRY TO THE STUDY OF TRANSIENT INTERMEDIATES

by Paul Joseph Kudirka

Reduction of a group of sulfonephthalein acid-base indicators in aqueous solutions has been used to evaluate the theory of cyclic volt-ammetry for disproportionation reactions initiated electrolytically. Predictions of the theory are in excellent agreement with experimental results, and rate constants were measured by cyclic voltammetry for nine sulfonephthalein radicals. Moreover, the rate constant measured for disproportionation of phenol red radical [k = $(3.4 \pm 0.3) \times 10^2$ \underline{M}^{-1} - \sec^{-1}] agrees exactly with conventional spectrophotometric measurements.

The effect of maximum suppressors on measured rate constants by cyclic voltammetry was investigated using several sulfonephthalein compounds. Gelatin was found to have no effect on measured disproportionation rate constants. Thus, at least for these systems, use of gelatin is an expedient and acceptable approach. Qualitatively, the effects of gelatin and Triton X-100 were found to be the same. However, apparent rate constants measured with cyclic voltammetry in the presence of Triton X-100 depended upon the concentration of this suppressor as well as on scan rate and sulfonephthalein concentration. Thus, Triton X-100 is unacceptable for quantitative measurements.

APPLICATIONS OF CYCLIC VOLTAMMETRY TO THE STUDY OF TRANSIENT INTERMEDIATES

Ву

Paul Joseph Kudirka

A THESIS

Submitted to
Michigan State University
in partial fulfillment of the requirements
for the degree of

DOCTOR OF PHILOSOPHY

Department of Chemistry

1971

Mohar

ills s

for he

ACKNOWLEDGMENT

The author wishes to express his appreciation to Professor Richard S. Nicholson for his guidance and encouragement throughout this study.

Thanks are also given to Janet M. Kudirka, the author's wife, for her encouragement and understanding.

I. III. A. B. HAROGER HO AR COMMENT ARE COMMENT AND ARE THE TARREST AND ARE THE TARREST AND ARE COMMENTED AND AREA COMMENTED AND AR

TABLE OF CONTENTS

		Page
I.	INTRODUCTION	1
	A. Some Aspects of Voltammetry	3 5 8
	Species of Transient Existence	19
II.	EXPERIMENTAL	29
	A. Electrochemical Apparatus	29 38 39 46 48 50
III.	ELECTROCHEMICAL REDUCTION OF CARBON TETRACHLORIDE IN NON-AQUEOUS SOLUTIONS	53
	A. Some Aspects of Dihalocarbene Chemistry	54
	Carbon Tetrachloride in Nonaqueous Solutions C. Electrochemical Reduction of Halomethanes in Non-	61
	aqueous Solutions	64
IV.	ELECTROCHEMICAL REDUCTION OF HALOBENZENE COMPOUNDS IN N,N-DIMETHYLFORMAMIDE	72
	A. Results	74 80
٧.	REDUCTION OF SULFONEPHTHALEIN ACID-BASE INDICATORS	85
	A. Compounds Investigated	85 87 92 93 99 100 103 106 109 118
	L. Considerations of Kinetic Effects	163

Tab Y--7---工. II. E. Ŋ, m. M. Titt. KI. Ŋ.

--

... '-

ΞX

Ï

Y

LIST OF TABLES

Table		Page
I.	Polarographic Data of Wawzonek and Duty (56)	22
II.	Polarographic Data of Wawzonek and Wagenknecht (58)	25
III.	Half-Wave Potentials and Diffusion Current Constants for Halobenzene Compounds	73
IV.	Potentials at which Limiting Current vs. $\underline{h}^{1/2}$ Studies were Conducted for Halobenzene Compounds	75
٧.	Half-Wave Potentials and Disproportionation Rate Constant for Sulfonephthalein Indicator Radicals	s 86
VI.	Disproportionation Rate Constants for Cresol Purple Radical by Polarographic Monitoring of Decay of Oxidation Wave of the Radical	105
VII.	Disproportionation Rate Constants for Phenol Red Radicals in Acetate Buffered Aqueous Solutions from Conventional Second Order Plots	
vIII.	Cyclic Voltammetric Data on Cresol Purple	120
IX.	Cyclic Voltammetric Data on Cresol Purple	121
х.	Cyclic Voltammetric Data on Thymol Blue	122
XI.	Cyclic Voltammetric Data on Thymol Blue	123
XII.	Cyclic Voltammetric Data on Bromothymol Blue	124
XIII.	Cyclic Voltammetric Data on Bromocresol Green	125
xIV.	Cyclic Voltammetric Data on Phenol Red	126
xv.	Cyclic Voltammetric Data on Phenol Red	127
xVI.	Cyclic Voltammetric Data on Phenol Red	128
XVII.	Cyclic Voltammetric Data on Phenol Red	129
XVIII.	Cyclic Voltammetric Data on Phenol Red	130
XIX.	Cyclic Voltammetric Data on Phenol Red	131
xx.	Cyclic Voltammetric Data on Phenol Red	132

Ist M

XII

MI

DI.

Mil

T.T.

H

MI.

MO

MI

DD.;

MII.

LIST OF TABLES

(continued)

Table	Pa	age
XXI.	Cyclic Voltammetric Data on Phenol Red]	L33
XXII.	Cyclic Voltammetric Data on Phenol Red]	L34
xxIII.	Cyclic Voltammetric Data on Phenol Red]	L35
xxIv.	Cyclic Voltammetric Data on Phenol Red]	L36
xxv.	Cyclic Voltammetric Data on Phenol Red	L37
XXVI.	Cyclic Voltammetric Data on Phenol Red	138
XXVII.	Cyclic Voltammetric Data on Phenol Red	L39
XXVIII.	Cyclic Voltammetric Data on Cresol Red	140
xxIv.	Cyclic Voltammetric Data on Cresol Red	141
xxx.	Cyclic Voltammetric Data on Cresol Red	L42
XXXI.	Cyclic Voltammetric Data on Cresol Red	L43
XXXII.	Cyclic Voltammetric Data on Cresol Red	լ 44
XXXIII.	Cyclic Voltammetric Data on Bromophenol Red]	L45
xxxiv.	Cyclic Voltammetric Data on Bromophenol Red]	L46
xxxv.	Cyclic Voltammetric Data on Bromophenol Red]	L47
XXXVI.	Cyclic Voltammetric Data on Chlorophenol Red	L48
XXXVII.	Cyclic Voltammetric Data on Bromocresol Purple]	L49
XXXVIII.	Effect of Gelatin on Disproportionation Rate Constants by Cyclic Voltammetry for Radicals of Cresol Red and Phenol Red in Aqueous Solutions	L60

FIRE

la.

lb.

3.

2.

5.

€.

ê. ,

9.

10. ;

12. :

13. 1 s a

11. C. 25. 25. 25. 25.

LIST OF FIGURES

FIGURE		Page
la.	Variation of electrode potential with time for cyclic voltammetry	6
lb.	Cyclic current function for reversible charge transfer	6
2.	Current-potential curves for various values of $\underline{k}/\underline{a}$ for first order chemical reaction following reversible charge transfer	10
3.	Ratio of the anodic to cathodic peak current as a function of $\underline{k}\underline{\tau}$ for first order chemical reaction following reversible charge transfer	13
4.	Cyclic current-potential curves showing effect of charge transfer parameter, Ψ	16
5.	Block diagram of circuit configuration	30
6.	Block diagram of circuit used for coulometry	34
7.	Cell arrangement	36
8.	Electrochemical vacuum line apparatus	40
9.	Vacuum line electrochemical cell	42
10.	Polarogram of 1.5 \underline{mM} CCl $_{l_1}$ in acetonitrile with 0.10 \underline{M} tetrabutylammonium perchlorate as supporting electrolyte.	66
11.	$\underline{\underline{E}}_{1/2}$ vs pH behavior of Cresol purple	88
12.	Polarographic waves for the controlled potential electrolysis of a sulfonephthalein indicator that is reduced to a moderately stable radical which subsequently disproportionates	94
13.	Limiting current vs time behavior of the polarographic waves following controlled potential electrolysis of a sulfonephthalein indicator that is reduced to a moderately stable radical which subsequently disproportionates	97
14.	Comparison of theory (points) and experiment (curve) for disproportionation reaction mechanism for cyclic voltammetry	101
15.	Esr spectrum of cresol purple following controlled potential electrolysis on first reduction wave	107

HHE ÷. 22

16

20

LIST OF FIGURES

(continued)

F	IGURE		Page
	16.	A typical experimental curve for reduction of phenol red with $V({\rm II})$, and the following generation of phenol red by disproportionation of the radical	112
	17.	A typical second order plot of phenol red radical vs time	115
	18.	Cyclic voltammogram on unpurified sample of phenol red in the absence of gelatin	151
	19.	Cyclic voltammogram on purified sample of phenol red in the absence of gelatin	153
	20.	Conventional polarogram on unpurified sample of phenol red in the absence of gelatin	155
	21.	Conventional polarogram on purified sample of phenol red in the absence of gelatin	157
	22.	Variation of apparent rate constant with scan rate and phenol red concentration in the presence of 0.014 % Triton X-100	161

theory Eeyrov record Progre refere availa ematic aivano electr: in of intra Taking ಾಗಿತೆಬಾರ instru achieva ë:e3:1 Mise 1 terinite. species Sterios. tteresor 2020202 Vier va its fee.

C:

I. INTRODUCTION

Truly spectacular advances have been made in electrochemical theory and methodology since the discovery of polarography by Heyrovsky in 1922 (1,2), and the first report of an automatically recording polarograph by Heyrovsky and Shikata in 1925 (3). Progress has been especially rapid over the last decade (4-12 and references contained therein) for several reasons. First, the availability of high speed computers has permitted successful mathematical modeling of very complex electrode processes. Second, advances in electronics have permitted corresponding advances in electrochemical instrumentation. For example, commercial availability of operational amplifiers has made it possible to construct instrumentation embodying features such as positive feedback, thereby making precise electrochemical measurements practicable in low conductivity media, including even ethers. Moreover, with modern instrumentation, measurements can be made on a time scale not achievable even a decade ago. Thus, it is now possible to observe directly with electrochemical methods extremely reactive species whose lifetimes are of the order of milliseconds, or less.

Of course, during this same period other extremely powerful techniques and tools have been developed for studying chemical species of very short lifetimes. Nevertheless, modern electrochemical methods possess some unique features in this context, and therefore complement other more standard methods. For example, controlled potential electrolysis permits the generation of a far wider variety of intermediates than any other single technique. This feature, coupled with the extremely rapid response of recently

ievelog versat: to the re fer excitiz receive sitei t to iate electro ievelop ite to Cess?i electro tiis ze wat of Wolle . iesorib; trig instar Milier IL Some Tilta<u>tte</u> ## E t Specia

A.

Ĵ;

developed methods, gives modern electrochemistry its power and versatility. To date, actual applications of modern electrochemistry to the generation and observance of highly reactive intermediates are few, but it is readily apparent that such methods provide an exciting tool for studying reactive entities.

Although a number of related electrochemical techniques have received extensive attention and development (4-12 and references cited therein), cyclic voltammetry is the most versatile developed to date, and has reached a popularity unequaled by any of the other electrochemical techniques. This predominance is due to concomitant developments in instrumentation, making the method simple to use due to the ease of interpreting the experimental data, and to successful mathematical modeling of the method for many important electrolysis mechanisms (13-52). Because of the predominance of this method, and because this laboratory has been responsible for most of the theory that has popularized it (24,25,27,42-44,48-52), cyclic voltammetry was embraced as the primary tool for measurements described in this thesis.

Cyclic voltammetric data will be presented ubiquitously throughout this thesis, and therefore it may be useful to provide some discussion of the technique for the uninitiated reader. Hence, the remainder of this introduction is divided into the following areas:

(A) Some General Aspects of Voltammetry; (B) Description of Cyclic Voltammetry; (C) Applications of Cyclic Voltammetry to Chemical Kinetics; and (D) Applications of Cyclic Voltammetry to the Investigation of Species of Transient Existence.

such d

se s

7

arretr intric

(1) to

ei as (

(2) el

(3) in

e_

acr

(5) in:

to (6) ohe

בתיל (ווי שתל (ווי

ejeciroje e

Profiterall

A Some Aspects of Voltammetry

The current in an electrochemical cell is a function of the voltage applied to the cell. Voltammetry encompasses methods by which such currents are studied when the current-voltage characteristics depend on the rate of the overall electrolysis mechanism.

In general, a variety of processes must be considered when voltammetric techniques are employed, since electrolysis mechanisms are intricate and comprise many steps. Electrode processes may be regarded as occurring formally in the following sequence (53):

- (1) transport of the depolarizer (reactant) to the vicinity of the electrode;
- (2) chemical changes in this depolarizer leading to an electroactive form;
- (3) influence of the electric field leading to further changes in the electroactive form;
- (4) actual electron transfer between the electrode and this electroactive form leading to an activated product;
- (5) influence of the electric field on this activated product leading to an intermediate product;
- (6) chemical changes in this intermediate product leading to a final product; and
- (7) transport of this final product into the bulk of the solution. Steps 1 and 7 involve mass transport, Steps 2 and 6 are homogenous chemical reactions, and Steps 3, 4, and 5 formally constitute the electrode reaction.

Three modes of mass transport must be considered, (54), namely, migration, convection, and diffusion. Migration is defined as the

rent i en be or gre smpor are co or by centra: Froduct qui es de iinere Terrs e of supp iis tr 13 (E. L.) fision Present

mtion

C

D:

Ţr

Terry is Pizzhez

ويُروسين وهي Neen vo

Carrett

iechniqu

Bot

motion of charged particles in an electric field. Since electric current in a solution is carried by all ions in the solution, migration can be minimized by employing an excess (usually in a ratio of 100/1, or greater) of an electrochemically inert electrolyte, termed the supporting electrolyte. Tetraalkylammonium and alkali metal salts are commonly employed for this purpose.

Convection arises from stirring by mechanical or ultrasonic means, or by density differences which in turn are primarily caused by concentration and temperature gradients. Mass transport of reactants and products by convection is minimized by conducting measurements in quiescent solutions.

Diffusion results from concentration gradients, or more rigorously, differences in chemical potential. Hence, if electrochemical measurements are conducted in quiescent solutions containing a large excess of supporting electrolyte, diffusion is essentially the sole means of mass transport of reactants and products. These latter conditions are usually selected, because of the three mass transport processes, diffusion is easiest to describe mathematically.

Traditionally, electrochemical terminology is in disarray, and presently no single terminology is standard. Nevertheless, voltammetry is generally regarded as the generic term for such techniques. Furthermore, either the voltage or current applied to the electrochemical cell is controlled. Hence, a clear distinction exsists between voltammetry at controlled potential and voltammetry at controlled current (54).

Both polarography and cyclic voltammetry are controlled potential techniques, but they differ in several major respects. First, cyclic

volta cours volta

tial,

soan y

even r

triang formei

a two-

errang

such as

tottaki japome

Ę

Fi Vith ti

ite exp

Which is

Petrotio Potentie

so stat

is the I

is beld (

Rivertial

voltammetry employs a stationary electrode, whereas polarography, of course, employs a dropping mercury electrode (DME). Second, cyclic voltammetric experiments are conducted with a linearly changing potential, whereas polarography is a constant potential technique.

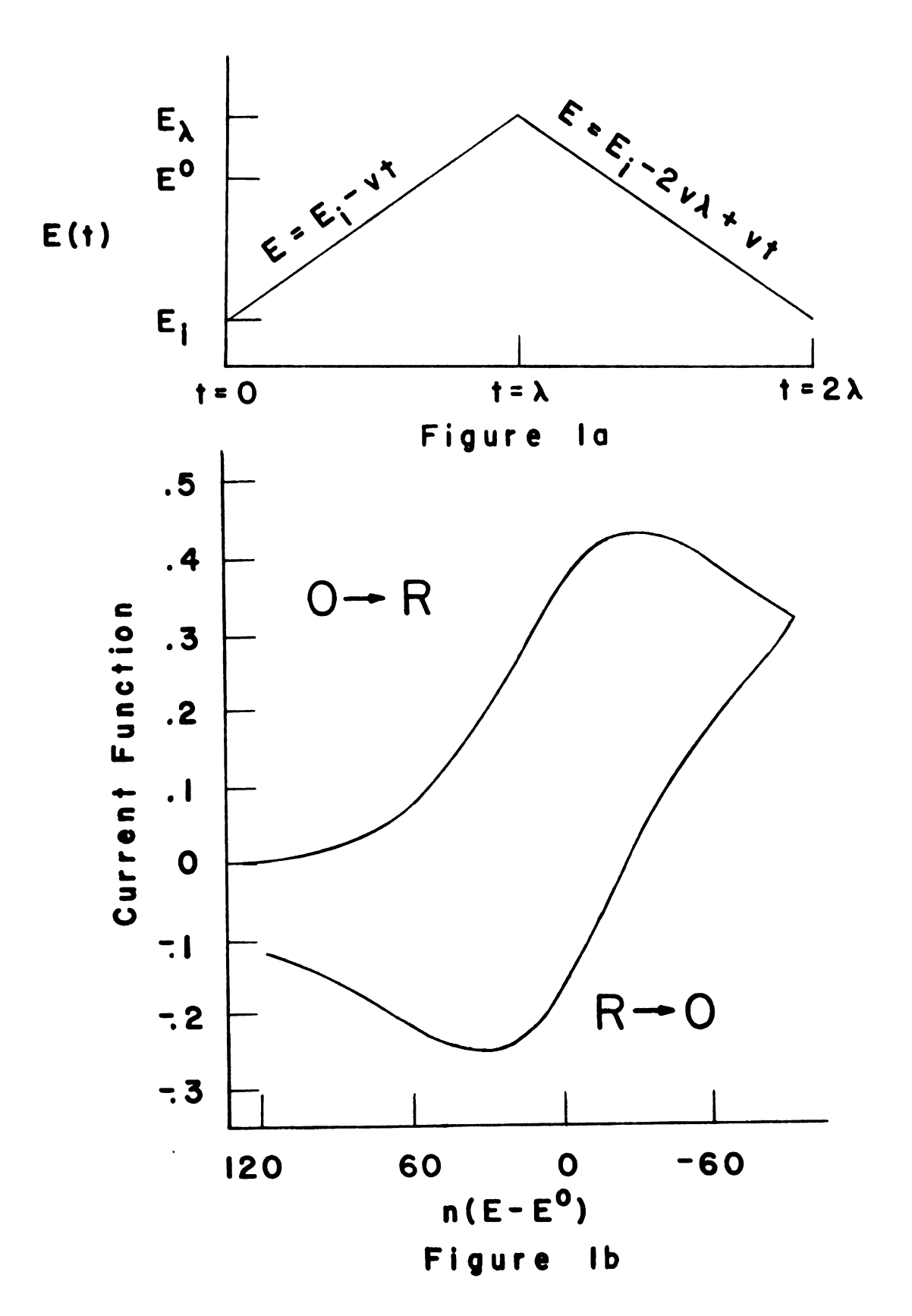
Although cyclic voltammetry is similar to polarography, it is even more akin to another technique, commonly termed linear potential scan voltammetry (LPSV). The primary difference between cyclic voltammetry and LPSV is that with cyclic voltammetric experiments, a triangular-wave potential is used, whereas LPSV experiments are performed with a ramp potential function. Hence, cyclic voltammetry is a two-step technique, whereas LPSV is a one-step method. The greatly enhanced versatility and power of cyclic voltammetry over techniques such as LPSV is due primarily to this two-step feature (55). This important aspect of cyclic voltammetry will become apparent in the following discussion.

B <u>Description</u> of <u>Cyclic</u> <u>Voltammetry</u>

Figure la illustrates the variation of electrode potential, $\underline{E}(\underline{t})$, with time for a cyclic voltammetric experiment. At the beginning of the experiment (\underline{t} = 0) the electrode is at an initial potential, \underline{E}_{i} , which is anodic of the formal potential, \underline{E}^{0} , for the given oxidation-reduction couple. During the time interval $0 < \underline{t} < \underline{\lambda}$ the electrode potential is made to vary linearly with time in a negative direction so that it passes the formal potential. At time $\underline{t} = \underline{\lambda}$ the direction of the linear scan is reversed (the rate of change of potential, \underline{v} , is held constant), and the potential is returned to the initial value. Figure la also includes mathematical relationships for the electrode potential in terms of the scan rate and the electrolysis time.

Figure la. Variation of electrode potential with time for cyclic voltammetry.

Figure 1b. Cyclic current function for reversible charge transfer.



for elec

is progr

the reve

<u>0</u> + <u>t.e</u> +

at the e

the meye

The own.

377.A6 6X

oathoate

C .

as the co

solution

Citer re

the char.

geste s

00±1 **: ±130:

Figure 1b is a plot of the electrolysis current function (the current function is directly proportional to current density) for a reducible depolarizer (reactant), 0, which undergoes reversible electron (charge) transfer. During the initial linear scan the electrolysis current varies from zero to a maximum, and then decreases. This decrease in current occurs because the amount of depolarizer available for electrolysis decreases, since as electrolysis proceeds depolarizer is progressively removed from solution in the immediate vicinity of the electrode. On the initial linear scan and the beginning part of the reverse scan, the current arises from the reduction process, $0 + ne \rightarrow R$, and the reduced substance, R, is continuously generated at the electrode. At some potential sufficiently positive of $\underline{\mathtt{E}}_{\lambda}$ on the reverse scan some of the accumulated R is oxidized back to O. The current for the $R \rightarrow 0 + ne$ portion of the current-potential curve exhibits a minimum for reasons analogous to the origin of the cathodic maximum.

C Applications of Cyclic Voltammetry to Chemical Kinetics

In reality, electrolysis mechanisms are generally not as simple as the one discussed in connection with Figure 1. There the depolarizer was assumed to be identical with species \underline{O} in the bulk of the solution. Furthermore, the reduced species, \underline{R} , did not undergo any other reactions following charge transfer. In addition, the rate of the charge transfer step was limited only by the mass transfer rates for substances \underline{O} and \underline{R} . Thus, the current-potential curve of Figure 1b reflects only the diffusion processes for \underline{O} and \underline{R} .

Complications of the electrolysis mechanism depicted in Figure 1b, and discussed in the above paragraph, can take many forms. For example,

the depolareaction we the charge therical retransfer reaction we have a result as addressed transfer,

Mitially

Product (

of B will

(lettitet

Faraneter

ಚಿತ್ರ ಸಂಪ

ire is

₹£is ze

)Olential

At t

respication

the depolarizer may be an intermediate resulting from a chemical reaction which precedes the charge transfer, and/or the product of the charge transfer step may be an intermediate which undergoes a chemical reaction in the bulk of solution. In addition, the charge transfer rate may vary from reversible to irreversible, and thus also may be a rate-limiting step in the electrolysis. Other complications such as adsorption on the electrode surface may participate in the overall electrolysis mechanism.

Consider the following complication of a reversible electron transfer, where a chemical reaction of \underline{R} forms \underline{P} , an electroinactive product (24,44).

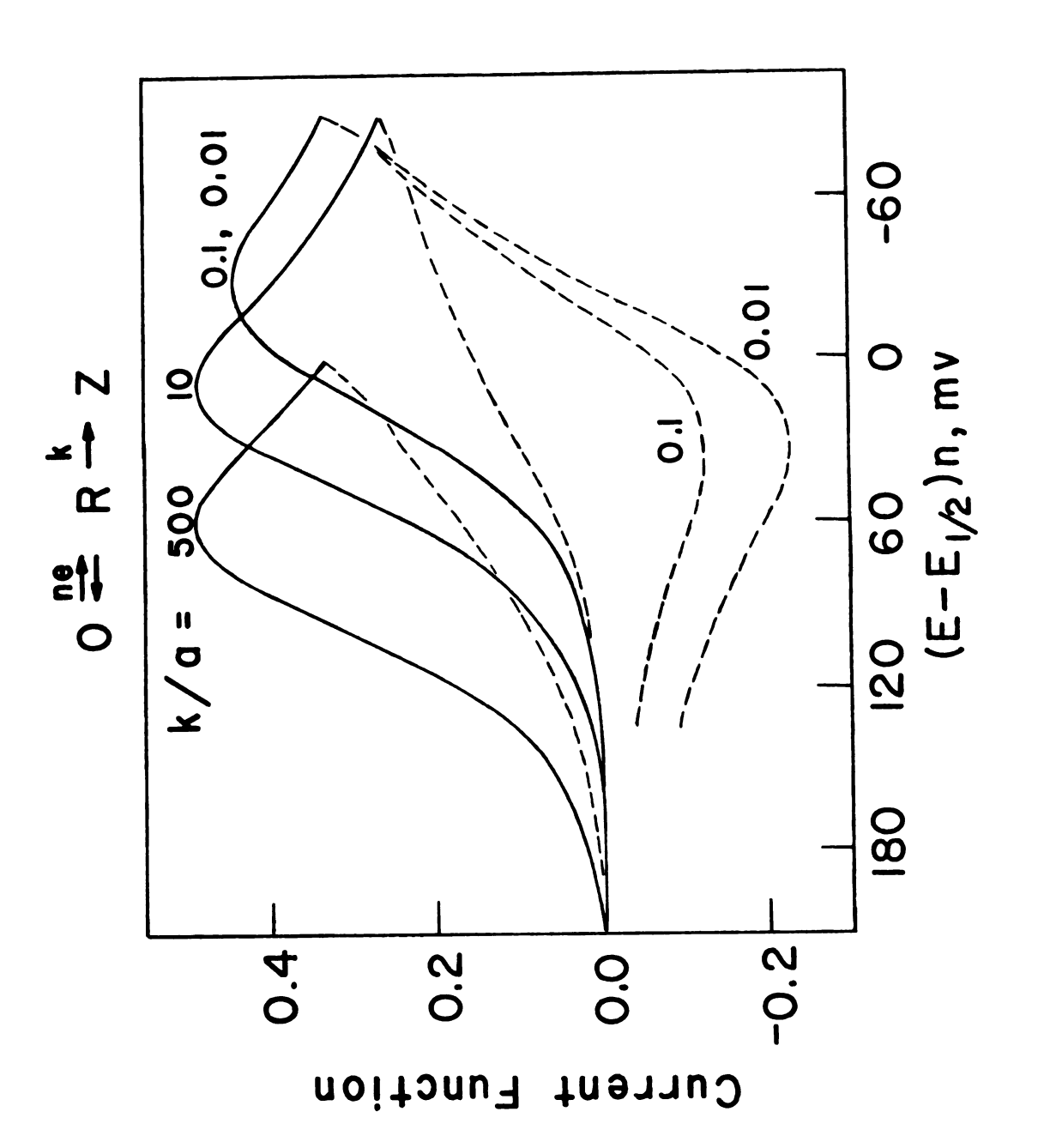
$$0 + ne \neq R \tag{I}$$

$$R \stackrel{k}{\rightarrow} P$$
 (II)

Initially, if the scan duration (time of the experiment) is small with respect to the half life of Reaction II, an insignificant amount of \underline{R} will have time to react to form \underline{P} before \underline{R} is oxidized to \underline{O} . Quantitatively, this idea is equivalent to stating that the kinetic parameter $\underline{k}/\underline{a}$ (where \underline{k} is the rate constant in \sec^{-1} , $\underline{a} = \underline{nFv}/\underline{RT}$ also in \sec^{-1} , and \underline{v} is scan rate) is less than about 0.01 (24). In this case no measurement of \underline{k} is possible and, in fact, the current-potential curve is essentially the one for a reversible charge transfer (where $\underline{k}/\underline{a}$ is zero) without any perturbation by Reaction II. A current-potential curve for this value of $\underline{k}/\underline{a}$ is shown in Figure 2.

At the other extreme, current-potential curves can be obtained by employing such large scan durations with respect to the half life of Reaction II that all of \underline{R} has sufficient time to form \underline{P} before any \underline{R} can be oxidized to \underline{O} . Quantitatively, this case corresponds to values

Figure 2. Current-potential curves for various values of $\frac{k/a}{a}$ for first order chemical reaction following reversible charge transfer.



value of \underline{k} To de tion of \underline{R} prior to o rates such for <u>Ma</u> eq Qroli orier irre Working ou ostacáic g is the : between po Expe Many in 1 (1) the Pote (2) the . froz 3) the מַייַבַיי ēχţę i ing A sin ्य **म**/इ_{हर}

it the re

Townset at

(280/05 (

of <u>k/a</u> gre

of $\underline{k}/\underline{a}$ greater than about 10 (24). A current-potential curve for this value of $\underline{k}/\underline{a}$ also is shown in Figure 2.

To determine \underline{k} , scan rates must be selected so that only a fraction of \underline{R} (ideally from about 10 to 50 % of \underline{R}) reacts to form \underline{P} prior to oxidation. Quantitatively, this idea corresponds to scan rates such that $\underline{k}/\underline{a}$ is between 0.01 and 1. A current-potential curve for $\underline{k}/\underline{a}$ equal to 0.10 also is included in Figure 2.

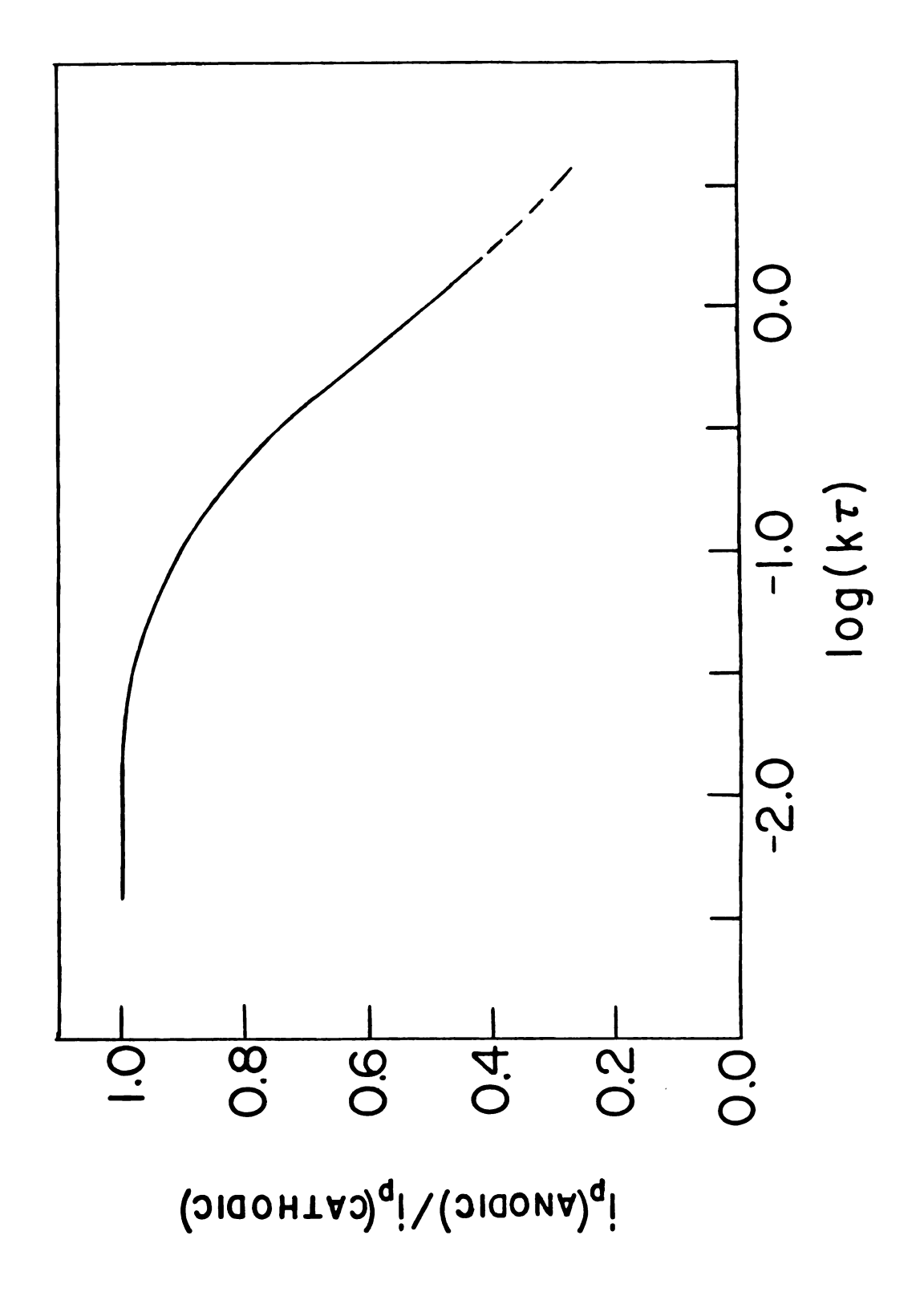
Cyclic voltammetric theory $(2^{\frac{1}{4}}, \frac{1}{4})$ for determining rates of first-order irreversible succeeding chemical reactions is presented as a working curve, shown in Figure 3, which relates ratios of anodic to cathodic peak currents $(\underline{i}_a/\underline{i}_c)$ to a parameter designated $\underline{k}\underline{\tau}$. Here \underline{k} is the rate constant in \sec^{-1} and $\underline{\tau}$ the elapsed time during the scan between potentials \underline{E}_{λ} and \underline{E}° (see Figure 1).

Experimentally, a rate constant is measured with cyclic voltammetry in the following manner:

- (1) the $\frac{i}{a}/\frac{i}{c}$ ratio is determined from the experimental current-potential curve (see Figure 2);
- (2) the value of $\underline{k}\underline{\tau}$ corresponding to this value of $\underline{\underline{i}}_a/\underline{\underline{i}}_c$ is read from the curve shown in Figure 3;
- (3) the value of <u>t</u> (in seconds) is determined from the experimental current-potential curve and the scan rate used for the particular experiment; and
- (4) finally, division of $\underline{k}\underline{\tau}$ by $\underline{\tau}$ gives \underline{k} .

A simple calculation shows that by varying scan rate between 10 mV/sec and 10^{14} V/sec , one can determine first-order rate constants in the range 10^{-2} to 10^{6} sec^{-1} . Similar calculations based on cyclic voltammetric theory for second-order chemical reactions, such as dimerization (51) and disproportionation (52), show that rate constants

Ratio of the anodic to cathodic peak current as a function of $\underline{k_{\rm T}}$ for first order chemical reaction following reversible charge transfer. Figure 3.



II IV/se able in te varie several long tin the sole tiat as wed to rapadati iaradai d Eftermat but gene ot court Steps at stati rati 21,821,281 e sot ಳುಭ್ಯಾ Mars. er Es es

And

A 3

Pates la

Cargo t

No Editor

in the 1

ÁS

in the range 10 to $10^8 \, \underline{\text{M}}^{-1}$ -sec⁻¹ can be obtained with scan rates from 10 mV/sec to $10^4 \, \text{V/sec}$.

As implied by the above discussion, scan rate is the primary variable in cyclic voltammetry. Experimentally, scan rates generally can be varied from about 10 mV/sec to 10 4 V/sec. This range is set by several experimental limitations, the lower is set by the fact that at long times convection becomes significant, making diffusion no longer the sole means of mass transport. The upper limit is set by the fact that as scan rate is progressively increased the fraction of current used to charge the electrical double-layer becomes dominant, because capacative current is directly proportional to scan rate whereas faradaic current is proportional to the square root of scan rate (54). Information on faradaic processes can still be obtained in such cases, but generally such data are only of qualitative value.

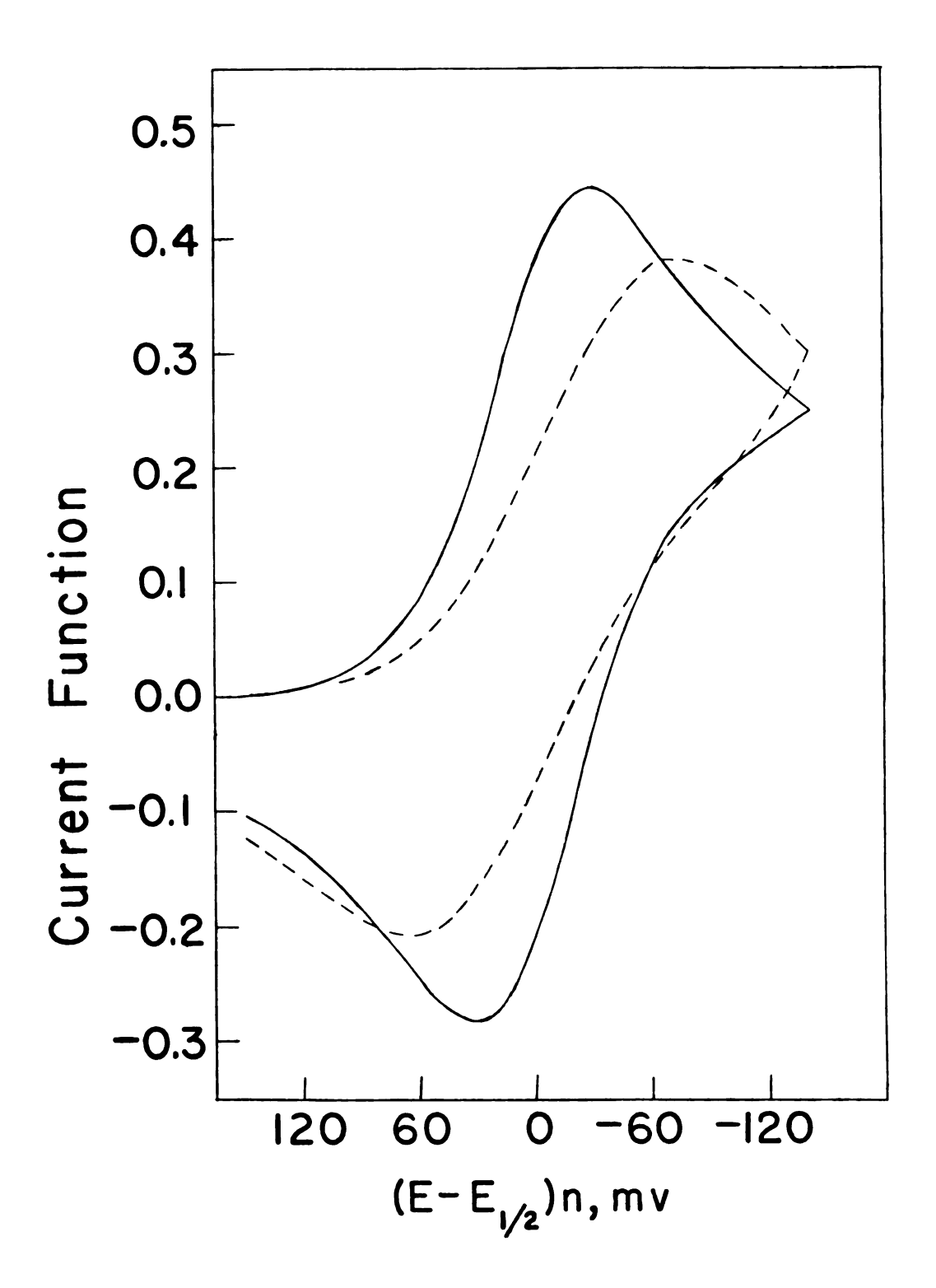
Another limitation in using cyclic voltammetry to determine rates of coupled chemical reactions is that kinetics of charge transfer steps at the electrode alter the shape of current-potential curves as scan rate is varied. Obviously, information on rates of coupled chemical reactions can only be garnered when charge transfer kinetics are not completely rate-determining.

A significant effect of charge transfer kinetics is that the anodic-to-cathodic peak separation (about 60 mV for reversible charge transfer) becomes progressively larger as scan rate is increased (27). This effect is shown in Figure 4, and is frequently observed when scan rates larger than about 100 V/sec are employed. For example, if the charge transfer rate constant is 0.1 cm/sec (a typical value), then the morphology of the current-potential curve will essentially

Figure 4. Cyclic current-potential curves showing effect of charge transfer parameter, Ψ .

---- Ψ = 7.0; α = 0.5

---- $\Psi = 0.25$; $\alpha = 0.5$



corre Edwere be ab : separa metry : mechan i :5: of versibl creases Hals, s is is g is obser ratios (ite pesk attodie Crease in fili inor Mrst-ora ATO 33 1126712611 ite pathod ser rate r title teal Tool office iniots sim

Ė.

Estate (21,

correspond to reversible electron transfer at a scan rate of 1 V/sec. However, at a scan rate of 10 V/sec the peak potential separation will be about 80 mV, and at a scan rate of 100 V/sec the peak potential separation will be about 130 mV.

At this point it may be useful to illustrate how cyclic voltammetry can be used as a diagnostic tool for elucidation of electrolysis mechanisms. As shown in Figure 2, for small values of $\underline{k}/\underline{a}$ the morphology of the current-potential curve corresponds to that for a simple reversible charge transfer. However, as the kinetic parameter $\underline{k}/\underline{a}$ increases the cathodic peak ($\underline{0} + \underline{ne} + \underline{R}$) shifts toward positive potentials, and the peak height increases by about 10 %. Moreover, when $\underline{k}/\underline{a}$ is greater than about 1, an anodic peak ($\underline{R} + \underline{0} + \underline{ne}$) no longer is observed. Hence, when $\underline{k}/\underline{a}$ is greater than about 1 peak current ratios ($\underline{i}_{-\underline{a}}/\underline{i}_{-\underline{c}}$) cannot be used to measure rate constants since only one peak is present. Nevertheless, when $\underline{k}/\underline{a}$ is greater than about 10, cathodic peak potentials shift $30/\underline{n}$ mV anodically for a 10 fold increase in $\underline{k}/\underline{a}$, or, equivalently, shift $30/\underline{n}$ mV cathodically for a 10 fold increase in scan rate. This fact indicates the presence of a first-order irreversible succeeding chemical reaction.

Anodic peaks also are absent for second-order reactions such as dimerization when $\underline{k}/\underline{a}$ is greater than about 1. In this case, however, the cathodic peak potentials shift $20/\underline{n}$ mV for a 10 fold increase in scan rate when $\underline{k}/\underline{a}$ is greater than about 10 (24). Thus, even when anodic peaks are absent, cyclic voltammetry can be employed as a diagnostic tool to distinguish between first and second-order chemical reactions simply on the basis of cathodic peak potential \underline{vs} scan rate shifts (24,51).

Foi mrrhol. element many c iate th mitam smitei iwes p ize ele tize of criers lives e sible a Merical

ini_{nes} Mich s Plance Pris ;

illinet; %e 455€

Witter; is 25 5

ور وقير 13. e For systems which display any or all of these complications, the morphology of the current-potential curves will be related to the elementary steps in the electrolysis mechanism. Hence, cyclic voltammetry can be used as an extremely valuable diagnostic tool to elucidate the nature of these steps and to measure their rates. Cyclic voltammetry has two outstanding features which make it especially suited for such mechanistic studies. First, a cyclic potential scan makes possible the investigation of both the reactants and products of the electron (charge) transfer in a single experiment. Second, the time of the experiment can be varied over a wide range (about six orders of magnitude). Thus, intermediates with a variety of half lives can be detected and their reaction rates measured.

D Applications of Cyclic Voltammetry to the Study of Species of Transient Existence

The original objectives of this research were to evaluate possible applications of modern electrochemistry to the investigation of chemically interesting species of transient existence. Although many choices were possible, it seemed logical to consider only systems for which some prior electrochemical data and observations (primarily polarography) already existed. In this regard, three classes of compounds seemed most amenable to further study: (1) reduction of tetrahalomethanes in nonaqueous solvents, since there is some evidence for the intermediacy of dihalocarbenes (56,57); (2) reduction of o-dihalobenzene compounds in nonaqueous solvents, since there is some evidence for the intermediacy of dehydrobenzene (58); and (3) reduction of certain common acid-base indicators in aqueous solutions, since there is reasonable evidence for the intermediacy of free radicals

which are

a brief s

three are

rezainier

search in

Two (

sible ele:

€:es <u>1.e</u>

tal reduct

interesti:

Stemiosl t

The e

reductions

of cases,

insei or y

electrolys

mie, for

Seterally:

Tu, the

ें इक्ष ध्रांभी

which are moderately stable in aqueous media at room temperature (59). A brief survey of the prior electrochemical research in each of these three areas constitutes the remainder of this introduction, and the remainder of this thesis is devoted to results and discussion of research in these three areas.

Two of the above areas for which the literature indicates possible electrochemical generation of chemically interesting intermediates (<u>i.e.</u>, dihalocarbenes and dehydrobenzene) involve electrochemical reductions of organic halogen compounds in nonaqueous solutions. Interestingly, both reports differ from the generally accepted electrochemical behavior of organic halogen compounds (60-76).

The electrochemical literature literally abounds with reports of reductions of both alkyl and aryl halogen compounds. In the majority of cases, unless some other group of the molecule is more readily reduced or unless organo-metallic compounds are formed, the overall electrolysis results in proton substition for the halide. For example, for $\underline{X} = \underline{I}$, \underline{Br} , \underline{Cl} , the overall electrochemical reduction is generally:

$$R - X \xrightarrow{2e, H} R - H + X$$

Thus, the electrochemical reduction of CCl_4 in 75 % dioxane-water proceeds as follows (60):

$$CCl_{4} \xrightarrow{2e, H^{+}} CCl_{3}H + Cl^{-}$$
 Wave I
$$CCl_{3}H \xrightarrow{2e, H^{+}} CCl_{2}H_{2} + Cl^{-}$$
 Wave II
$$CCl_{2}H_{2} \xrightarrow{2e, H^{+}} CCl_{3}H + Cl^{-}$$
 Wave III
$$CCl_{3}H_{2} \xrightarrow{2e, H^{+}} CH_{4} + Cl^{-}$$
 Wave IV

Simila

such as meta

stoichiomet





Neverth

to investiga firile (E)

ierent behav

lable I com:

ीं tiese oo

Vii a meney

ietoe the ha

Mential of

ध्याच्या १० ००

re ejectrof

Based c

tetts (Tabl

ite following

₹ %;

Similarly, electrochemical studies of aryl halogen compounds such as meta-dibromobenzene have found the following overall reduction stoichiometry in both aqueous and nonaqueous media:

Nevertheless, Wawzonek and Duty (56,57), who used polarography to investigate the electrochemical reduction of halomethanes in acetonitrile (AN) and N,N-dimethylforamide (DMF), reported entirely different behavior. Wawzonek and Duty studied six halomethanes, and Table I contains the polarographic behavior reported by these authors for these compounds. These authors used a two-electrode polarograph with a mercury pool combination reference and counter electrode; hence the half-wave potentials in Table I are with respect to the Potential of a mercury pool. Their polarographic solutions were reported to contain 0.175 M tetrabutylammonium bromide as the supporting electrolyte.

Based on largely indirect evidence from polarographic experiments (Table I in this introduction), Wawzonek and Duty proposed the following mechanism for the electrochemical reduction of ${\rm CCl}_{\rm h}$ in AN:

Table I. Polarographic Data of Wawzonek and Duty (56).

Compound	Solvent	-E _{1/2} (V) I _d	I	-E _{1/2} (V)	Id	-E _{1/2} (V) I _d	Id
CH ₂ C1 ₂	DMF					2.14	(6.37)
CHC13	DMF			1.45	(3.18)	2.14	(3.24)
CC1 7	DMF	0.25	(62.29)	1.49	(1.42)	2.17	(1.92)
CC1 7	DMF-10% water	0.27	(7.30)	1.61	(4.35)	2.25	(4.75)
CH ₂ Cl ₂	AN		no red	no reduction wave	observed		
CHC13	AN			1.32	(67.5)		
CC1 ₄	AN	0.25	(4.40)	79.0	(07.4)		
CC17	AN-10% water	0.33	(07.7)	1.64	(5.22)		
CBr _h	DMF	0.08	(6.43)	1.36	(2.20)	1.94	(1.62)
CHCLF ₂	DMF		no red	no reduction wave observed	observed		
ccl ₂ F2	DMF	1.45	(14.2)				

Itese au
chloroca
In
denlere
Serionne
of reage
Pested t
7.00
of the f
tie pres
Remoione
1,1-11 ah
Pirorato
ever, wh
is the p
17,7-31
Pesence
ie stoen
The extra
*250308)
Tarie,
et the v

$$CCl_{4} + 2e \rightarrow CCl_{3}^{-} + Cl^{-}$$
 (I)

$$\operatorname{ccl}_{3}^{-} \quad \neq \quad \operatorname{ccl}_{2} + \quad \operatorname{cl}^{-}$$
 (II)

$$CCl_2 + 2e \rightarrow CCl_2$$
 (III)

$$CC1_2^{=} + 2 CH_3CN \rightarrow H_2CC1_2 + 2 [CH_2CN]^{-}$$
 (IV)

These authors also proposed that CCl₄ reduction in DMF produces dichlorocarbene, but to a lesser extent than in AN.

In an attempt to provide direct evidence for the formation of dichlorocarbene suggested by this mechanism, Wawzonek and Duty also performed macroscale electrolytic reductions of CCl₄ in the presence of reagents such as tetramethylethylene and cyclohexene which are expected to trap any dichlorocarbene.

Thus, Wawzonek and Duty found that gas chromatographic analysis of the final solution of the macroscale electrolysis of CCl_h in AN in the presence of tetramethylethylene gave a component (no yields mentioned) possessing the same retention time as a pure sample of 1,1-dichloro-2,2,3,3-tetramethylcyclopropane, and regarded this gas chromatographic peak as proof of dichlorocarbene generation. However, when these authors performed a similar macroscale electrolysis in the presence of cyclohexene, none of the expected product (7,7-dichlorobicyclo[4.1.0]heptane) was observed, which makes the presence of dichlorocarbene less than certain. This ambiguity is heightened when one considers the way electrolyses were performed. The experimental procedures described by Wawzonek and Duty for their macroscale electrolyses are, to say the least, a bit unclear. For example, they stated that "Direct current was used for all electrolyses, and the voltage output was 120 volts." For the macroscale electrolysis

of SC		
H Marriago		
reaii		
ice I		
age his		
mang 		
grā o		
		
20.78		
≎ <u>*</u> ``,		
creas		
ଞ୍ଚିତ୍ର ଆଧାର		
are,		
92900		
Sisser		
(EDEXE		
57 <u>6</u> -7		
1000		
ં રેક્ક્		
Ţ		
Region		
\$\$\C\$ _e		
tetzet.		
it Tab		

of CCl₄ in AN in the presence of cyclohexene, they reported that "Current was controlled at 0.3 amp. After 21 hours, the current reading was 0.16 amp., and the reduction was stopped." And, for the macroscale electrolysis of CCl₄ in AN in the presence of tetramethylethylene, they reported that "Direct current was allowed to pass through the solution for 37 hours during which no visible color change was observed. The direct current was controlled at 0.30 amp and fell off to a final value of 0.15 amp."

Based on these statements, it appears that the macroscale electrolyses were conducted by impressing 120 V across the electrolysis cell, and then halting the electrolyses after the current had decreased to about one-half of its initial value. In other words, it appears that neither controlled current nor potential was employed.

In summary, although the analytical data of Wawzonek and Duty are, at best, not very convincing, their results suggest that modern electrochemical techniques might be used to generate and then directly observe species such as dichlorocarbene. This possibility is quite interesting since carbenes are known to be highly reactive, and generally are studied only by indirect methods. Therefore, in spite of doubts about the proposed mechanism of Wawzonek and Duty, reduction of tetrahalomethanes using cyclic voltammetry was investigated.

In another paper from Wawzonek's laboratory, Wawzonek and Wagenknecht (58) described the polarographic reduction of several halobenzene compounds, among them o-dibromobenzene and o-bromochlorobenzene, in nonaqueous media. These polarographic data are reproduced in Table II. Again, half-wave potentials are vs a mercury pool.

E-pactors

Pirozo:

Morobe Liverate

> Princing Princing

> > irozobe

2455 2455

> 3-116; 3-116;

> > }=::

Proper

Table II. Polarographic Data of Wawzonek and Wagenknecht (58).

		1			
Compound	Solvent	 - E _{1/2} (v) I _d	 -E _{1/2} (v) I _d
Bromobenzene	DMF			1.85	(3.28)
o-dibromobenzene	DMF	1 1.28	(6.53)	 	
<u>m</u> -dibromobenzene	DMF	l 1.40	(3.79)	l 1.88	(2.68)
<u>p</u> -dibromobenzene	DMF	1 1.53	(3.02)	1.82	(3.49)
Chlorobenzene	DMF	!		l 2.00	(2.95)
o-bromochlorobenzene	DMF	1.38	(4.50)	l 2.02	(1.44)
<u>m</u> -bromochlorobenzene	DMF	1.49	(3.32)	1 2.04	(2.83)
p-bromochlorobenzene	DMF	1.60	(3.09)	1 2.02	(2.61)
Chlorobenzene	AN	 no reduction wave observed 			
o-bromochlorobenzene	AN	1 1.54	(5.50)	 	
m-bromochlorobenzene	AN	1.65	(4.85)	 -	
p-bromochlorobenzene	AN	1.81	(4.50)	 	
Bromobenzene	AN	not in	vestigate	ı d	
<u>o</u> -dibromobenzene	AN	1.41	(9.77)		
<u>m</u> -dibromobenzene	AN	l 1.55	(5.00)	 2.05	(3.90)
<u>p</u> -dibromobenzene	AN	1.70	(4.12)	2.02	(4.12)
<u>o</u> -dibromobenzene	82% Dioxane	1.40	(4.15)	 	
<u>m</u> -dibromobenzene	82% Dioxane	1.56	(2.66)	l 1	
o-dibromobenzene	75% Dioxane	1.40	(3.84)	 	
<u>m</u> -dibromobenzene	75% Dioxane	1.56	(2.57)	' 	
o-dibromobenzene	60% Dioxane	1.40	(3.42)	 	
-dibromobenzene	60% Dioxane	1 1.56	(2.28)	 	

26 <u>2</u>re tic ---Tae; ier. 30<u>8</u>] ing. :0<u>1</u>; (5; 6,63 . V. Although Wawzonek and Wagenknecht apparently performed no coulometric experiments, they nevertheless stated that the reduction of o-dibromobenzene in both AN and DMF results in a single 4-electron reduction. On the basis of their polarographic data (Table II), these authors proposed the following mechanism, which involves the intermediacy of dehydrobenzene in DMF and AN.

$$\frac{\text{Br}}{\text{Br}}$$
 $\frac{2e}{\text{Br}}$ + Br (I)

$$k$$
 + Br (II)

They also proposed that, under similar electrolysis conditions, reduction of o-bromochlorobenzene results in dehydrobenzene intermediacy.

In an attempt to provide direct evidence for the intermediacy of dehydrobenzene suggested by this mechanism, they also performed a macroscale electrolytic reduction of o-dibromobenzene in the presence of furan, which is expected to trap dehydrobenzene. Specifically, they found that a macroscale electrolytic reduction of o-dibromobenzene (at -35° C, DMF as solvent, tetrabutylammonium iodide as supporting electrolyte) in the presence of furan yielded products which on acid hydrolysis gave a 1 % yield of a compound which possessed the same glc retention time as a peak due to a pure sample of α -napthol, and interpreted this as direct proof of dehydrobenzene generation.

Although the analytical data of Wawzonek and Wagenknecht are not conclusive, their results suggest that cyclic voltammetry could be used first to generate and then directly observe dehydrobenzene. Such a study would be highly informative since dehydrobenzene, like dichlorocarbene, is a highly reactive species which generally is studied only by indirect methods.

Of all the possibly reactive species that can be studied electrochemically, free radicals have received by far the greatest attention (8-12 and references contained therein). In the majority of studies nonaqueous solvents have been used because organic free radicals generally are less reactive in aprotic, or nearly aprotic media, where protonation of electrogenerated radical ions is greatly diminished. Nevertheless, meaningful experiments in nonaqueous solutions are very difficult, as will be illustrated repeatedly throughout this thesis, and therefore much of the extant research on free radical electrochemistry is not an unambigous evaluation of the potential of electrochemical relaxation techniques for studying reactive intermediates. Hence, the recent experiments (primarily polarography) of Senne and Marple (59) on the electrochemical reduction of phenol red, the structurally simplest of the sulfonephthalein acid-base indicators, are particularly interesting because their data suggest that free radicals of moderate stability can be produced electrochemically in aqueous solution. These authors postulated a mechanism which rationalizes the results of their experiments. Essentially, this mechanism consists of a one-electron reduction yielding a product which disproportionates to form starting material and the fully-reduced (two-electron) product, phenolsulfonephthalein.

ploye **L**etho accon وغتت thesi recen ters : to the Stiest ::e g: indica erea. is the lerize: ed in t

:

Hence, it appeared that compounds such as phenol red could be employed to evaluate the efficacy of modern electrochemical relaxation methods for studying free radical reactions, without the complications accompanying the use of nonaqueous solutions. Thus, sulfonephthalein compounds were selected as the third class for investigation in this thesis research.

The research described in this thesis was initiated by applying recently-developed electrochemical techniques to all three of the systems mentioned above, with the intention of devoting the major effort to the systems that appeared most promising in the terms of the major objectives stated above. As results in following chapters will show, the greatest promise seemed to lie in the study of the sulfonephthalein indicators, so that the most detailed investigations were made in this area. Nevertheless, very interesting preliminary results were obtained in the other two areas, and therefore the most salient features of experiments on halomethanes and o-dihalobenzene compounds are also included in this thesis.

0h:

Mercury

signifi

solvent

wately

iosses

voltage

this ci

Th

Potenti

two vol

٧غ۶٤.).

Ce

:esisto

^{jevices}

etperiz

Tektro

357 (t

Tekero

II. EXPERIMENTAL

A Electrochemical Apparatus

Ohmic potential losses are a possible source of serious error in all of the electrochemical measurements made in this study. A conventional three electrode potentiostatic circuit does not compensate for resistance between the working electrode and reference electrode probe. This iR drop is especially significant when a conventional dropping mercury electrode (DME) is used. Also, the solution resistance is significant in low conductance solvents and even in high conductance solvents when fast scan rates (large currents) are employed. Fortunately, it is possible to compensate electronically for ohmic potential losses by using a three electrode potentiostatic circuit with positive voltage feedback. Figure 5 is a block diagram of the circuit used here; this circuit is similar to one described by Smith and Deford (77).

The control amplifier (C.A.) was a commercial instrument (Wenking potentiostat, Model 61RS, Brinkmann Instruments, Westbury, N.Y.). The two voltage followers (F_1 and F_2) and inverter (I) were solid state operational amplifiers (Philbrick Researches, Inc., Model P25AU, Dedham, Mass.).

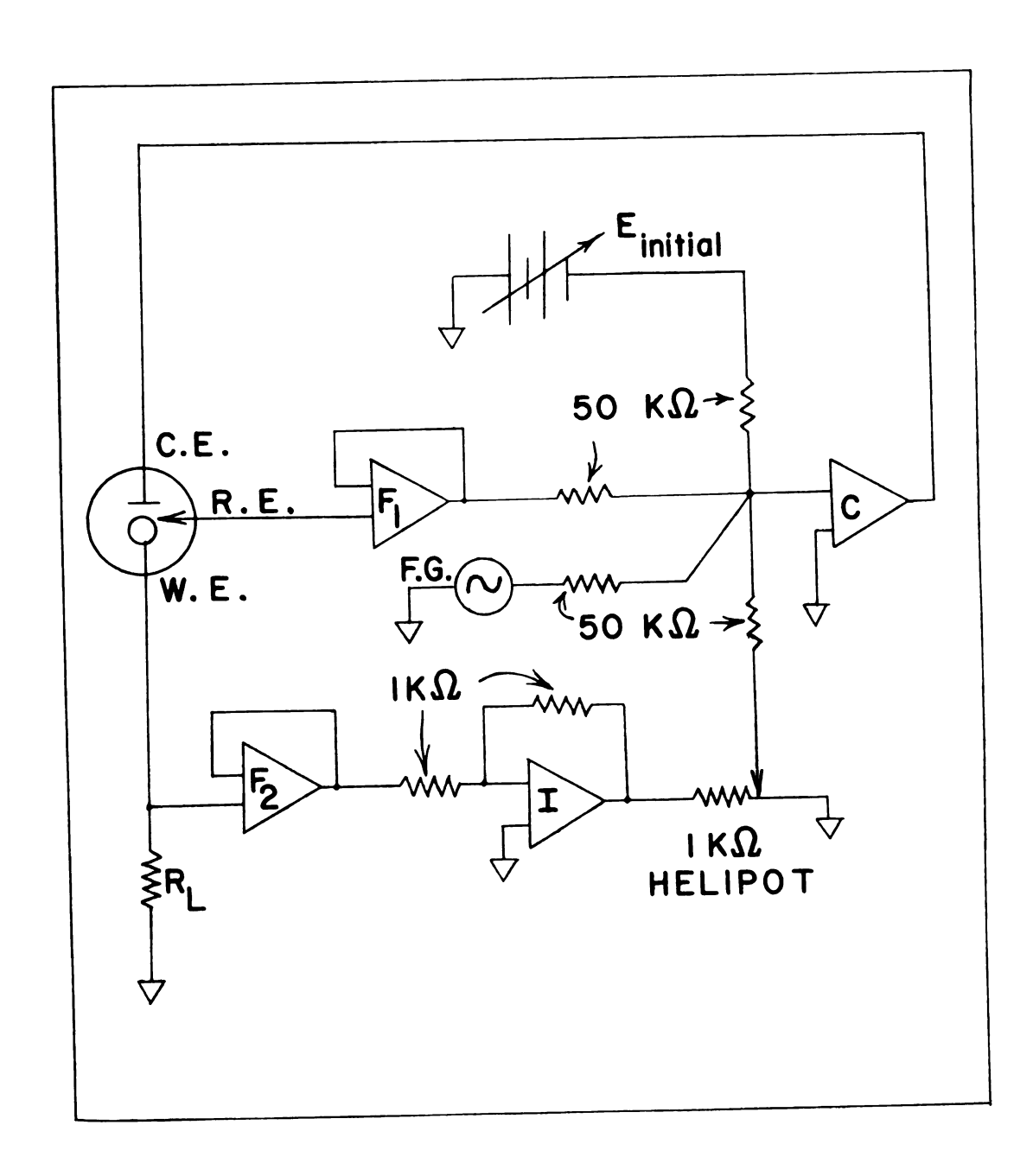
Cell current was determined from the potential drop across the load resistor, R_L. To measure this potential drop two different recording devices were used depending on the time scale of the experiment. For experiments less than about one second duration a storage oscilloscope (Tektronix, Inc., Beaverton, Ore., Type 564 with 2A63 (vertical) and 2B67 (horizontal) plug-in units) with Polaroid camera attachment (Tektronix Type C-12) was employed. For longer time experiments an

Figure 5. Block diagram of circuit configuration

R. E.: Reference electrode
C. E.: Counter electrode
W. E.: Working electrode
R. : Load resistor
C : Control amplifier

F : Voltage follower amplifier
F1 : Voltage follower amplifier
I : Inverter amplifier

I² : Inverter amplifier
F. G.: Function Generator
E_i : Initial potential



x-y re

ograph

_

ii ffer

perimen

to have

Wave.

then h

This re

erator

14 111

erators

Tiers:

Secera:

istin:

W of

E batte

F;

£2 ,736

ireque:

C;

in about

381 31

يوندن

ilei re

x-y recorder (Honeywell, Inc., Model 520, San Diego, Calif.) was used.

The various electrochemical techniques used in this study (polarography, cyclic voltammetry, constant potential electrolyses) require different potential-time functions. For some cyclic voltammetry experiments involving measurements of anodic currents it was necessary to have a base line constructed from the extension of the cathodic wave. This was obtained by scanning just past the cathodic peak, and then holding the potential constant to record the current-time curve. This required a voltage waveform consisting of the first leg of the triangular wave, followed by a constant potential. The function generator for experiments of this nature has been previously described (78). In addition to this function generator, two commercial function generators (Exact Electronics, Inc., Model 255, Hillsboro, Ore., and Interstate Electronics Corp., Model F52, Anaheim, Calif.) were used to generate triangular waves for cyclic voltammetry and polarography. No distinction could be made between experimental results obtained with any of these three function generators.

For constant potential electrolyses the initial potential source, a battery-operated low voltage power supply, of the Wenking potentiostat was used to set the potential of the working electrode.

Coulometric measurements were made by means of a voltage-to-frequency conversion technique previously described by Bard and Solon (79). Instrumentation consisted of a commercial potentiostat (Wenking, described above) and a Heath Universal Digital Instrument (UDI, Model EU-805A) used simultaneously as a voltage-to-frequency converter and a frequency counter. The voltage measured by the UDI was the ohmic drop across a load resistor, \underline{R}_{I} , placed in the current-carrying loop of the three

elec

oir:

Ng.

Zach Sem

Stell Tig

1385 1875

177.3

14. 14.

1104

lin.

electrode potentiostatic circuit. Figure 6 is a block diagram of this circuit.

The cell arrangement employed for most aqueous studies is shown in Figure 7. The cell consists of a glass weighing bottle with a \$\mathbb{E}\$ 60/20 ground glass joint on the top. The cell lid is made of Teflon and is machined to fit this joint. Holes were drilled in the lid to allow insertion of the various cell components (Figure 7).

The counter electrode consists of a one foot length of 26 guage platinum wire wound around 6 mm soft glass tubing. One end of the platinum was sealed in the glass tubing, and electrical contact was made through mercury contained in the glass tubing.

The reference electrode contained three separate sections separated by 10 mm fine porosity glass discs. The left hand compartment (Figure 7) was a saturated calomel electrode, and the right hand compartment contained the solution being investigated. Because, on occasion, this latter solution contained perchlorate, a 1 M aqueous sodium nitrate solution was used in the middle compartment to prevent precipitation of potassium perchlorate. Liquid junction potentials clearly arise when different solutions are contacted in this manner. However, in this work only relative potential measurements were critical. Presumably the liquid junction potential for a given solution would remain constant during the course of an experiment. In fact, half-wave potentials for a given system never varied more than about 10 mV during the course of an entire investigation. The right hand compartment of the reference electrode was a tube with a 10 mm fine porosity glass disc in contact with the solution in the cell.

For experiments requiring a stationary mercury electrode, a hanging

Figure 6. Block diagram of circuit used for coulometry.

C : Control amplifier (Wenking potentiostat)

E; : Initial potential

R. E.: Reference electrode

W. E.: Working electrode

C. E.: Counter electrode

R_L : Load resistor

V.F.C.: Voltage-to-frequency converter

F. C.: Frequency counter

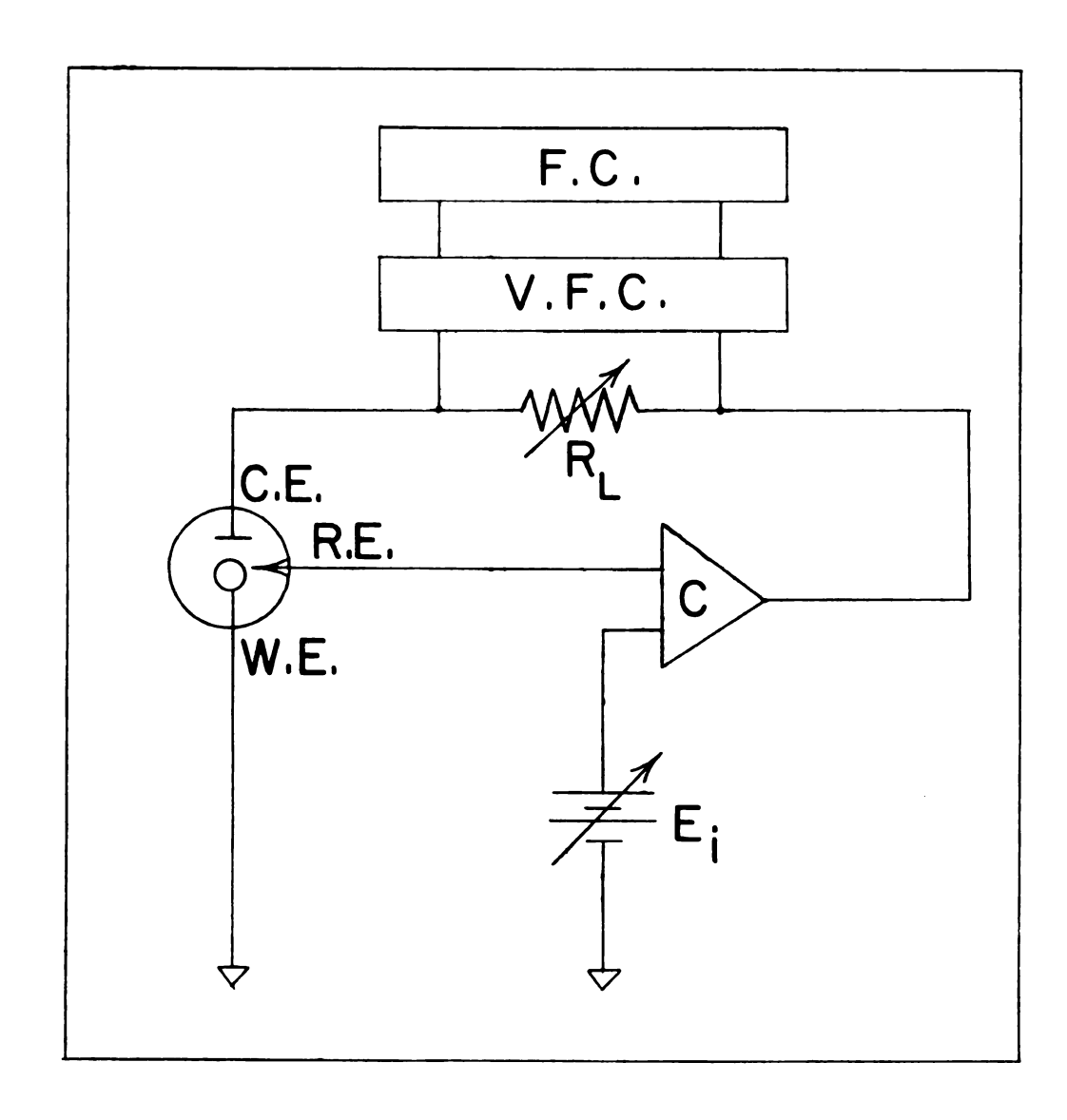
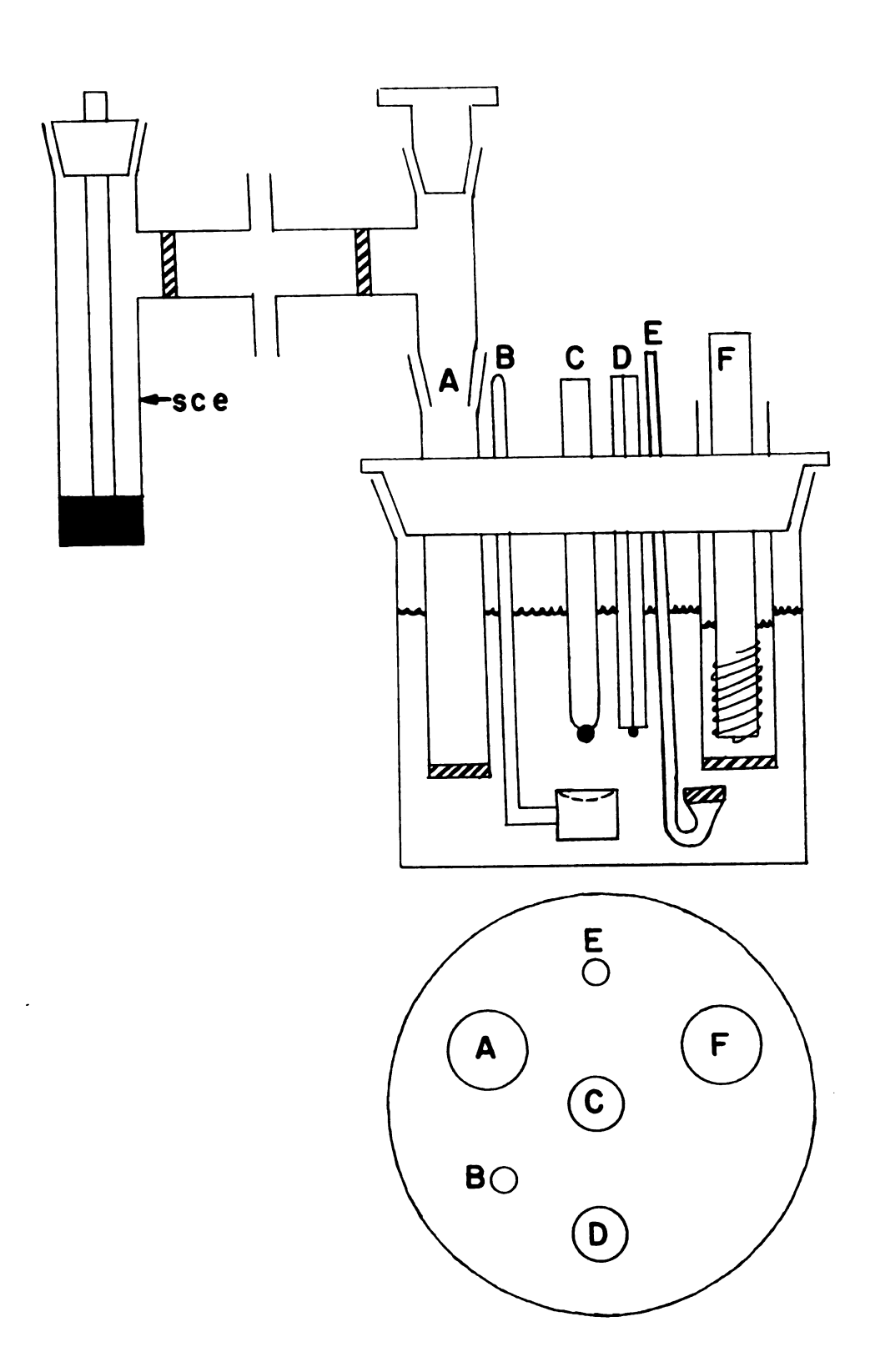


Figure 7. Cell arrangement.

- A: Reference electrode
- B: Scoop
- C: Hanging mercury drop electrode
 D: Dropping mercury electrode
- E: Deaerator
- F: Counter electrode



mercury

Ross, Si

irops fo

vorking

A :

a miero:

the tip

spite o

mating

tained

studies

causing

it less

tite, s

Ti

STILETE

Tell II e

gerere]

5.

iratei

tiett.

 ε

Tai Ting

iczątie.

tie ei

mercury drop electrode (HMDE) constructed in the manner described by Ross, Shain, and DeMars (80) was used. Generally one or two mercury drops from the DME were collected in a scoop and suspended from the working electrode.

A Kemula HMDE (Metrohm Ltd., Type EBM 5-03, Herisau, Switzerland), a micrometer type electrode that permits extruding mercury drops from the tip of a capillary, was also tried, but without any success. In spite of repeated attempts involving a large variety of cleaning and coating procedures of the capillary, reproducible data were never obtained with the Kemula HMDE in nonaqueous solutions. Even in aqueous studies it was found that solution started to creep up the capillary, causing a broken mercury thread, and hence a broken electrical contact, in less than one hour.

The deoxygenator was of conventional design, a small gas dispersion tube, and could be raised above the solution to provide an inert atmosphere (either nitrogen or argon was used) over the solution while measurements were being made.

pH was measured with a Heath pH meter (Model EU-302A) and a Beckman general purpose glass electrode (Model 41263). The pH meter was calibrated with standard Beckman buffers over the pH range studied.

All measurements were made in a constant temperature room at ambient temperatures of 23-24°C.

B Procedures for Aqueous Electrochemical Experiments

Precautions such as deoxygenating solutions with nitrogen, maintaining a nitrogen blanket over the solution when measurements are being conducted, and running blank (everything present in the solution except the electroactive material) experiments were always observed. The weight of mercury drops was determined in the usual manner by weighing out 50 drops.

The solvent was either 25 % (by weight) methanol-water or strictly water. Citrate buffered solutions were made up by dissolving citric acid to give a 0.10 \underline{M} solution with subsequent addition of sodium hydroxide to give a particular pH as measured by a pH meter. Acetate buffered solutions were made up in a similar manner. Namely, first sodium acetate was dissolved to give a 0.20 \underline{M} solution with subsequent addition of concentrated acetic acid to give a particular pH as measured by a pH meter.

C Vacuum Line and Associated Apparatus

A serious obstacle to conducting nonaqueous electrochemical studies is the presence of small amounts of water in the nonaqueous solutions. For example, 0.01 % water is approximately 1 mM water which is equal to the concentration of electroactive materials usually employed in electrochemical techniques. Water contamination arises from the solvent, the supporting electrolyte, the atmosphere, and residual water remaining on surfaces in the electrochemical cell. Therefore a vacuum line and integral electrochemical cell were constructed in an attempt to avoid these problems. This vacuum apparatus is similar to one previously described by Bard (7), and is shown in Figure 8.

The electrochemical cell, shown in Figure 9, was connected to the vacuum line by means of a § 18/9 ground glass joint. Five electrodes could be positioned in the cell by means of five § 14/20 ground glass joints situated at the top of the cell. For example, an arrangement consisting of a DME, a HMDE, a scoop, a reference electrode, and a counter electrode and compartment could be placed in this cell. The

Figure 8. Electrochemical vacuum line apparatus

A: BASF BTS O_2 removal catalyst B: Molecular sieve plus ${\rm Mg}({\rm ClO}_{\rm L})_2$

C: Liquid N₂ traps

D: Electrochemical cell

E: Glass-to-metal seal

F: C.V.C. Type 100C vacuum discharge gauge

G: To vacuum pumps

H: To inert gas

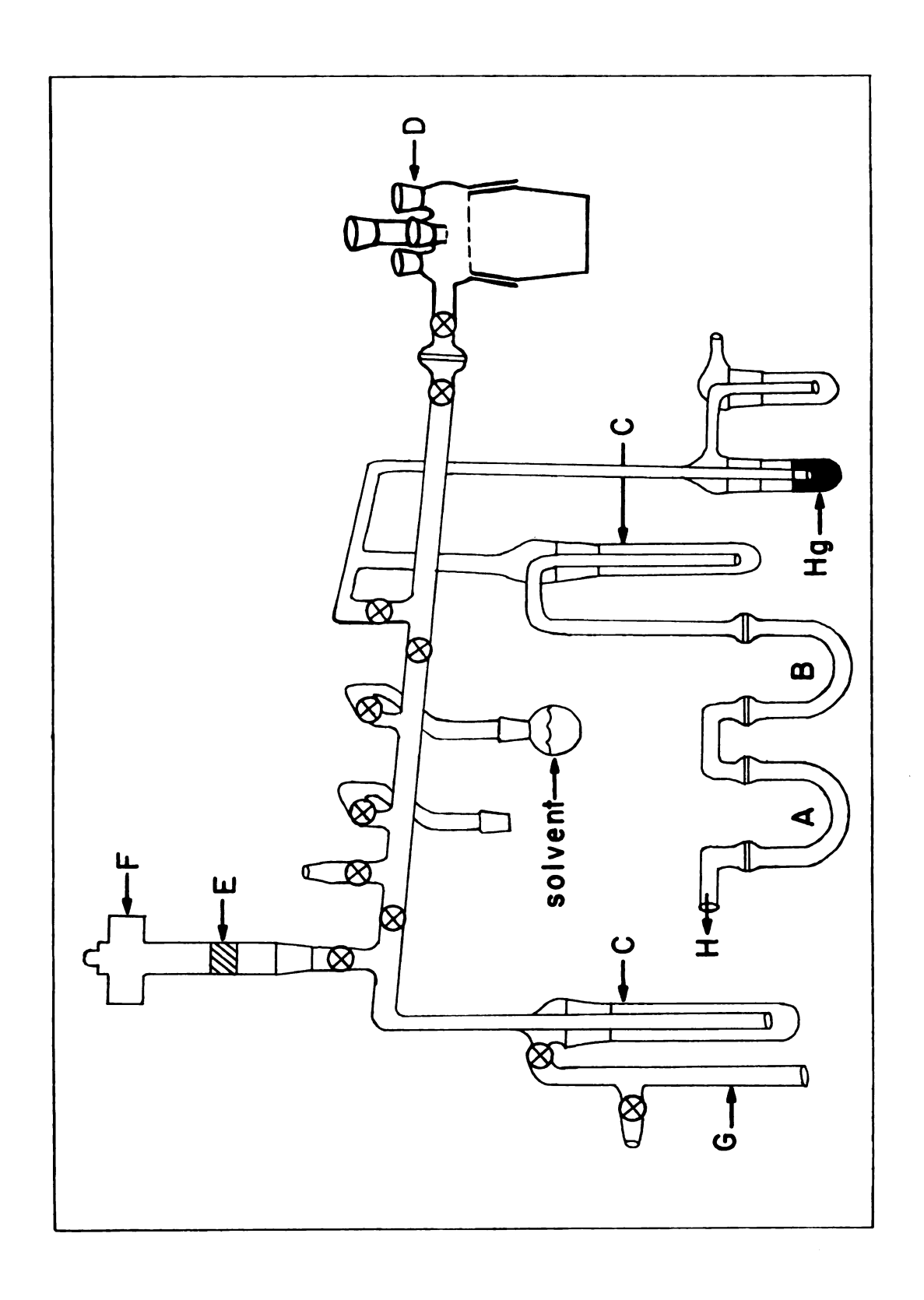


Figure 9. Vacuum line electrochemical cell.

- A: Combination scoop and mercury pool contact
- B: Hanging mercury drop electrode (HMDE)
- C: Reference electrode (sce)
- D: Dropping mercury electrode (DME)
- E: Counter electrode (platinum wire)
- F: Cell bottom (male portion of a \$\ 60/50 joint sealed flat 5 cm from ground glass portion of joint)
- G: F 60/50 joint
- H: Adapter, threaded (Ace Glass Incorporated, part no. 5029-10)
- I: § 14/20 joint
- J: 4 mm vacuum stopcock (ground glass)

All ground glass joints, except the main \S 60/50 joint, are \S 14/20 joints.

referer

the one referer

the bot

chamber

A zero:

letry a

tact to

of the

electro

imers.

a iewa:

the va

-

conven-

"Eigh

ಕ್ಷಿಯಾನೆ

errear

Edwerre

longer

vork i

appara

દે-કડ

of Dow

1 1

[%] है हैं

Givae

reference electrode had a three compartment configuration identical to the one described above for aqueous solution studies. The arm of this reference electrode configuration that fits into the cell is closed at the bottom with a fine porosity glass frit. The counter electrode chamber was also closed at the bottom with a fine porosity glass frit. A mercury pool could be introduced at the bottom of the cell for coulometry and other macroscale electrolysis experiments. Electrical contact to this pool was made by a platinim wire that was an integral part of the scoop which was inserted through the top of the cell. The electrochemical cell is designed so that the bottom half of it can be immersed in another solution. For example, immersion of the cell into a dewar containing liquid nitrogen is necessary to transfer solvent from the vacuum line manifold to the cell, and to degas solvents.

The vacuum stopcocks and joints used on this apparatus were of the conventional ground-glass type. Both silicone lubricant (Dow Corning "High Vacuum Grease") and Apiezon N grease were used to lubricate these ground-glass joints. The chemical inertness of these two lubricants appeared to be about equal towards solvents used in these studies. However, Apiezon N was found to be superior in that it appeared to make longer-lasting seals, which is important since a great deal of time and work is involved in dismantling, regreasing, and reassembling the vacuum apparatus. Furthermore, manipulations of stopcocks and other ground-glass joints appeared to require less effort when Apiezon N, instead of Dow Corning lubricant, was used.

The use of ground-glass joints on the vacuum apparatus results in one unsatisfactory feature. Namely, solvents such as 1,2-dimethoxyethane (Glyme) and tetrahydrofuran (THF) rapidly dissolve both of the above

mentioned va apparatus wa forazide and most versati because of apparatus co electrochemi Commerc cooled cil c Plainview, ! (Jentral So of the oil ¥€:. Co., ½ air supply Said (Cent) Pressu ischarge g 1.Y.). Thi ed 25 torr 2 m vacuum tiis stopeo Periodic cla As dep aciam atta ing why dro-

13e11, Act:

catalyst, E

Ger.) pri

mentioned vacuum lubricants. However, it was found that this vacuum apparatus was quite suitable for use with solvents such as N,N-dimethyl-foramide and acetonitrile. Thus, since the amides and nitriles are the most versatile and commonly-employed nonaqueous electrochemical solvents (because of their relatively high dielectric constants), the vacuum apparatus constructed for this research is suitable for most nonaqueous electrochemical studies.

Commercial vacuum pumps were employed for the vacuum line. An air-cooled oil diffusion pump (Veeco Instruments Inc., Model EP 2A-1, Plainview, N.Y.) was operated in conjunction with a mechanical forepump (Central Scientific, Model 91138 Hyvac &, Chicago, Ill.). The heater of the oil diffusion pump was rigged with an air flow switch (Rotron Mgf. Co., Model 2A, Woodstock, N.Y.) so that the heater shut off if the air supply stopped. The oil used in this diffusion pump was silicone fluid (Central Scientific, Type 93262-003, Chicago, Ill.).

Pressure in the vacuum line was measured by means of a cold cathode discharge guage (consolidated Vacuum Corp., Model GPH-100C, Rochester, N.Y.). This guage was capable of monitoring the pressure between 10⁻⁷ and 25 torr, and was isolated from the manifold of the vacuum line by a 2 mm vacuum stopcock. A # 24/40 ground glass joint was situated above this stopcock for ease of removal of the entire guage assembly for periodic cleaning.

As depicted in Figure 8, a gas train is an integral part of the vacuum apparatus. This train directs inert gas through U-tubes containing anhydrous magnesium perchlorate, molecular sieve (Matheson Coleman & Bell, Activated "Linde" Type 3A), and an oxygen removal catalyst (BTS catalyst, Badische Anilin und Soda Fabrik, A.G., Ludwigshafen am Rhein, W. Ger.) prior to entry into the electrochemical cell. The U-tube

containing the oxygen removal catalyst was wrapped with heating tape and the temperature kept at approximately 200°C. The reason for the inclusion of this gas train is that it is necessary to have a positive pressure of an inert gas (nitrogen or argon) blanketing the electrolysis cell when measurements are being made. This is done to prevent introduction of water and oxygen from the atmosphere into the cell during electrode manipulations that arise in the course of a series of experiments.

D Procedures for Nonaqueous Electrochemical Experiments

The primary reason for constructing a vacuum apparatus for electrochemical experiments was to obtain a dry environment for conducting experiments using nonaqueous solutions. Solvents, supporting electrolytes, and other materials were purified (discussed below) prior to introduction into the vacuum line apparatus. The electrochemical cell (Figure 9) was designed so that measurements could be made with solution volumes from 30 to 100 ml.

Taking acetonitrile as an example, the following statements list the sequence of operations carried out using this vacuum apparatus for a nonaqueous electrochemical experiment. First, a weighed amount of purified tetrabutylammonium perchlorate, the supporting electrolyte usually employed, was placed in the electrochemical cell. Then the cell was assembled with the counter electrode and compartment, the HMDE, the scoop, and two plugs placed in the top of the cell (the DME and reference electrode were placed in the cell in a later operation). The cell was then attached to the vacuum line, the proper stopcocks manipulated, and the contents of the cell exposed to the vacuum manifold. The cell was pumped until a pressure of about 10⁻⁶ torr was obtained for at least

from th aceton: 720UII the mar mitroge four ti ocemica. ransfe Gen tem stopede: Eroria. ei to w tions), turning them pla Prevent: ejestroc After th ¥as aide kε Mis app iliei a timite. Sing I,

ites be

ingrater.

one ho

one hour. Then, by further stopcock manipulation, the cell was isolated from the vacuum line manifold. Next, from 30 to 50 ml of purified acetonitrile, contained in a round bottomed flask, was attached to the vacuum line manifold, the contents of this flask being separated from the manifold by a vacuum stopcock. The solvent was frozen with liquid nitrogen, and this stopcock turned and the solvent degassed at least four times. Then, by further stopcock manipulations, the electrochemical cell was reconnected to the vacuum line manifold and the solvent transferred directly into the cell which was maintained at liquid nitrogen temperature. The cell and vacuum manifold were then reisolated by stopcock manipulations, and the liquid nitrogen bath removed from around the electrochemical cell. Then the cell and contents were allowed to warm to room temperature (about two hours for acetonitrile solutions), and a positive pressure of argon introduced into the cell by turning the proper stopcocks. The reference electrode arm and DME were then placed into the cell, with the positive pressure of argon (hopefully) preventing contamination by oxygen and water from the atmosphere. Then electrochemical experiments were carried out on this blank solution. After these blanks were run, a measured amount of electroactive material was added, and the electrochemical experiments initiated.

As indicated by the above statements, operations performed with this apparatus were quite time consuming. For example, it always required at least 18 hours to run even preliminary experiments when acetonitrile was employed as the solvent. Furthermore, experiments conducted using N,N-dimethylforamide (DMF) as the solvent required far longer times because of the much lower vapor pressure of DMF. For example, transfer of 30 ml of acetonitrile from the storage flask on the manifold

into the cell required about one hour whereas transfer of an equivalent volume of DMF required about six hours.

E Spectroscopy Apparatus and Procedures

Sulfonephthalein indicators absorb strongly in the visible region ($\lambda_{\rm max}$ for phenol red is 430 nm) whereas the one and two electron reduction products are colorless, absorbing in the uv region ($\lambda_{\rm max}$ for phenol red is 265 nm). Thus, absorbance measured at 430 nm can be used to determine the concentration of phenol red. For example, if a 4 x 10⁻⁵ M solution of phenol red is reduced chemically to 2 x 10⁻⁵ M, then at equilibrium the absorbance at 430 nm corresponds to 3 x 10⁻⁵ M. Of course, experiments of this type performed with rapid mixing provide a means of measuring the rate of disproportionation. Experiments along these lines were performed using two procedures, one involving the use of a stop flow apparatus and the other a conventional spectrophotometric apparatus. All phenol red solutions in these studies were aqueous solutions containing 0.20 M acetic acid and 0.20 M sodium acetate. The preparation of solutions of chemical reductants is discussed below.

Approximately half of the rate measurements were conducted with a stop flow apparatus which is described by Beckwith and Crouch (81). In a typical experiment a solution of phenol red was contained in one syringe and a solution containing approximately half an equivalent of V(II) was contained in the other syringe. Mixing into a 2.00 cm length cell was complete within a few milliseconds and transmittance through the cell was recorded as a function of time with a Heath (Model EU-201V) multi-speed strip chart recorder, operated at a speed of one inch per minute. Zero % Transmittance was set with the shutter closed, and 100 % Transmittance with a blank (everything present in the solutions except

phenol red and V(II)) solution in the cell. Measurements were made at ambient temperatures of 23-24°C.

Other rate measurements were made with a Heath (Model EU-701) single-beam spectrophotometer in conjunction with a Heath (Model EU-703-31) photometric readout module. The current output of this photometric readout module was connected to a Heath (Model EU-20-28) log/linear current module which was incorporated in a Heath (Model EU-201) multi-speed strip chart recorder, operated at a speed of one inch per minute. The reaction cell was a standard 1.00 cm spectrophotometric cell surrounded by a brass jacket through which water at 23 + 0.01°C was circulated. Zero % Transmittance was set with the shutter closed and 100 % Transmittance with a blank solution in the cell. 2 ml of phenol red solution was placed in the cell and the absorbance recorded. Then 0.50 ml of a V(II) solution, about half an equivalent of V(II), was injected into this cell using a 0.50 ml tuberculin syringe. Rapid mixing was obtained by this technique, as seen by the fact that these experimental curves were identical in appearance to those obtained using the stop flow apparatus. This syringe injection technique was found to be necessary since the use of a magnetic stirring bar (Teflon coated) in the standard 1.00 cm spectrophotometric cell did not give sufficiently rapid mixing. No discernable differences were observed in measured rate constants obtained by this conventional procedure vs the stop flow method.

Other spectrophotometric measurements in the ultraviolet and visible regions were made with a Unicam SP 800 spectrophotometer. Studies were carried out in a conventional manner using standard 1.00 cm spectrophotometric cells, with a cell containing blank solution in the reference

beam.

throug

cordec

]

specti

Conver

-

tient

system

calib:

a west

7.

cedure distil

1,1-32

iisti]

Tisco

Parisi - 66.1

1,2-11:

1,1-110

tion u

siere (

dettane

stor_{ege}

beam. Both sample and reference cells were surrounded by a brass jacket through which water at $23 \pm 0.01^{\circ}$ C was circulated. Spectra were recorded from 200 to 850 nm.

Infrared measurements were made with a Perkin-Elmer 237 B grating spectrophotometer. Spectra were recorded between 625 and 4000 nm. Conventional techniques employing nujol mulls and KBr pellets were used.

EPR experiments were run in a constant temperature room at an ambient temperature of about 23°C using a Varian E-4 EPR spectrometer system. An aqueous solution cell was used. The instrument was first calibrated with a strong pitch sample (Varian part no. 904450-01) and a weak pitch sample (Varian part no. 904450-02).

F Materials

Nonaqueous solvents were purified according to the following procedures. Acetonitrile (Fisher, B.P. 81.4 - 81.7 °C) was purified by distillation under nitrogen according to the procedure of Mann (82).

N,N-dimethylformamide (Fisher, B.P. 152.5 - 153.2 °C) was purified by distillation under reduced pressure according to the procedure of

Visco (6). N,N-dimethylacetamide (Fisher, B.P. 165.9 - 166.6 °C) was purified in the same manner as DMF. Tetrahydrofuran (Baker, B.P. 65.9 - 66.4 °C) was purified according to the procedure of O'Donnell (83).

1,2-dimethoxyethane (glyme) (Eastman red label, B.P. 83 - 84 °C) was purified according to the procedure of Mann(6). Tetrahydrothiophene
1,1-dioxide (Sulfolane) (Shell, Sulfolane-W) was purified by distillation under reduced pressure from either calcium hydride or molecular sieve (Matheson Coleman & Bell, Activated "Linde" Type 5A). Nitromethane (Matheson Coleman & Bell, B.P. 100 - 102 °C) was purified by storage over barium oxide for several days followed by a reduced pressure

distillation from barium oxide.

Aqueous solutions were prepared using distilled water. Methanol (Matheson Coleman & Bell, B.P. 64.4 - 65.0 °C), acetone (Matheson Coleman & Bell, B.P. 55.9 - 56.0 °C), and methylene chloride (Matheson Coleman & Bell, B.P. 38.3 - 41.3 °C) were used without further purification.

Tetraalkylammonium perchlorate salts were generally used for studies conducted in nonaqueous solvents. Both the tetraethyl and tetrabutyl salts were made by the metathesis of their respective chlorides (Eastman red label) with sodium perchlorate (G.F. Smith Chemical Co.). These salts were then purified by crystallization according to published procedures (6). Furthermore, shortly before usage in electrochemical experiments, the salts were dried under vacuum at 80 °C for at least 24 hours. Other supporting electrolytes such as sodium perchlorate, lithium perchlorate, potassium chloride, and sodium sulfate were used without further purification.

All halomethane and halobenzene compounds were obtained commercially (Eastman Organic Chemicals, Aldrich Chenical, J.T. Baker Chemical, K & K Laboratories, and Fisher Scientific) and were used without further purification, except for carbon tetrachloride which was distilled under nitrogen at atmoshperic pressure.

The purification procedure employed for phenol red and other sulfonephthalein indicators has been described previously (84).

Phenolsulfonephthalein (phenol red) was obtained from Aldrich Chemical Co., Inc. and from the stockroom (Allied Chemical). 3',3",5',5"-tetra-bromo-m-cresolsulfonephthalein (bromocresol green), 5',5"-dibromo-o-cresolsulfonephthalein (bromocresol purple), o-cresolsulfonephthalein

(cresol red), and 3',3"-dibromo-5',5"-dichlorophenolsulfonephthalein (bromochlorophenol blue) were obtained from Aldrich Chemical Co., Inc. Meta-cresolsulfonephthalein (cresol purple), thymolsulfonephthalein (thymol blue), 3',3"-dibromothymolsulfonephthalein (bromothymol blue), 3',3"-dichlorophenolsulfonephthalein (bromophenol red), 3',3"-dichlorophenolsulfonephthalein (chlorophenol red), 3',3",5',5"-tetrabromophenolsulfonephthalein (bromophenol blue), and 3',3",5',5"-tetrachlorophenolsulfonephthalein (chlorophenol blue) were obtained from Matheson Coleman & Bell.

Gelatin used in these studies was purified calfskin (Eastman red label). Triton X-100 was obtained from LaPine Scientific.

Ti(III) solutions were made by dilution with 0.10 \underline{M} HCl of a commercially-available (Matheson Coleman & Bell) 20 % titanium (III) chloride solution. V(II) solutions were prepared by dissolving vanadyl sulfate in 0.10 \underline{M} HCl, reducing this solution with amalgamated zinc, and then diluting with 0.10 \underline{M} HCl to the desired concentration. The amalgamated zinc (8-30 mesh) was obtained from Fisher Scientific Co.

III EI

NO

1

methar.

was br

Potent

carben

synthe

to bas

Presen

iechri

tures Ated i

employ

ketere:

tetrac

ierrir.

Sich al

je ver

3 101 B

The to

:5%[0]

797

III ELECTROCHEMICAL REDUCTION OF CARBON TETRACHLORIDE IN NONAQUEOUS SOLUTIONS

The work of Wawzonek and Duty on the reduction of several halomethanes in acetonitrile (AN) and N.N-dimethylformamide (DMF), which was briefly summarized above, suggested the intermediacy of dichlorocarbene during electrolytic reduction of carbon tetrachloride. One potentially significant aspect of this report is that electrolytic carbene generation possesses several advantages over any other single synthetic procedure for producing carbenes. For example, as opposed to basic hydrolysis techniques, base sensitive substrates could be present in the generative solutions. Also, as opposed to thermolysis techniques, syntheses could be carried out at relatively low temperatures so that thermally sensitive or labile substrates could be tolerated in the generative solutions. Moreover, as opposed to techniques employing more exotic compounds (diazo compounds, diazirines, and ketenes) as carbene precursors, the starting material could be a safely handled, readily available, and inexpensive compound such as carbon tetrachloride. Furthermore, syntheses could be conducted without interferring side reactions from products of the carbene generative reaction, such as the alcohol produced in the basic haloform hydrolysis technique. In addition, the potential of the reducing agent (the electrode) can be very carefully controlled, thereby minimizing possible side reactions, such as further reductions of carbene products which may be reduced by alkali metals. Finally, the possibility of direct detection of carbenes with the aid of modern rapid-response electrochemical techniques is of obvious signifance.

Hence, experiments involving reduction of carbon tetrachloride in

nonaqueous solvents have been performed by several workers in this laboratory over the past several years. For example, prior to initiation of this thesis research, Lundquist and Nicholson (85) studied the reduction of carbon tetrachloride in tetrahydrofuran (THF); the most salient features of their research are included here because they complement this thesis research, and because they have not been published elsewhere. In addition, a brief discussion of dihalocarbene chemistry also is incorporated in this chapter to provide a foundation for following discussions of electrochemical studies on carbon tetrachloride reduction. Hence, the remainder of this chapter is divided into the following sections: (A) Some Aspects of Dihalocarbene Chemistry; (B) Previous Studies on Electrochemical Reduction of Carbon Tetrachloride in Nonaqueous Solutions; and (C) Electrochemical Reduction of Halomethanes in Nonaqueous Solutions.

A Some Aspects of Dihalocarbene Chemistry

A great deal is now known about the chemistry of carbenes; most of this knowledge has been gained over the last two decades, and has been summarized in a number of excellent reviews (86-91). Briefly, a carbene is a neutral divalent carbon species in which the carbon atom has two of its four electrons in nonbonding orbitals with the remaining two electrons forming covalent bonds. Two possibilities exist for the electronic state of a carbene, depending on the relative configuration of the nonbonding electrons of the carbon atom. These electrons may occupy either a single orbital with paired spins (singlet quantum state) or they may have unpaired spins and occupy separate orbitals (triplet quantum state). A carbene in the singlet state exhibits the properties of an electron-deficient species since electrons occupy

only three of the four atomic orbitals of the carbon atom. Hence, the electrophilic character of carbenes is usually a dominant feature. However, the presence of a nonbonded pair of electrons on the carbon atom of singlet state carbenes leads to a different reactivity pattern than for other electrophilic species such as carbonium ions. Triplet carbenes generally behave as diradicals by virture of the two unpaired electrons of the carbon atom.

Dihalocarbenes are very reactive species, but are far less energetic than the simplest carbene, methylene (: CH_2). This reduced reactivity of dihalocarbenes is usually explained on the basis of ground state stabilization of dihalocarbenes by lone pairs of electrons of the halogens interacting with the empty \underline{p} orbital of the carbon atom. The importance of these interactions is of the order of $F >> \mathrm{Cl} > \mathrm{Br} > \mathrm{I}$. Hence, chlorofluorocarbene (: CCl_2), and so on.

Modern dihalocarbene chemistry began with the work of Hine and coworkers (92-97) when they elucidated the basic hydrolysis mechanism of chloroform, and demonstrated that trichloromethide ion and dichlorocarbene are both intermediates in the hydrolysis reaction. Dichlorocarbene was shown to be formed from the decomposition of trichloromethide ion in the rate-determining step of the hydrolysis;

CCl₃ → :CCl₂ + Cl⁻. In addition, these workers showed that the presence of perchlorate, nitrate, and fluoride ions does not affect the hydrolysis rate of chloroform. However, they demonstrated that the hydrolysis rate is decreased by addition of iodide, bromide, or chloride ion. Iodide ion decreases the hydrolysis rate to the greatest extent, chloride to the least extent, and bromide ion exhibits an intermediate

effe

back

of h

Heno

£1110.

that iroly

trika

of ha

1,2-1

nonnu

έε ε<u>:</u>

tase (

Jamely

iin c

tie di

techni O

ote or

rique.

alkox:

Obtaine

ict res

4

effect. This decreased rate is attributed to an acceleration of the back reaction: $X^- + :CCl_2 \to CCl_2 X^-$.

Hine and coworkers also determined that the relative ease of loss of halide ion in the rate-determining step is in the order ${\rm Br} \approx {\rm I} > {\rm Cl} >> {\rm F}$. Hence, basic hydrolysis of dibromofluoromethane (CHBr₂F) yields bromofluorocarbene (:CBrF), and so on. In addition, these workers found that CHXF₂ haloforms undergo a concerted HX elimination on basic hydrolysis so that difluorocarbene (:CF₂) is generated directly without trihalomethide ion intermediacy.

Successful generation of dihalocarbenes <u>via</u> the basic hydrolysis of haloforms has been found generally to require the use of aprotic and nonnucleophilic solvents such as benzene, toluene, tetrahydrofuran, 1,2-dimethoxyethane, etc. In addition, the use of a strong base which is also a poor nucleophile is required, potassium <u>t</u>-butoxide being the base of choice. This generation technique has been widely used in organic synthesis in spite of possessing several important disadvantages. Namely, only moderate yields are generally obtained because of formation of t-butyl alcohol from <u>t</u>-butoxide (the alcohol then reacts with the dihalocarbene). Moreover, the use of alkoxides restricts this technique to substrates which are not sensitive to strong bases.

Other sources of trihalomethide ions have been found which avoid one or both of the disadvantages of the basic haloform hydrolysis technique. For example, trichloromethide ion is formed by reaction of alkoxides with ethyl trichloroacetate. Carbene adducts are sometimes obtained in better yields with this technique because the reaction does not result in alcohol production as a by-product.

Another technique for dihalocarbene generation involves the

thermolysis of trihaloacetate salts. As with the above two techniques, dihalocarbenes are generated <u>via</u> decomposition of trihalomethide ions. However, as opposed to the above two techniques, this method can be used for synthesis in the presence of base sensitive substances.

Still another dihalocarbene generative method proceeds $\underline{\text{via}}$ thermally induced α -elimination reactions. For example, thermolysis of phenylbromodichloromethyl mercury (PhCBrCl₂Hg) yields dichlorocarbene and phenylbromo mercury (PhHgBr).

Carbene generation has also been carried out using a wide variety of other techniques. For example, the photolysis or thermolysis of diazo compounds results in the loss of a stable molecule, nitrogen, and provides a common route to carbenes. Formation of carbenes by this method is believed to be quite general when reactions are conducted in aprotic solutions. Photolysis of substituted diazirines, the cyclic isomers of diazo compounds, also results in loss of nitrogen and generates carbenes. This procedure is now a well established carbene generation technique, and is somewhat better than the use of equivalent diazo isomers because the diazirines tend to be somewhat less hazardous than the corresponding diazo compounds. Halodiazirines have been used to generate halocarbenes. Ketenes have also been used as carbene precursors. This reaction, as with the above two techniques, involves the loss of a stable molecule which in this case is carbon monoxide. The carbene generative procedures that have been mentioned here constitute most of the common generative methods. Other techniques, such as pyrolysis of chloroform or carbon tetrachloride at 1500°C, are generally not very amenable to widespread synthetic

applications.

Carbene intermediacy is generally postulated on the basis of product analysis, and it is now generally thought that in some cases free carbenes are not involved in the reactions. Moreover, some generative procedures are more likely to result in free carbenes than others. Comparative precursor techniques are sometimes used to indicate whether or not a free carbene is involved in a given reaction, and identical product chemistry is taken as presumptive evidence for free carbene intermediacy. For example, conparative precursor experiments have shown that the intermediate generated by the thermolysis of phenylbromodichloromethyl mercury and the sodium salt of trichloroacetic acid result in identical product chemistry, and both of these methods are thought to yield free dichlorocarbene.

The reaction of alkyl lithium compounds with carbon tetrahalides in the presence of olefins results in dihalocyclopropanes. Alkyl lithium compounds are thought first to undergo lithium-halogen exchange with carbon tetrahalides so that α-halolithium complexes are formed, which subsequently lose lithium halide in forming cyclopropanes with olefins. A question remains as to whether α-halolithium complexes react directly with olefins, or first lose lithium halides so that free carbenes react with the olefins. However, it is now generally thought that α-halolithiums, and not free dihalocarbenes, are the actual intermediates. Exact structures of such carbeneoid complexes are unknown, and all that can be said is that lithium halides are apparently associated with the transition state entities during the formation of dihalocyclopropanes. For example, in a recent review article on carbeneoid complexes, Köbrich (88) stated the following:

"The formation of dichlorocyclopropanes from trichloromethyl lithium and olefins is more complex than was originally thought. The trichloromethyl lithium produced from bromotrichloromethane in diethyl ether undergoes several secondary reactions even at temperatures below -100°C. It is therefore difficult to decide whether the formation of 7,7-dichloronorcarane observed under these conditions with cyclohexene is due to a reaction of trichloromethyl lithium itself or of an initially formed cleavage product. Trichloromethyl lithium is stable in tetrahydrofuran at -100°C, but it is also inert towards cyclohexene under these conditions. However, its slow decomposition in this solvent at -72°C is accelerated by cyclohexene and other olefins. Moreover, the difference between the amount of decomposition with and without cyclohexene roughly corresponds to the yield of 7,7-dichloronorcarane. In view of these results it is probable that trichloromethyl lithium can react with olefins without first decomposing to dichlorocarbene, and that this cyclopropane formation competes successfully with other reactions of the carbeneoid."

The principal reaction of dihalocarbenes with olefins is addition to form dihalocyclopropanes. Moss (98) has stated the following about this reaction: "The relative rates of addition of dihalocarbenes to olefinic carbon bonds usually increases with increasing alkyl substitution at the olefinic group since carbenes are predominantly electrophilic in nature. However, it has also been shown that steric hindrance is an important factor in controlling the rate of dihalocarbene addition to even the most simple olefins. Adverse steric factors presumably cut down the rate enhancements obtainable by alkylation of the olefinic carbon bonds."

Dich

iety of a

can inser

base. Mon

silicon-h;

Furthermor

with dichi

rediates.

adis acros

across the

In es

this speci

iepend on

cial facto

tion of tr

or perchlo:

iodile, bro

tele genere

the trichlo

isrutating

Were not su

With the so

rests shoul

electrolyti

Dichlorocarbene is so reactive that it also undergoes a wide variety of addition and insertion reactions. For example, dichlorocarbene can insert into some carbon-hydrogen bonds, in the absence of strong base. Moreover, dichlorocarbene insertions into carbon-mercury, silicon-hydrogen, and silicon-carbon bonds have also been reported. Furthermore, secondary and tertiary amines have been shown to react with dichlorocarbene, giving amides on acid hydrolysis of the intermediates. In addition, it has been reported that dichlorocarbene adds across the nitrile bond of trifluoromethyl cyanide, and adds across the carbonyl bond of hexafluorodimethyl ketone.

In essence, then, the literature on dichlorocarbene indicates that this species is so highly reactive that successful generative procedures depend on a variety of factors. Thus, there appear to be several crucial factors for successful dichlorocarbene generation via decomposition of trichloromethide ions. First, the presence of fluoride, nitrate, or perchlorate ion would have little or no effect, but the presence of iodide, bromide, or chloride ion would retard the rate of dichlorocarbene generation. Second, if the solvent were not sufficiently aprotic, the trichloromethide ions would react to form chloroform instead of dismutating to dichlorocarbene and chloride ion. Third, if the solvent were not sufficiently nonnucleophilic, dichlorocarbene might well react with the solvent. Hence, choices of supporting electrolytes and solvents should be crucial in any attempt to generate dichlorocarbene by electrolytic reduction of carbon tetrachloride.

B <u>Previous Studies on Electrochemical Reduction of Carbon</u> Tetrachloride in Nonaqueous Solutions

Wawzonek and Duty (56) may have proposed an essentially correct electrolysis mechanism for carbon tetrachloride reduction based on inconclusive analytical data. Therefore, Lundquist and Nicholson (85) reduced carbon tetrachloride electrolytically in THF (a commonly used solvent for carbene generative procedures) using lithium perchlorate as the supporting electrolyte to determine whether dichlorocarbene could be produced under such conditions. The remainder of this section summarizes this work.

All electrolyses were performed in a cell of conventional design (see Figure 7) in which the anode compartment was separated from the cathode compartment by a fine porosity glass frit. The cathode was a mercury pool for macroscale electrolyses, and, of course, a dropping mercury electrode (DME) for polarographic electrolyses. The anode was a spool of platinum wire. The reference electrode was a saturated calomel electrode (sce) with a flowing junction compartment between the sce and the electrolysis solution.

All electrolyses were performed with the aid of an electronic three-electrode potentiostat, so that precise control of the potential of the working electrode could be maintained even in solutions of very high resistance such as THF. Macroscale electrolyses were performed in THF, however, the anode compartment always contained AN because oxidation of THF resulted in rapid formation of tar. The supporting electrolyte was 1.0 M lithium perchlorate.

Macroscale electrolyses of carbon tetrachloride were performed in the presence of a 5 fold molar excess of both cyclohexene and

1-5

The

wor:

graj

This

redu

bicy Thus

Ges (

sever

poner

samp]

bieye

001<u>1</u>e

Spect

ļ

Washir

lithiu

in see

Was est

irst i

jograph

Pú

Piblishe Thermal

cereties

1-methylcyclohexene (neither of these olefins are reducible in THF).

These electrolyses were conducted by setting the potential of the working electrode at -1.40 V vs sce, which corresponds to the polarographic limiting current for reduction of carbon tetrachloride in THF.

This potential is considerably anodic of the half-wave potentials for reduction of 7,7-dichlorobicyclo[4.1.0]heptane and 1-methyl-7,7-dichlorobicyclo[4.1.0]heptane which are reduced at about -2.7 V vs sce in THF.

Thus, reduction of neither of these dichloronorcaranes could take place.

Gas chromatographic analysis with two different columns operated at several different temperatures indicated two well resolved major components with retention times always identical with those of authentic samples of 7,7-dichlorobicyclo[4.1.0]heptane and 1-methyl-7,7-dichlorobicyclo[4.1.0]heptane. These two gas chromatographic fractions were collected, and their IR and NMR spectra were identical in every respect with those of authentic samples of these dichloronorcaranes.

All macroscale electrolyses solutions were analyzed after first washing the contents of the cathode compartment with water to remove lithium perchlorate. After this step, solutions were directly analyzed by gas chromatography. By similar treatment of standard solutions, it was established that none of the dichloronorcaranes was lost in this water washing step. To obtain IR spectra, the dichloronorcaranes were first isolated by vacuum distillation, and then purified by gas chromatography.

Pure samples of dichloronorcaranes were prepared according to published procedures, (99) wherein dichlorocarbene is generated by thermal decarboxylation of sodium trichloroacetate. The dichloronorcaranes were all characterized by boiling point, IR spectra, and NMR

spect

chlor

the A

pound

this :

the in

relati

interm

that t

ate to

Welch.

the val

IF in

l-Tethy

Fublish

electro

of an i

as a lit

 I_{n}

distion

ce trich

Furtherm

carbon te

itaraqeni

spectra. In addition, for comparative purposes, a sample of 7,7-di-chlorobicyclo[4.1.0]heptane (7,7-dichloronorcarane) was purchased from the Aldrich Chemical Company (Milwaukee, Wis.). This commercial compound was identical in every respect with the compound prepared in this laboratory.

These macroscale electrolysis experiments were also conducted with the intention of using the method of competing reactions to determine relative rate constants of addition of the electrochemically generated intermediates to cyclohexene and 1-methylcyclohexene. It was found that the rate of addition of the electrochemically generated intermediate to 1-methylcyclohexene was about 10 times the rate of addition to cyclohexene. This ratio of relative rate constants (1:10) agrees with the value obtained for the reaction of chloroform and lithium metal in THF in the presence of a 5 fold molar excess of both cyclohexene and 1-methylcyclohexene. This ratio is also in fairly good agreement with published values (about 8:1) (99). Therefore, it was concluded that electrolysis of carbon tetrachloride in THF had resulted in formation of an intermediate which was either dichlorocarbene or a species such as a lithium-carbeneoid complex that gave dichlorocarbene-like products.

In summary, this work demonstrated that controlled potential reduction of carbon tetrachloride in THF must lead to initial generation of trichloromethide ion, and, possibly even to free dichlorocarbene.

Furthermore, this work indicates that controlled potential reduction of carbon tetrachloride in THF may be a very useful synthetic route to preparation of substances such as dichloronorcaranes.

reported :

used as th

electroche marsing t

Unior

aboratory

ity (see I polarograph

in Dur, the

optosed to .

iustion wave tetrachlorid

tertor of thi

C <u>Electrochemical Reduction of Halomethanes in Nonaqueous</u> Solutions

With the exception of macroscale electrolyses in AN, the work of Wawzonek and Duty (56) consisted of conventional polarography in AN and DMF. Hence, prior to applying more modern electrochemical techniques to the study of halomethane reductions, conventional polarographic experiments were performed in these two solvents in an attempt to duplicate the data reported by these authors.

All electrochemical experiments performed in this thesis study on halomethane reductions in AN and DMF were conducted with the aid of a vacuum line apparatus, described above, to obtain the driest conditions possible. In addition, tetrabutylammonium perchlorate (TBAP) was employed as the supporting electrolyte except, when experiments were conducted in an attempt to rigorously duplicate the solution conditions reported by Wawzonek and Duty, tetrabutylammonium bromide (TBABr) was used as the supporting electrolyte. However, no differences in the electrochemical behavior of any of the halomethanes were observed by changing the supporting electrolyte from TBAP to TBABr.

Unfortunately, the polarographic experiments performed in this laboratory in DMF differed grossly from those reported by Wawzonek and Duty (see Table I for the data of these authors). Specifically, three polarographic waves were obtained for reduction of carbon tetrachloride in DMF, the same number of waves reported by Wawzonek and Duty, but as opposed to their results, relative limiting currents of all three reduction waves were equal within 10 %. In fact, reduction of carbon tetrachloride in DMF appeared very similar to the polarographic behavior of this compound in aqueous solutions (60). Moreover, addition

of f ing form reiu equa In a oklor this sugge both oppos. 110<u>11</u>0 tetrac Wiere cur, 1 and pos are thr Siver i gi ffere shown in ietrach. The ėramatie Pater. itree wel When a sm

of from 1 % to 10 % water had no significant effect on either limiting currents or half-wave potentials. Furthermore, addition of chloroform and methylene chloride demonstrated that the second and third
reduction waves for carbon tetrachloride in DMF occurred at exactly
equal potentials for chloroform and methylene chloride, respectively.
In addition, coulometry on the first reduction wave for carbon tetrachloride in DMF gave an n-value of 2.0, the same value reported for
this compound in aqueous solutions (61). Hence, these data strongly
suggest conventional stepwise reduction of carbon tetrachloride in DMF
both in the presence and absence of added proton donors. Thus, as
opposed to the report of Wawzonek and Duty, these data suggest that no
dichlorocarbene is generated by the electrolytic reduction of carbon
tetrachloride in DMF.

Conventional polarographic experiments were also performed in AN where reduction of carbon tetrachloride resulted in three, or possibly four, waves. All these reduction waves except the last were drawn out and poorly defined so that it is difficult to determine whether there are three or four waves present. A polarogram showing this behavior is given in Figure 10. The morphology of these waves is dramatically different from that described by Wawzonek and Duty, who reported, as shown in Table I, two polarographic waves of equal height for carbon tetrachloride in AN.

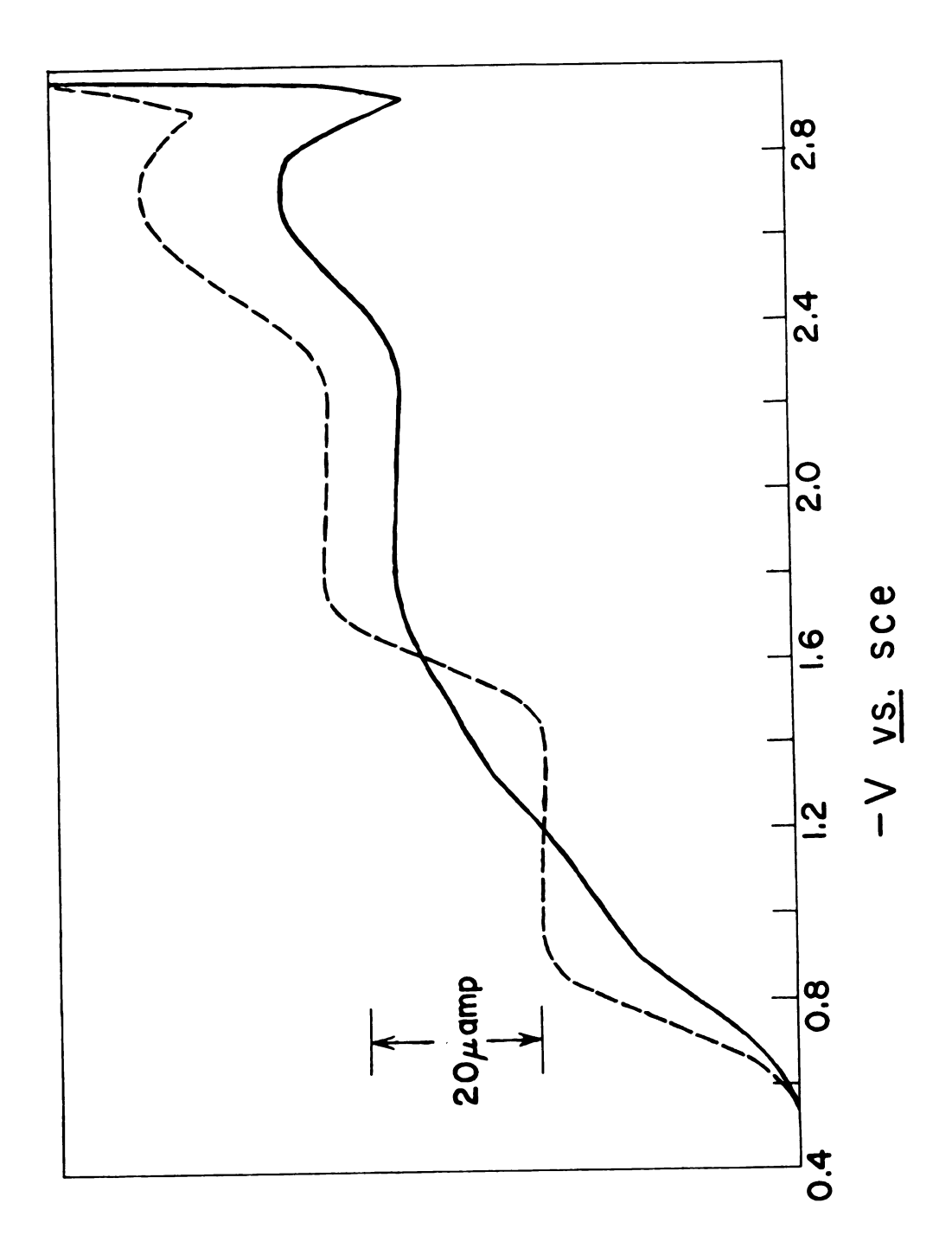
The polarographic behavior of carbon tetrachloride in AN was dramatically affected by additions of small amounts (about 1%) of water. This behavior is also depicted in Figure 10. Specifically, three well defined waves were obtained for carbon tetrachloride in AN when a small amount of water was added. Additions of chloroform and

Polarogram of 1.5 $\underline{mM}^{a,b}\text{CCl}_{l_1}$ in acetonitrile with 0.10 \underline{M} tetrabutylammonium perchlorate as supporting electrolyte. Figure 10.

(----) no water added

(----) 1% water added

amercury column height = 60 cm. $b_m 2/3 t^{1/6} = 1.1 t$



meth seco of c of o effe Fres step of o ident iefin the a of car Proton mi Di chlori somethi Eerce, obloria. eathodic nititic tat the tion Were

+ 3

tively.

Bents, cy

Moride i

methylene chloride to these "wet" AN solutions demonstrated that the second and third waves for carbon tetrachloride are due to reduction of chloroform and methylene chloride, respectively. Moreover, addition of other proton donors such as phenol and benzoic acid has the same effect as adding water. Hence, polarographic reduction in AN in the presence of small amounts of proton donors results in conventional stepwise reduction for carbon tetrachloride. In other words, reduction of carbon tetrachloride under these conditions results in behavior identical to that in DMF or aqueous solutions.

Again, as seen in Figure 10, three or four rather broad and poorly defined waves are obtained for carbon tetrachloride reduction in AN in the absence of added proton donors. Hence, the polarographic behavior of carbon tetrachloride in AN both in the presence and absence of added proton donors differs greatly from the morphology reported by Wawzonek and Duty.

The poorly defined polarographic waves obtained for carbon tetrachloride in AN in the absence of added proton donors suggested that something other than conventional stepwise reduction might be occurring. Hence, cyclic voltammetric experiments were performed on carbon tetrachloride under these conditions. Surprisingly, only three irreversible cathodic peaks were observed for carbon tetrachloride in AN under these conditions. Addition of chloroform and methylene chloride demonstrated that the second and third cathodic peaks for carbon tetrachloride reduction were due to reduction of chloroform and methylene chloride, respectively. Hence, in contrast to the conventional polarographic experiments, cyclic voltammetry suggested that reduction of carbon tetrachloride in AN in the absence of added proton donors also occurs in a

conventional stepwise manner.

Sometimes a fourth irreversible cathodic peak was observed for carbon tetrachloride reduction in AN solutions. Specifically, on addition of very small amounts of water (about 0.1%), a new cathodic peak appeared at a potential midway between the reduction peaks for carbon tetrachloride and chloroform. This new peak was extremely non-reproducible, and, in fact, always vanished when the amount of added water was increased to about 1%. Furthermore, addition of other proton donors such as phenol and benzoic acid had the same effect as small incremental additions of water. This unusual and interesting behavior was not investigated in any further detail, only because it did not appear that such behavior could be related to dichlorocarbene generation.

The polarographic and cyclic voltammetric experiments conducted in this laboratory indicated that dichlorocarbene is not generated by electrolytic reduction of carbon tetrachloride in either DMF or AN. This conclusion was substantiated by conducting a macroscale electrolysis of carbon tetrachloride in AN in the presence of cyclohexene (this compound is not reducible under these conditions) with tetrabutylammonium perchlorate as the supporting electrolyte. The electrolysis was performed at a mercury pool and controlled potential of -1.0 V vs sce, which corresponds to the limiting current of the first reduction wave for carbon tetrachloride in AN. Only two polarographic waves remained following exhaustive electrolysis of the first wave. The two remaining waves corresponded to chloroform reduction ($\underline{E}_{1/2} = -1.6$ V vs sce) and methylene chloride reduction ($\underline{E}_{1/2} = -2.5$ V vs sce). No wave was observed for reduction of 7,7-dichloronorcarane ($\underline{E}_{1/2} = -2.8$ V

vs sce) implying that dichlorocarbene was not generated.

The remarkable differences between results obtained in this laboratory and the laboratory of Wawzonek and Duty probably can be attributed to some or all of the following factors. First, nonaqueous electrochemical experiments performed for this thesis research were conducted with the aid of a vacuum line apparatus which minimized water contamination. In contrast, Wawzonek and Duty used a polarographic cell which essentially consisted of a rubber-stoppered beaker which, in turn, was partially immersed in a thermostated water bath. Hence, the data of Wawzonek and Duty correspond to a far higher degree of water contamination than data reported here. In addition, electrochemical measurements performed for this thesis research were generally made using modern three-electrode instrumentation so that iR drop was compensated electronically. On the other hand, Wawzonek and Duty used two-electrode electrolysis cells so that their data must reflect effects of uncompensated resistances.

In summary, the electrochemical behavior of carbon tetrachloride in both DMF and AN was found to be completely different than reported by Wawzonek and Duty. For example, these authors reported that methylene chloride was not reducible in AN, whereas it was found in this thesis research that this compound always gives a well defined polarographic wave in AN ($E_{1/2} = -2.5 \text{ V} \text{ vs} \text{ sce}$). However, more significantly, the experiments performed in this thesis research strongly suggest that no significant amount, if any, of dichlorocarbene is generated by electrolytic reduction of carbon tetrachloride in either DMF or AN. Nongeneration of dichlorocarbene in these two solvents is probably due to the fact that trichloromethide ion, the initial electrode reduction

product of carbon tetrachloride, is protonated forming chloroform at a far greater rate than the rate at which this ion can decompose to dichlorocarbene and chloride ion. In fact, Hine and coworkers (97) have reported that the rate of protonation of trichloromethide ion is about five orders of magnitude larger than the rate of decomposition into dichlorocarbene and chloride ion. Thus, even in such relatively aprotic solvents as DMF and AN, the rate of protonation of trichloromethide ion is probably still significantly larger than the rate of decomposition of this ion.

IV. ELECTROCHEMICAL REDUCTION OF HALOBENZENE COMPOUNDS IN N.N-DIMETHYLFORMAMIDE

Wawzonek and Wagenknecht (58) proposed that dehydrobenzene is formed during electrolytic reduction of o-dibromobenzene and o-bromochlorobenzene in both DMF and AN in the presence of 0.20 M tetrabutyl-ammonium bromide as supporting electrolyte. Their work is summarized in the introduction to this thesis, and their data are reproduced in Table II. Briefly, they proposed that o-dibromobenzene undergoes an initial two-electron reduction to form the o-bromophenyl anion which, instead of being protonated to form bromobenzene, loses bromide to form dehydrobenzene. Furthermore, primarily from the fact that a single reduction wave is obtained for o-dibromobenzene, they proposed that the formal potential for reduction of dehydrobenzene is anodic of that for o-dibromobenzene so that when dehydrobenzene is formed, it is immediately reduced to benzene.

On the basis of the results of Wawzonek and Wagenknecht, several o-dihalobenzene and monohalobenzene compounds were studied, first to verify the electrolysis behavior reported by Wawzonek and Wagenknecht, and then to attempt to detect directly dehydrobenzene with the aid of cyclic voltammetry.

In general, both conventional polarography (but with a three-electrode potentiostat) and cyclic voltammetry were used, and experiments were performed with the vacuum line apparatus described earlier. The compounds studied are listed in Table III; all experiments were conducted in DMF with 0.1 $\underline{\text{M}}$ tetrabutylammonium perchlorate as supporting electrolyte.

Table III. Half-wave Potentials and Diffusion Current Constants for Halobenzene Compounds.

1.87 1.87 1) _d ~1.9	(4.8) _c
1) ~1 Q	(0.5)
-'d -1.9	(8.0) _c
2.57	(4.7) _e
7) _c	
2.79	(4.5) _c
8) _e 2.79	(9.1) _c
7) 0.70	(8.7) _c
	8) _e 2.79 7) _e 2.79

 $a_{\text{in V }\underline{\text{vs}}}$ sce $b_{\underline{I}_{\underline{d}}} = \underline{i}_{\underline{d}}/C_{\underline{o}}^{*} m^{2/3} t^{1/6}$

 $^{^{\}rm c}$ measured at -2.90 V $_{
m vs}$ sce $^{\rm d}$ measured at -1.80 $_{
m vs}$ sce

e_{measured} at -2.70 V <u>vs</u> sce

A Results

Before discussing the results of these experiments for the individual compounds, a few general remarks are appropriate. First, all of the compounds exhibited complex behavior, so that in many cases polarography served only to indicate the number of reduction steps involved. For example, polarograms for iodobenzene, o-diiodobenzene, and o-dibromobenzene exhibited maxima or prewaves which are indicative of adsorption and/or stirring phenoma (100). Unfortunately, these effects preclude any quantitative treatment of the polarographic data. However, these effects were absent or minimal for the other four compounds in Table III. The dependence of limiting current on mercury column height can be used to determine whether the reduction is diffusion controlled (100), and studies of this nature were conducted for all of the compounds except o-diiodobenzene. In every case, limiting current vs $h^{1/2}$ plots were linear, indicating that the electrode reaction is diffusion controlled. Table IV lists the potentials at which these limiting current studies were conducted.

The cyclic voltammetric data also was very complex. Most of these compounds exhibited either one or two broad cathodic waves. These waves generally exhibited decreasing values of $\frac{i}{p}/v^{1/2}$ with increasing scan rate. Moreover, peak potentials for all waves shifted cathodically with increasing scan rate. Data of this nature suggests the presence of a succeeding chemical reaction following charge transfer. The data, however, was not amenable to further analysis with any of the available theories for cyclic voltammetry because of complications such as adsorption and/or stirring phenomena. In essence,

Table IV. Potentials at which Limiting Current $\underline{vs} \ \underline{h}^{1/2}$ studies were conducted for Halobenzene Compounds.

Compound	-E ^a
chlorobenzene	2.90
o-dichlorobenzene	2.70 and 2.90
o-bromochlorobenzene	2.50 and 2.90
<u>o</u> -dibromobenzene	2.40
bromobenzene	2.90
iodobenzene	2.10

 $a_{in \ V \ \underline{vs}}$ sce

sufficient that results are presented below for each compound individually.

1. Iodobenzene

Polarograms were obtained for this compound at concentrations of 0.47, 1.13, and 1.85 $\underline{\text{mM}}$. One reduction wave, with $\underline{\text{E}}_{1/2}$ = -1.87 V $\underline{\text{vs}}$ sce, was found. Each polarogram exhibited a maximum centered at -1.95 V vs sce.

Cyclic voltammetry also was performed on this compound at concentrations of 0.47, 1.13, and 1.85 $\underline{\text{mM}}$. The scan rate was varied from 40 mV/sec to 100 V/sec. Under these conditions, a single broad cathodic wave was always found. The value of $(\underline{E}_p - \underline{E}_{p/2})$ increased with scan rate from 90 mV at the slowest scan rate to 350 mV at 100 V/sec. These peak potential shifts also depend on concentration. For example, the peak potential for the 0.47 $\underline{\text{mM}}$ solution shifted 80 mV cathodically for a 10-fold increase in scan rate, whereas, for the 1.85 $\underline{\text{mM}}$ solution, it shifted 200 mV cathodically for the same increase in scan rate. The value of $\underline{i}_p/v^{1/2}$ decreased with increasing scan rate.

2. <u>o</u>-diiodobenzene

Polarograms were obtained for this compound at concentrations of O.25, 0.50, 1.00, 1.51, and 2.08 mM. All polarograms were very complex. First, a small prewave started at about -1.4 V vs see on every Polarogram. This prewave was concentration independent, indicating strong adsorption of the electrode reaction product (100). After this prewave, a second more conventional wave appeared with $\underline{E}_{1/2} = -1.73$ V vs see. Following this, a third wave appeared which exhibited a large maximum on the first portion of the wave. This third wave and the maximum both showed small cathodic shifts with decreasing

<u>o</u>-diiodobenzene concentration. Because of the maximum, $\underline{E}_{1/2}$ for this third wave could only be estimated as -1.9 V <u>vs</u> sce. In addition, because of the prewave, $\underline{E}_{1/2}$'s and \underline{I}_d 's always were measured at the highest <u>o</u>-diiodobenzene concentration where the effect of adsorption is minimized.

A few cyclic voltammetric experiments were performed on this compound at a concentration of 0.56 mm. However, as was the case for the conventional polarograms, these current-potential curves were very complex, and were unsuitable for purposes of obtaining additional quantitative information.

3. Bromobenzene

Polarograms were obtained for this compound at concentrations of 0.39, 1.01, and 1.97 $\underline{\text{mM}}$. One reduction wave, with $\underline{\text{E}}_{1/2}$ = -2.57 V $\underline{\text{vs}}$ sce, was found. No prewaves or maxima were observed.

Cyclic voltammetry also was performed on this compound at concentrations of 0.39, 1.01, 1.97 mm. The scan rate was varied from 50 mV/sec to 40 V/sec. Under these conditions, a single broad cathodic wave was always observed. The value of $(\frac{E}{p} - \frac{E}{p/2})$ was independent of concentration, but increased with scan rate from 130 mV at the lowest scan rate to 200 mV at 40 V/sec. The peak potential shifted 150 mV cathodically for a 10-fold increase in scan rate, and was independent of concentration. The variation of $\frac{i}{p}/v^{1/2}$ with scan rate was very erratic and showed no clear trends for any of the concentrations studied.

4. <u>o</u>-dibromobenzene

Polarograms were obtained for this compound at concentrations of 0.20, 0.44, 1.00, and 1.88 $\underline{\text{mM}}$. One reduction wave, with $\underline{\text{E}}_{1/2}$ = -2.05 V sce, was found. The 0.20 $\underline{\text{mM}}$ solution exhibited no maximum, but the

other three solutions all showed a maximum centered at -2.1 V vs sce.

Cyclic voltammetry also was performed on this compound at concentrations of 0.20, 0.74, and 1.92 mM. The scan rate was varied from 75 mV/sec to 500 V/sec. Under these conditions, a single broad cathodic wave was always observed. The value of $(\frac{E}{p} - \frac{E}{p/2})$ increased with scan rate from 100 mV at the lowest scan rate to 400 mV at 500 V/sec. Peak potential shifts were also a function of concentration. For example, the peak potential for the 0.20 mM solution shifted 100 mV cathodically for a 10-fold increase in scan rate, whereas, for the 1.92 mM solution, it shifted 330 mV cathodically for the same increase in scan rate. The value of $\frac{i}{p}/v^{1/2}$ also was concentration dependent, but decreased with increasing scan rate.

5. Chlorobenzene

Polarograms were obtained for this compound at concentrations of 0.31, 0.78, and 1.68 mM. One reduction wave, with $\underline{E}_{1/2}$ = -2.79 V \underline{vs} sce, was found. No prewaves or maxima were observed.

Cyclic voltammetry also was performed on this compound at concentrations of 0.31, 0.78, and 1.68 $\underline{\text{mM}}$, with a scan rate range from 25 mV/sec to 1 V/sec. One broad cathodic wave, which began to merge with the background current at scan rates of greater than 1 V/sec, was observed. The value of $(\underline{E}_p - \underline{E}_{p/2})$ ranged from 80 to 100 mV, and increased slightly with increasing concentration. However, this value was independent of scan rate. The value of $\underline{i}_p/v^{1/2}$ was independent of concentration, and decreased with increasing scan rate.

6. <u>o</u>-dichlorobenzene

Polarograms were obtained for this compound at concentrations of 0.29, 0.56, 0.83, 1.13, 1.40, 1.66, and 1.96 $\underline{\text{mM}}$. Two reduction waves,

with $\underline{E}_{1/2}$ of -2.53 and -2.79 V \underline{vs} sce respectively, were found. No prewaves or maxima were observed. Addition of chlorobenzene to these solutions indicated that the second wave is due to chlorobenzene reduction.

Cyclic voltammetry also was performed on this compound at a concentration of 0.29 mM. The scan rate was varied from 40 mV/sec to 20 V/sec. Two broad cathodic waves were observed for scan rates below 1 V/sec, whereas only one peak was found for faster scan rates. When two peaks were observed, they both shifted cathodically with increasing scan rate. The behavior of the second wave was identical to that found for chlorobenzene itself (cf., above). The value of $(\underline{\mathbf{E}}_{\mathbf{p}} - \underline{\mathbf{E}}_{\mathbf{p}/2})$ for the first wave was 100 mV, and was independent of scan rate. The peak potential of the first wave shifted 70 mV cathodically for a 10-fold increase in scan rate. Finally, $\underline{\mathbf{i}}_{\mathbf{p}}/\mathbf{v}^{1/2}$ decreased with increasing scan rate.

7. <u>o-bromochlorobenzene</u>

Polarograms were obtained for this compound at a concentration of 0.86 mm. Two reduction waves, with $\underline{E}_{1/2}$ of -2.10 and -2.79 V vs sce respectively, were found. No prewaves or maxima were observed. Addition of chlorobenzene to this solution indicated that the second wave is due to chlorobenzene reduction.

Cyclic voltammetry also was performed on this compound at a concentration of 0.86 mM, but only a few experiments were conducted because the polarographic data indicated simple stepwise reduction.

Two broad cathodic waves were found at scan rates below 1 V/sec, whereas only one peak was observed at greater scan rates. Both peaks shifted cathodically with increasing scan rate. The behavior of the

second wave was identical to that of chlorobenzene (cf., above). The first wave was very broad, with a value of $(\frac{E}{p} - \frac{E}{p}/2)$ of 140 mV that was independent of scan rate. The peak potential of the first wave shifted 200 mV cathodically for a 10-fold increase in scan rate. Finally, $\frac{i}{p}/v^{1/2}$ decreased with increasing scan rate.

B Discussion

As indicated above, most of the compounds in Table III, especially the iodo- and bromo-substituted ones, exhibit effects of adsorption and stirring phenomena associated with maxima. Unfortunately, maximum suppressors cannot be used in nonaqueous media. Thus, the maxima could not be eliminated in the conventional manner, which makes quantitative interpretation of the majority of the data impossible.

For cyclic voltammetry, one of the effects of adsorption is that the current-potential curves are broader than in the absence of adsorption (36). Of course, other factors also can cause wave broadening. For example, it is known that electrolysis of all these compounds, except perhaps o-dibromobenzene, consists of two-electron reduction steps, with two such steps occurring for the o-dihalobenzenes. Cyclic voltammetric theory for consecutive electron transfers (30) shows that current-potential curves will appear as a concerted two-electron transfer if the formal potential for the addition of the second electron is at least 200 mV anodic of the formal potential for the addition of the first electron. However, if the formal potential for the second electron transfer is within 100 mV of the formal potential for the first electron transfer, then the current-potential curves will be broadened. Thus, this also may be a factor in observed broadening

of the waves for compounds in Table III. Unfortunately, there is no way to separate unequivocally the various wave-broadening effects.

Nevertheless, for several of the compounds studied here, the data strongly suggest that both of the factors just described are operative.

In broad terms, the results described above are consistent with the polarographic data reported by Wawzonek and Wagenknecht (58). For example, the data demonstrate that o-dibromobenzene reduction in DMF does constitute an anomoly with respect to the reduction of compounds such as o-dichlorobenzene and o-diiodobenzene in this solvent. Although no coulometric studies were performed in either of the studies to determine n-values, the diffusion current constant, \underline{I}_d , for o-dibromobenzene indicates that reduction of this compound in DMF takes place by an overall four-electron process. Nevertheless, this fact neither proves nor disproves that dehydrobenzene is involved as an intermediate during the electrolysis of o-dibromobenzene.

As previously discussed, Wawzonek and Wagenknecht proposed that dehydrobenzene is generated by the decomposition of o-bromophenyl anion, implying that the rate of decomposition is much greater than the rate of protonation to form bromobenzene.

Also, it has been shown that the decomposition is reversible (101), an aspect that Wawzonek and Wagenknecht apparently did not consider. This could be an important point, since these authors conducted their experiments in the presence of 0.20 M bromide ion. Interestingly, this factor apparently is not very significant, since

the use of a perchlorate salt in the work described here resulted in, for most of the compounds studied, essentially the same polarographic behavior as reported by Wawzonek and Wagenknecht.

The electrolysis mechanism proposed by Wawzonek and Wagenknecht for the reduction of o-dibromobenzene seems implausible for several reasons. Specifically, even if the electrogenerated o-bromophenyl anion does undergo significant decomposition to dehydrobenzene in DMF, there are significant reasons for doubting whether dehydrobenzene is subsequently reduced at a formal potential anodic of or very close to that for o-dibromobenzene. For example, it is known that the formal potential for reduction of benzene is so cathodic that it lies beyond the decomposition potential of most supporting electrolytes and/or solvents that have been used. In fact, approximate molecular orbital calculations indicate that the formal potential for the reduction of benzene is about -3.5 V vs sce in solvents such as DMF (102). Furthermore, it is known that activated acetylenes (eg., diphenylacetylene) are reduced at slightly more negative potentials than their olefinic counterparts (eg., diphenylethylene). In view of these facts, the formal potential for the reduction of dehydrobenzene should be close to that of benzene. Hence, if dehydrobenzene is generated during the electrolysis of o-dibromobenzene, some other mechanism would seem to be necessary to account for the enhanced diffusion current constant.

When dehydrobenzene is generated by the decomposition of o-bromo-phenyl anion in the absence of competing substrates, the following reaction is known to proceed (103).

Nevertheless, this reaction was not considered by Wawzonek and Wagenknecht. Clearly, generation and subsequent reduction of bromobiphenyl and homologous compounds would constitute a more plausible explanation than dehydrobenzene reduction for the increased diffusion current constant observed for o-dibromobenzene. In addition, Wawzonek and Wagenknecht reported that in the absence of furan, reduction of o-dibromobenzene led to fluorescent products which they could neither identify nor explain. A mechanism involving the generation and subsequent reduction of bromobiphenyl and higher homologs does, however, account for the formation of fluorescent products.

Wawzonek and Wagenknecht did not report any experiments on the reduction of either o-diiodobenzene or o-dichlorobenzene. The data in Table III show that these two compounds, unlike o-dibromobenzene, undergo electrolysis in DMF in a conventional stepwise manner. For example, during the first polarographic wave, o-dichlorobenzene is reduced to chlorobenzene which, in turn, is reduced to benzene during the second reduction wave. Hence, both the o-chlorophenyl anion and the o-iodophenyl anion must be protonated to form the respective halobenzenes at a much faster rate than the rate at which either of these o-halophenyl anions can decompose to dehydrobenzene in DMF. Furthermore, the data show that o-bromochlorobenzene is reduced to the o-chlorophenyl anion which is protonated to form chlorobenzene, without

formation of dehydrobenzene.

In summary, these experiments substantiated the polarographic data reported by Wawzonek and Wagenknecht for the electrolytic reduction of o-dibromobenzene in DMF. However, there is a more plausible explanation for the enhanced current for this compound than the mechanism proposed by these authors. In addition, as opposed to the report of Wawzonek and Wagenknecht, these experiments indicated that the electrolytic reduction of o-bromochlorobenzene in DMF occurs in a conventional stepwise manner. In other words, the electrolytic reduction of o-bromochlorobenzene is analogous to that of o-dichlorobenzene since the initial electrode reduction product of both of these compounds is o-chlorophenyl anion, which is protonated forming chlorobenzene at a far greater rate than the rate at which this ion can decompose to dehydrobenzene and chloride ion. The fact that electrolytic reduction of o-bromochlorobenzene and o-dichlorobenzene in DMF results in chlorobenzene formation during the first polarographic wave is not very surprising, since, even in liquid ammonia (a more basic solvent than DMF), o-chlorophenyl anion is protonated 1.5 times faster than it looses chloride ion (104). Moreover, the fact that these two compounds exhibit behavior different from that of o-dibromobenzene is reasonable since it is known that the rates of loss of halides from o-halophenyl anions is in the order Br > Cl > F (104). Thus, this study showed that, except for o-dibromobenzene, the electrolysis of o-dihalobenzene compounds in DMF generally results in conventional stepwise reduction because the initial electrode reduction products (i.e., the o-halophenyl anions) are protonated at a faster rate than the rate at which these ions can decompose to dehydrobenzene.

V. REDUCTION OF SULFONEPHTHALEIN ACID-BASE INDICATORS

The work of Senne and Marple (59) on the reduction of phenol red, which was briefly summarized above, suggested that free radicals of moderate stability are produced in aqueous solutions. Hence, compounds such as phenol red provide an attractive system for the evaluation of the usefulness of electrochemical relaxation techniques for studying reactive intermediates, since the experiments can be conducted with aqueous solutions. Thus, cyclic voltammetry can be subjected to experimental evaluation without the complications that accompany non-aqueous electrochemical studies.

A Compounds Investigated

The compounds that are reduced according to the disproportionation mechanism are given in Table V. Although phenol red and cresol purple were studied most extensively, each of the nine compounds for which a rate constant is given was investigated in sufficient detail to confirm the mechanism. Moreover, the same mechanism appears to apply to chlorophenol blue even though the rate constant for this compound was too large to measure with cyclic voltammetry. Thus, although most subsequent discussions will pertain to phenol red and cresol purple, except for quantitative differences in thermodynamic and kinetic data, the discussions are applicable to all of the compounds listed in Table V. In addition to these ten compounds, bromophenol blue and bromochlorophenol blue were also investigated. These studies showed that the reduction mechanism for these two compounds is more complicated than for the compounds listed in Table V. The behavior of these two compounds was not, however, studied in sufficient detail to determine

Table V. Half-wave Potentials and Disproportionation Rate Constants for Sulfonephthalein Indicator Radicals.

Compound	pН ^с	- <u>E</u> _{1/2} V <u>vs</u> sce	Rate Constant, \underline{M}^{-1} - \sec^{-1}
cresol purple	4.8	0.56	1.8 ₇ x 10 ¹
thymol blue	4.8	0.66	3.2 ₅ x 10 ¹
bromothymol blue	4.8	0.61	$6.6_7 \times 10^1$
bromocresol green	2.5	0.38	$6.9_1 \times 10^1$
phenol red	2.5	0.47	1.6 ₂ x 10 ²
phenol red	4.8	0.60	1.6 ₅ x 10 ²
phenol red	6.8	0.72	1.6 ₄ x 10 ²
cresol red	4.8	0.65	6.6 ₂ x 10 ²
bromophenol red	2.5	0.46	$1.0_{1} \times 10^{3}$
chlorophenol red	2.5	0.40	1.0 ₆ x 10 ³
bromocresol purple	4.8	0.64	2.0 x 10 ⁵
chlorophenol blue	2.5	(0.32) ^e	

a 25% (by weight) methanol-water.

b Cyclic voltammetric data for these compounds are given in Tables VIII-XXXVII.

c 0.10 M total citrate buffer.

d First eight rate constants are within \pm 10% of stated values, and \underline{k} for bromocresol purple is within \pm 20% of stated value.

^e Apparent $\underline{E}_{1/2}$ since \underline{k} is too large to measure.

the actual mechanism of reduction.

B Mechanism

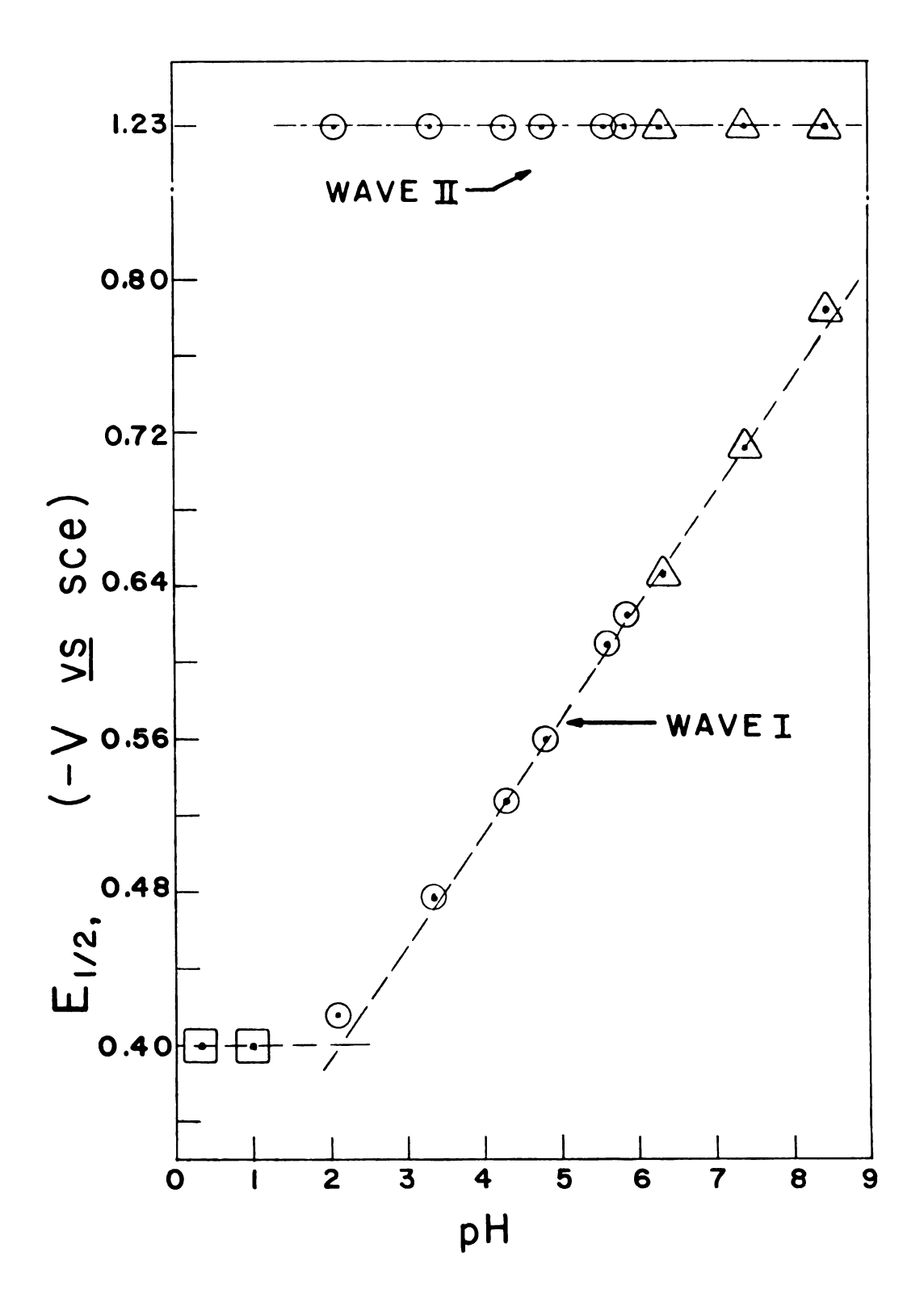
According to Bates (105), sulfonephthalein indicators are represented structurally as hybrid ions containing a central carbonium ion and a negative charge on the sulfonate group with color changes resulting from successive dissociations of the phenol groups. Thus, probable structures of the three indicator forms of cresol purple are

The color transformation intervals of cresol purple occur in the pH ranges of 1.2 to 2.8 (red to yellow) and 7.4 to 9.0 (yellow to purple) (105). Hence, form I is the predominant species in solution below pH 1.2, and so on.

Polarograms were obtained for cresol purple at ten pH's over a range from 0.3 to 7.4. Two reduction waves of equal height were obtained at each pH. The $\underline{E}_{1/2}$ \underline{vs} pH behavior of both waves is shown in Figure 11. Below pH 1.2, $\underline{E}_{1/2}$ of the first wave is pH-independent and equals -0.40 V \underline{vs} sce. Form I is the predominant species in solution in this pH region, and the polarographic data indicate that this form

Figure 11. $\underline{E}_{1/2}$ vs pH behavior of Cresol purple. a,b,c,d

- HCl solutions.
- Citrate buffer solutions.
- A Phosphate buffer solutions.
- a All solutions approximately 10% methanol-water.
- ^b $C_O^* \simeq 1.0 \text{ } \underline{\text{mM}} \text{ at each pH.}$
- $^{\rm c}$ Wave II is masked by hydrogen discharge below pH \simeq 2.
- ^d In pH region 2 to 8, $\underline{E}_{1/2}$ of Wave I shifts 59 mV cathodically with increase in unit pH.



is reduced directly under these conditions.

HO

$$CH_3$$
 CH_3
 CH_3

However, in the pH region 2.8 to 7.4, $\underline{E}_{1/2}$ of the first wave shifts 59 mV cathodically per unit increase in pH. Form Ia is the predominant species in solution in this pH region, and the polarographic data indicate that one proton is consumed in reducing species Ia to II. Hence, in this pH region, the stoichiometry for the first wave is

$$HO \longrightarrow CH_3 \longrightarrow CH_3 \longrightarrow HO \longrightarrow CH_3 \longrightarrow CH_3$$

The fact that the limiting current of the first reduction wave is

pH-independent, and that $\underline{E}_{1/2}$ shifts in the manner described above, indicates that the proton-transfer chemical equilibrium between species I and Ia is rapidly established. Moreover, it is known that undissociated forms of organic acids are generally reduced anodic of the dissociated forms (106). Hence, these data indicate, but do not prove, that, in the region where species Ia predominates in solution, species I is the form of the indicator undergoing reduction. Thus, the probable reduction mechanism, which is essentially the one cited by Senne and Marple, is

HO

$$CH_3$$
 CH_3
 CH_3

HO

$$CH_3$$
 CH_3
 CH_3

HO
$$\begin{array}{c}
CH_3 \\
CH_3
\end{array}
+ H^+$$

$$\begin{array}{c}
CH_3 \\
CH_3
\end{array}$$

$$\begin{array}{c}
CH_3$$

$$CH_3$$

C Polarography

The polarographic behavior of the compounds listed in Table V is similar to that reported by Senne and Marple (59) for phenol red and thymol blue. Two reduction waves are generally observed; for the most stable radicals the first reduction wave is reversible, but becomes progressively less so as the rate of Reaction 3c increases. The second reduction wave is always irreversible. The height of the first wave varies from apparently one electron for cresol purple to two electrons for chlorophenol blue, with the other eight compounds in

Table V having intermediate apparent <u>n</u>-values. In each case the first wave corresponds to Reaction 3a with enhancement from Reaction 3c for those compounds where Reaction 3c is rapid on the polarographic time scale. The second wave corresponds to Reaction 3b, and is always irreversible because of reaction 3d. Because of these kinetic complications, half-wave potentials for either wave are not directly of thermodynamic significance. The exception is those compounds, such as cresol purple, for which Reaction 3c is sufficiently slow on the polarographic time scale that the first wave is unperturbed.

It might be argued that Reaction 3c should be reversible, and indeed lie to the left. Of course, a thermodynamic analysis using half-wave potentials for these two waves would lead to this conclusion. However, such an analysis is not valid because the second wave is irreversible. In fact, the polarographic results, as well as all the other data presented below, suggest the reaction sequence as written. Reaction 3c is the rate-determining step in the disproportionation reaction, and is essentially irreversible because Reaction 3d is very rapid.

D Controlled Potential Reduction

Controlled potential electrolysis of the compounds in Table V on either the first or second reduction wave leads to the sulfonephthalin, IV. For cresol purple, thymol blue, bromothymol blue, and bromocresol green the corresponding radical, II, is sufficiently stable that a conventional polarographic wave is observed for II following controlled potential reduction on the first wave.

Figure 12 depicts the overall polarographic behavior at various

Figure 12. Polarographic waves for the controlled potential electrolysis of a sulfonephthalein indicator that is reduced to a moderately stable radical which subsequently disproportionates.

Curve A: Time prior to controlled potential electrolysis

Curve B: Time immediately following exhaustive electrolysis on first reduction wave

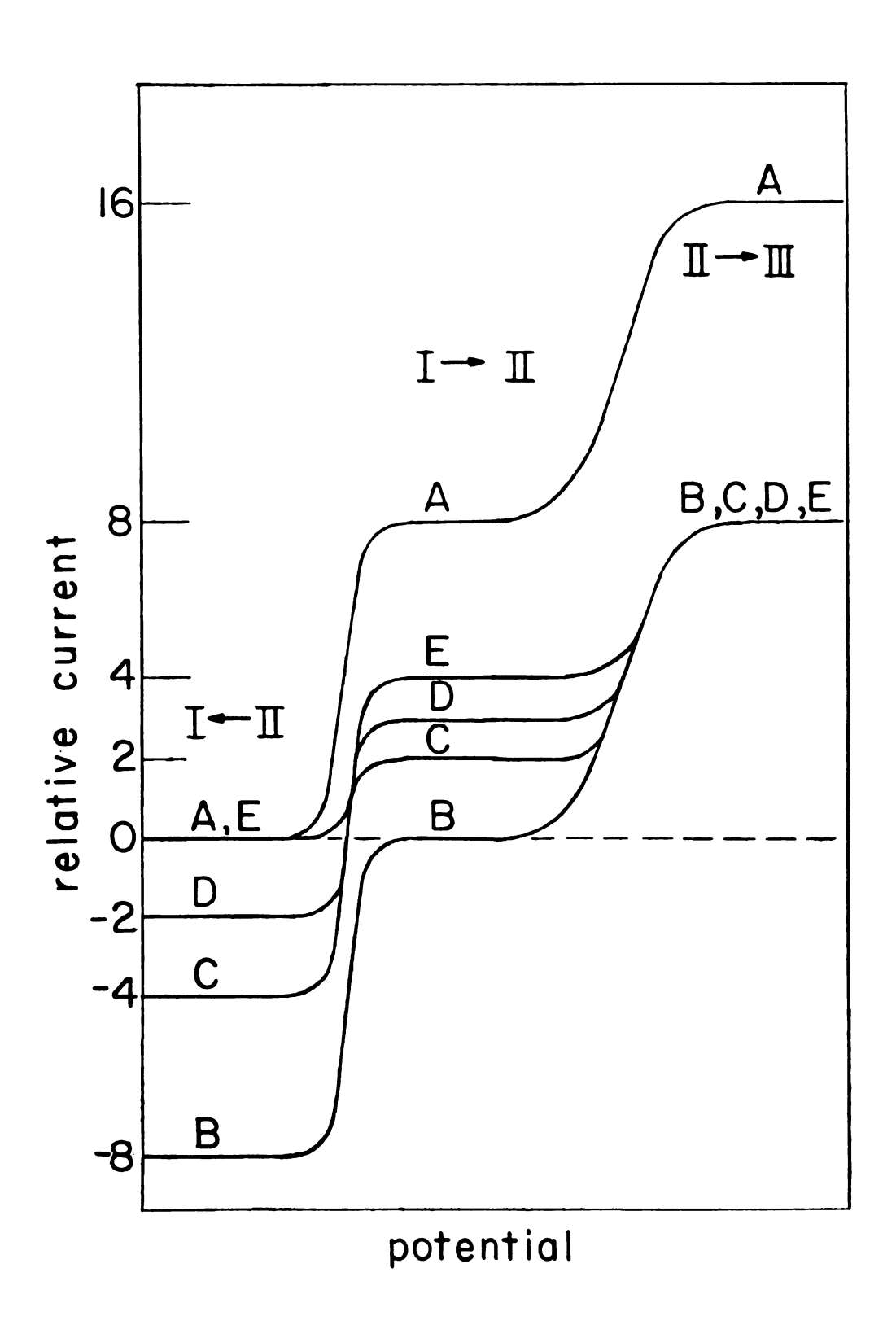
Curve C: Time at which 1/2 of the electro-generated radical has disproportionated

Curve D: Time at which 3/4 of the electro-generated radical has disproportionated

Curve E: Time at which all the radical has disproportionated

a At potential on limiting current of first reduction wave.

b Stable on macroscale electrolysis time scale.



times prior to and following controlled potential electrolysis on the first reduction wave for a sulfonephthalein indicator that is reduced to a moderately stable radical, one which subsequently disproportionates on a time scale that is longer than the time required for electrolysis. Figure 13 shows that the electrogenerated radical, II, decays in a second-order fashion while the carbonium ion, I, and carbanion, III, appear in a second-order manner. These simultaneous events constitute Reaction 3c. The total current height of the second reduction wave is equal to the sum of the currents of the oxidation wave plus twice that of the first reduction wave.

Controlled potential electrolysis experiments were performed on cresol purple, and the behavior agreed qualitatively with the morphology depicted in Figures 12 and 13. Thus, although this method was not used to determine rate constants, it provided further evidence of the disproportionation mechanism for cresol purple.

Coulometry was performed on cresol purple, and n-values of 1.8 and 1.9 were obtained by controlling the potential on the limiting current of the first and second reduction waves, respectively. These data also confirm the disproportionation mechanism for cresol purple, since exhaustive electrolysis on either reduction wave should result in an n-value of 2 for this mechanism.

No conventional polarographic oxidation waves were observed following controlled potential electrolysis on the first reduction wave for those compounds in Table V whose radicals disproportionate rapidly on a polarographic time scale (\underline{k} greater than about $10^3 \,\underline{\text{M}}^{-1}\text{-sec}^{-1}$). Hence, only the two reduction waves corresponding to Reactions 3a and 3b were observed for these compounds. For example, if a radical at an

Figure 13. Limiting current <u>vs</u> time behavior of the polarographic waves following controlled potential electrolysis of a sulfonephthalein indicator that is reduced to a moderately stable radical which subsequently disproportionates.

Curve X: Limiting current of oxidation wave (II \rightarrow I)

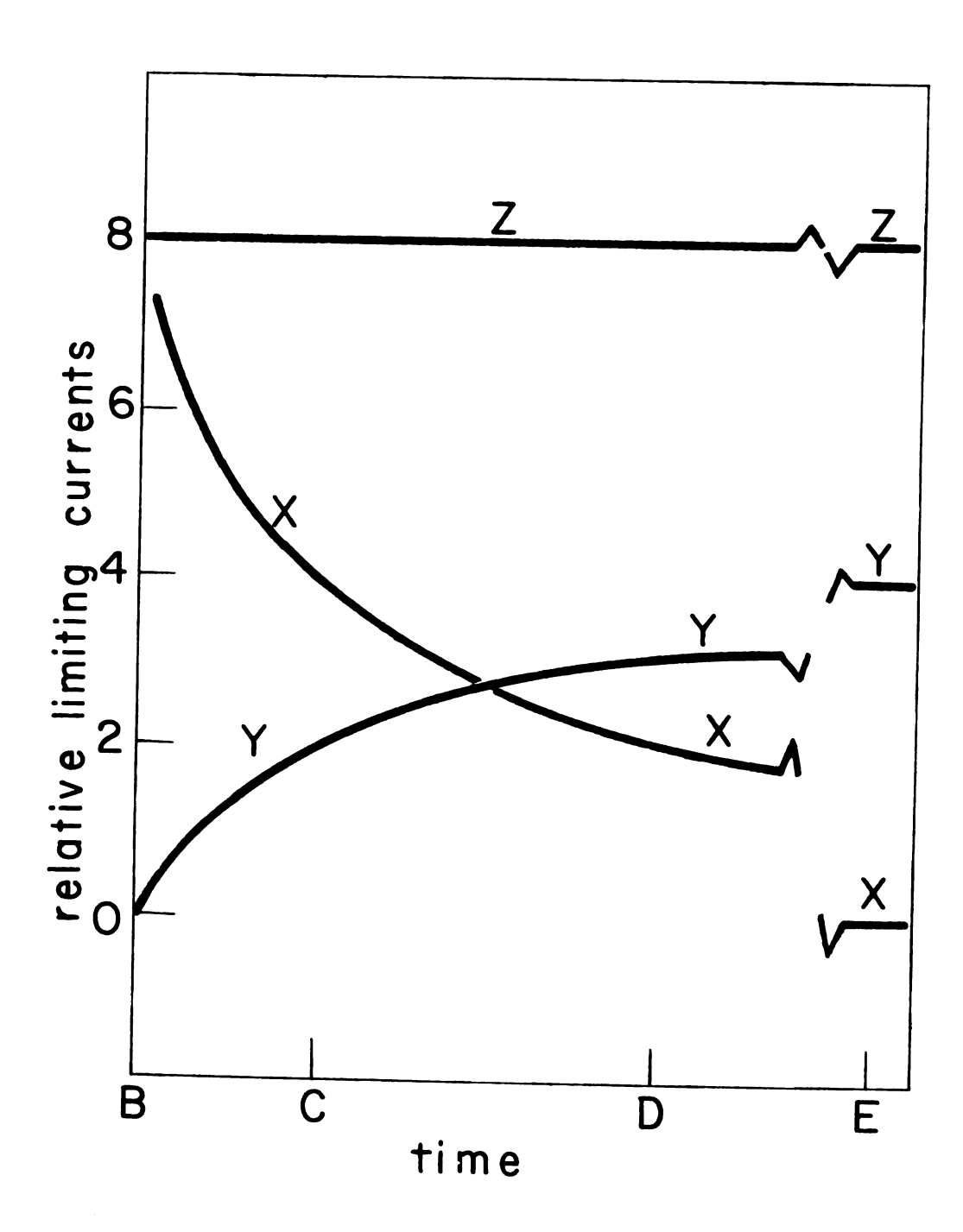
Curve Y: Limiting current of first reduction wave $(I \rightarrow II)$

Curve Z: Total limiting current at potential on second reduction wave (I \rightarrow II and II \rightarrow III)

- B: Time immediately following exhaustive electrolysis on first reduction wave
- C: Time at which 1/2 of the electro-generated radical has disproportionated
- D: Time at which 3/4 of the electro-generated radical has disproportionated
- E: Time at which all the radical has disproportionated

a At potential on limiting current of first reduction wave.

b Stable on macroscale electrolysis time scale.



initial concentration of $1 \, \underline{\text{mM}}$ possesses a disproportionation rate constant of $10^3 \, \underline{\text{M}}^{-1}$ -sec⁻¹, then half of the radical reacts in one second. Clearly in this case no conventional polarographic oxidation wave can be detected because polarographic experiments involve time scales of at least a few minutes duration. However, even though an oxidation wave is not observed for these rapidly disproportionating radicals, the enhancement effects of Reaction 3c are still manifested by the two reduction waves when incremental controlled potential reductions are conducted on the first wave. For example, as the controlled potential reduction on the first wave progresses, the relative limiting current ratio of the two reduction wave changes because the half-life of Reaction 3c is concentration-dependent, and increases as the concentration of species I decreases.

E Cyclic Voltammetry

At sufficiently high scan rates (less than about 10 V/sec), the first reduction wave for the first eight compounds listed in Table V is unperturbed by the disproportionation (Reaction 3c) and corresponds to a reversible (k greater than about 0.02 cm/sec) one-electron charge transfer. Experiments of this type are the source of the thermodynamically meaningful half-wave potentials in Table V. Bromocresol purple required scan rates of 30 V/sec to determine the rate of Reaction 3c. Nevertheless, in this case it was still possible to obtain a thermodynamically meaningful half-wave potential.

For every compound listed in Table V, the second reduction wave (Reaction 3b) is irreversible even at the highest scan rates employed (about 100 V/sec). Thus, direct evidence for Reaction 3d could not be

obtained, nor could meaningful half-wave potentials be measured.

For compounds where disproportionation is appreciable on the cyclic voltammetric time scale, the behavior of the first wave agrees quantitatively with theory for an irreversible disproportionation reaction following reversible electron transfer (52). The morphology of $\frac{i}{p}/v^{1/2}$ ($\frac{i}{p}$ is cathodic peak current and v is scan rate) with scan rate agrees with theory. Moreover, individual cyclic voltammograms agree exactly with theory. For example, the curve of Figure 14 is an experimental cyclic voltammogram for reduction of phenol red in an acetate-buffered aqueous solution at pH 4.8. The points are theoretical for disproportionation (52) and a rate constant of 3.40 x $10^2 \, \text{M}^{-1}$ -sec⁻¹. Nonelectrochemical experiments carried out under similar solution conditions, described below, also yield the same rate constant. Thus, the excellent agreement between cyclic voltammetric theory and experiment for phenol red was further substantiated by a completely different generation as well as measurement technique.

Furthermore, measurements of the rate constant of Reaction 3c for cresol purple (in 25 % by weight methanol-water with a citrate buffer at pH 4.8) by cyclic voltammetry agree with the rate constant obtained by polarographic monitoring of the oxidation wave of the radical following prior reduction with V(II), which is described below.

F Chemical Reduction

Reduction of all compounds listed in Table V with amalgamated zinc leads to the sulfonephthalin, IV. This is equivalent to controlled potential electrolysis on the limiting current of the second reduction wave (Reaction 3b). Chemical reduction can also be accomplished using either V(II) or Ti(III), both of which possess formal potentials

Figure 14. Comparison of theory (points) and experiment (curve) for disproportionation reaction mechanism for cyclic voltammetry.

Aqueous solution

 $C_0^* = 3.04 \text{ } \underline{\text{mM}} \text{ phenol red (unpurified sample)}$

0.020 % gelatin

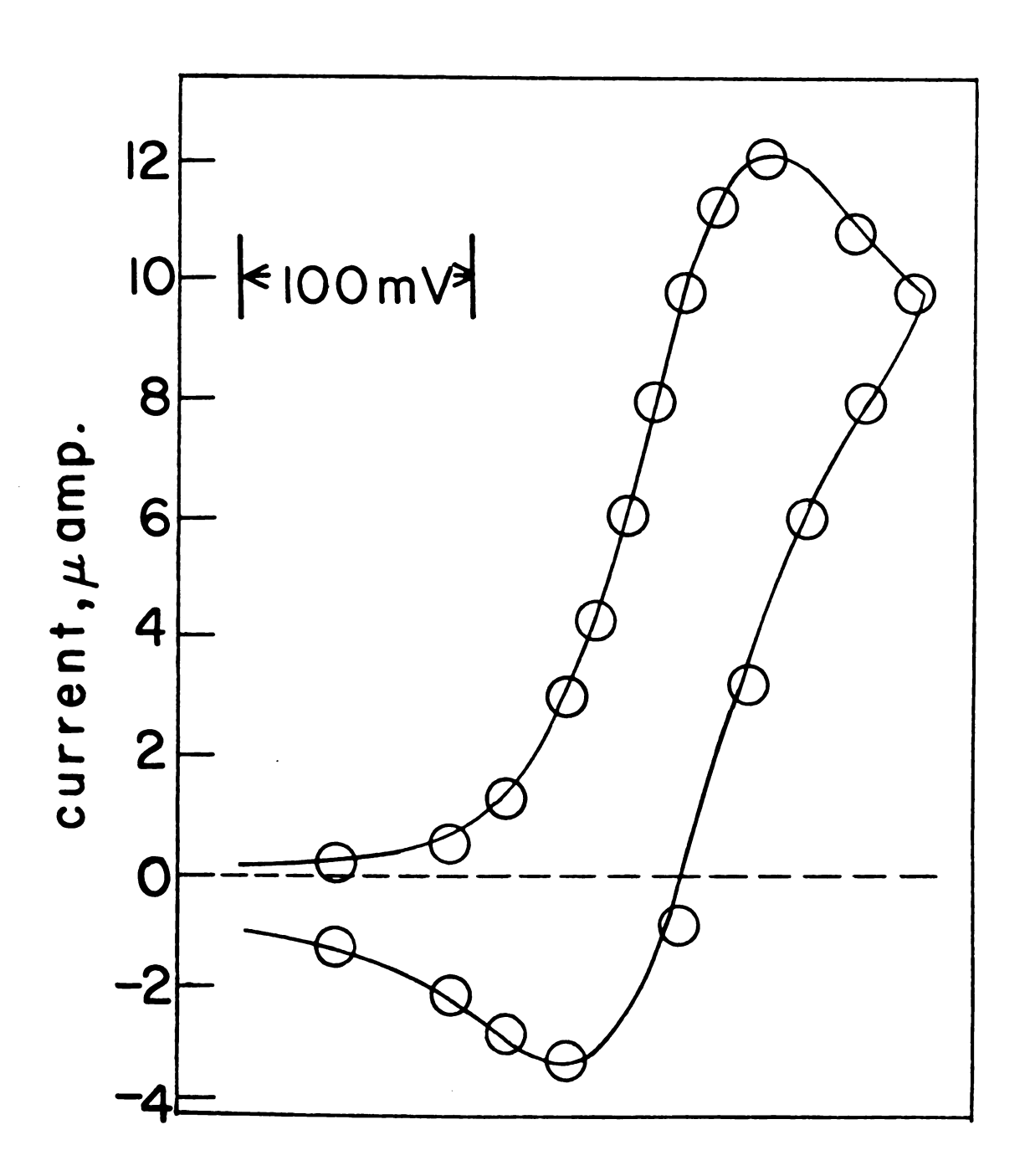
0.020 \underline{M} acetic acid

0.020 \underline{M} sodium acetate

Scan rate = 67 mV/sec

Theoretical points for $\Psi = 0.350$

Rate constant = $3.4 \times 10^2 \, \underline{\text{M}}^{-1} - \sec^{-1}$



corresponding to the limiting current region of the first reduction wave (Reaction 3a). Reduction with these two chemical reductants also ultimately leads to the sulfonephthalin because of the disproportionation reaction (Reaction 3c).

Preliminary experiments showed that the rate of reduction of phenol red with V(II) occurred at about twice the rate as when Ti(III) was used as the chemical reductant. Hence, most chemical reductions corresponding to reductions on the limiting current region of the first reduction wave were carried out with V(II). Relative rate of reduction by V(II) and Ti(III) of compounds other than phenol red were not studied because this aspect, although interesting, is outside the scope of this investigation.

G Chemical Generation with Electrochemical Detection

Reduction of most of the compounds listed in Table V leads to radicals which disproportionate so rapidly that no oxidation wave is observed following controlled potential macroscale electrolysis on the first reduction wave. However, the first four compounds listed in Table V are reduced to radicals of sufficient stability (k less than about 10^2M^{-1} -sec⁻¹) that oxidation waves are observed following controlled potential electrolysis on the first reduction wave. Hence, in these cases, radical concentration can be directly monitored with a DME at a potential corresponding to the limiting current region of the oxidation wave. Nevertheless, exhaustive electrolytic reduction of millimolar solutions of these compounds requires hours, even when rapidly stirred mercury pools are used, and therefore polarographic monitoring of the oxidation wave is quite difficult because a significant fraction of the radical reacts before polarographic monitoring

can be initiated. Thus, polarographic monitoring would lead to easier rate constant determination if the radical could be generated homogeneously during a relatively small time interval. As indicated above, such homogeneous reduction can be accomplished with V(II).

Polarographic monitoring experiments were performed with 2 mM solutions (about 0.04 millimoles) of cresol purple into which 1.00 ml (about 0.003 millimoles) of a V(II) solution was injected. (Rapid mixing is achieved by injecting the chemical reductant into the cresol purple solution with a syringe.) The decay of the oxidation wave (see Figures 12 and 13) was monitored with a DME set at -0.20 V vs sce. After the completion of the disproportionation reaction, the initial amount of radical formed (or V(II) added) was determined by measuring the decrease in the limiting current (the difference between curves A and E in Figure 12) of the first reduction wave for the cresol purple (with a correction for the volume change caused by adding the V(II) solution). As previously discussed, the decrease in the limiting current of the first reduction wave is directly proportional to the amount of radical that was initially generated.

The results of these experiments on cresol purple are given in Table VI. Rate constants for the disproportionation of cresol purple radical were determined by measuring the first two half-lives of the decay of the oxidation wave of the radical (times C and D on Curve X of Figure 13). As shown in Table VI, the rate constant for the disproportionation of cresol purple determined polarographically is $21 \pm 2 \text{ M}^{-1}$ -sec⁻¹. This value agrees reasonably well with the rate determined by cyclic voltammetry, namely, $19 \pm \text{ M}^{-1}$ -sec⁻¹.

Table VI. Disproportionation Rate constants for Cresol Purple Radical aby Polarographic Monitoring of Decay of Oxidation Wave of the Radical.

Initial Radical Concentration, mM	First half-life, sec	Second half-life, sec	Rate Constant, f
	292		20 ± 2
0.17		908	19 ± 2
0.11	442		21 ± 2
		1,360	20 ± 2
0.10	241		22 ± 2
0.19		706	23 ± 2

^a 25% (by weight) methanol-water, 0.10 $\underline{\text{M}}$ total citrate buffer, pH 4.8.

b Determined by measuring decrease in limiting current of first reduction wave.

c Time at which one-half of radical has reacted.

d Time at which three-quarters of radical has reacted.

 $[\]frac{e}{x} = 1/\underline{t}_{1/2} \times \underline{R}_{initial}$

Rate constants given to within about ± 10% since initial radical concentrations are within about ± 10% of stated values.

H ESR Spectroscopy

On the basis of the generally accepted structures of the sulfonephthaleins and sulfonephthalins (105), the reactant of Reaction 3a (I) and the product of Reaction 3b (IV) should both be diamagnetic, whereas the one-electron reduction product of Reaction 3a (II) should be paramagnetic. Esr measurements were used to confirm these assumptions. Since facilities for rapid mixing and observation by esr were not available, cresol purple was used exclusively for these esr measurements because its rate of disproportionation is the slowest of all compounds studied. Solutions of cresol purple gave no detectable esr signal, nor did solutions of this compound which were reduced over a mercury pool at potentials on the limiting current region of the second reduction wave. Moreover, cresol purple solutions reduced with amalgamated zinc gave no detectable esr signal. On the other hand, solutions reduced electrolytically at potentials on the limiting current of the first reduction wave, as well as solutions reduced with either V(II) or Ti(III), all gave identical esr spectra. A representative spectrum is shown in Figure 15. These results prove that both chemical and electrochemical reduction, at potentials on the limiting current region of the first reduction wave, lead to exactly the same paramagnetic species, presumably II, the product of Reaction 3a.

As shown in Figure 15, the esr spectrum of cresol purple radical consists of a single resolvable line about 22 gauss wide, with a g value of 2.00, very close to the free electron value. Only partially resolved hyperfine splitting is evident, and no attempt was made to assign the spectrum quantitatively. Nevertheless, the results are consistent with structure II, with the free electron localized on the

Figure 15. Esr spectrum of cresol purple following controlled potential electrolysis on first reduction wave.

Scan Range: 40 G.

Time Constant: 0.30 sec.

Modulation Amplitude: 1.0×10^{-1} G.

Microwave Power: 10 dB/20 mV.

Field Set: 3,371.2 G.

Scan Time: 16 min.

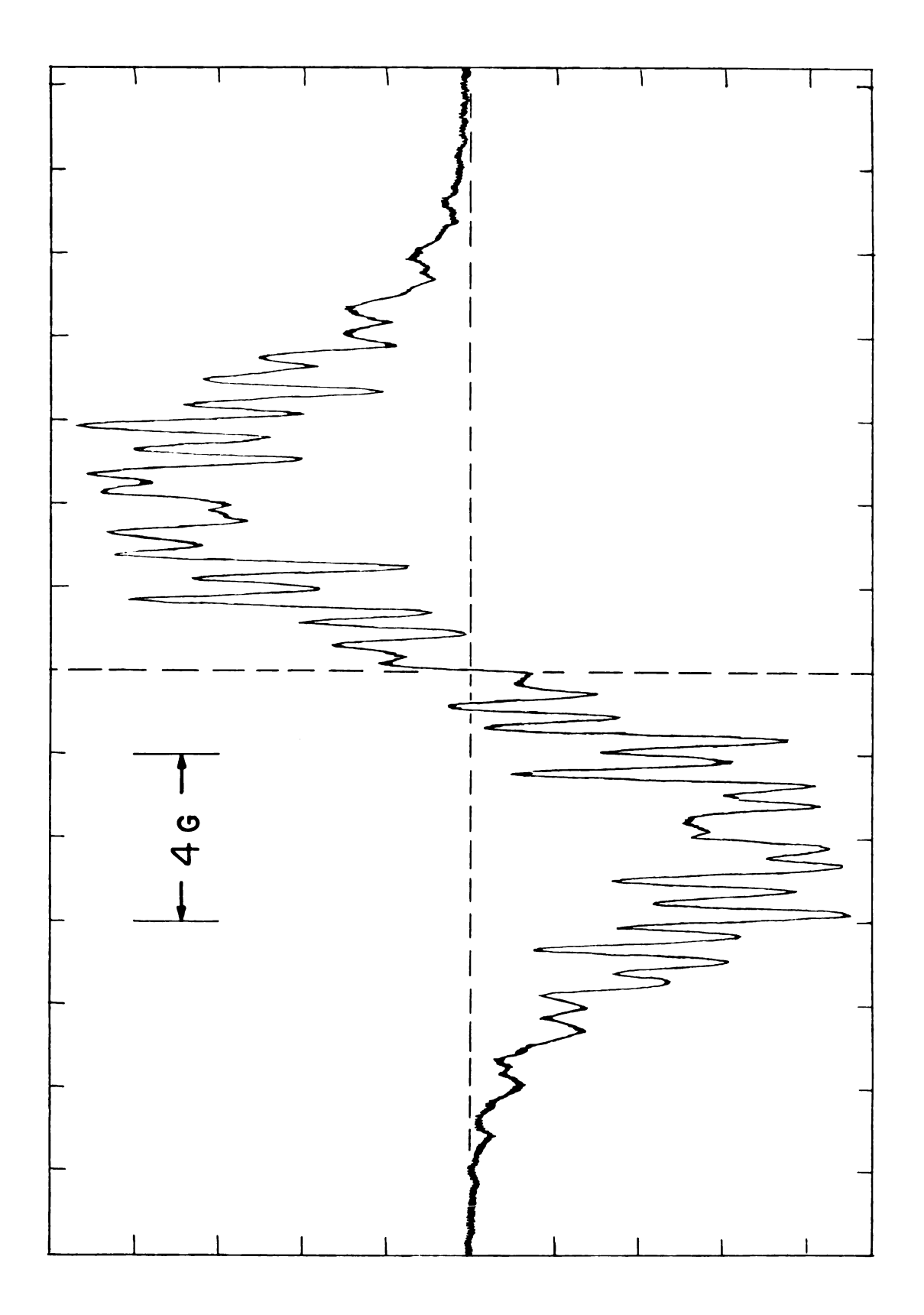
Modulation Frequency: 100 KHz.

Temperature: 23° C.

Microwave frequency: 9.42 GHz.

a At -0.80 V <u>vs</u> sce.

 $^{\rm b}$ Spectrum obtained approximately 3/4 hr. after removal of solution from electrolysis cell.



central carbon atom and undergoing only long range interactions with ring and methyl protons. This picture is consistent with the fact that none of the compounds containing the added electron (II, III, and IV) absorbs in the visible region of the spectrum (λ_{max} for m-cresol-sulfonephthalin, IV, is 275 nm), suggesting that the added electron is not highly delocalized on the radical, II. In contrast, the free electron on triphenylmethyl radical is highly delocalized into the rings (as shown, for example, by its well known esr spectrum), and this species absorbs strongly in the visible region. However, the fourth electron of the central carbon atom in triphenylmethane is localized on the central carbon atom, in the carbon-hydrogen bond, and this species does not absorb in the visible region.

For those compounds where disproportionation is slow, esr provides a convenient means of monitoring the concentration of free radical with time. For the radical generated by the reduction of cresol purple, the esr signal was observed to decay with time in a second order manner which is consistent with the disproportionation mechanism.

I Spectrophotometric Measurements

Sulfonephthalein indicators absorb strongly in the visible region ($\lambda_{\rm max}$ for the acid form of phenol red is 430 nm), whereas the one and two-electron reduction products of these compounds are colorless, absorbing in the uv region ($\lambda_{\rm max}$ for phenolsulfonephthalin is 265 nm). Thus, absorbance at 430 nm can be used to determine the concentration of phenol red. for example, if a 4 x 10⁻⁵ M solution of phenol red is reduced to 2 x 10⁻⁵ M, then from the stoichiometry for complete disproportionation, the equilibrium absorbance at 430 nm will correspond to 3 x 10⁻⁵ M phenol red. Hence, the disproportionation of the colorless

radical can be studied by monitoring the reappearance of the colored starting material. Of course, if experiments of this type are performed with rapid mixing, they provide a means of measuring the rate of disproportionation, and provide a completely independent confirmation of electrochemically measured rate constants.

Under conditions of electrochemical measurements the half-life of the free radical of phenol red is less than a few seconds, and therefore spectrophotometric experiments were initially performed with a stop-flow apparatus (81). In a typical experiment, a solution of phenol red in the same electrolyte used for electrochemical experiments was contained in one syringe, and a solution containing approximately half an equivalent of V(II) was present in the other syringe. Mixing into a 2 cm cell was complete in about 1 msec, and absorbance through the cell was recorded as a function of time. To have an absorbance of less than about one with this system, however, required the use of solutions of phenol red that were relatively dilute compared with those studied electrochemically. Phenol red concentrations in electrochemical experiments ranged from about 5 x 10^{-4} M to 5 x 10^{-3} M, whereas in these spectrophotometric experiments the concentration averaged about 5×10^{-5} M. Since the disproportionation is second order, this necessity of using lower concentrations resulted in a corresponding increase in the half-life of the chemical reaction. Thus, the use of a stop-flow apparatus was actually unnecessary since identical results could be obtained by simply mixing solutions in the cell compartment of a conventional spectrophotometer. Results presented below are a composite of both kinds of experiments.

A typical % Transmittance vs time curve for reduction of phenol

red with V(II) and subsequent disproportionation generating phenol red is shown in Figure 16. Clearly the reduction by V(II) is not instantaneous, and indeed could be studied conveniently by stop-flow, although this possibility was not pursued. Percent Transmittance vs time data were converted to concentration vs time data using the measured molar extinction coefficient for the acid form of phenol red (1.81 x $10^4 \, \text{M}^{-1}\text{-cm}^{-1}$). Concentrations of phenol red were then converted to concentrations of radical, II, by assuming the stoichiometry of a disproportionation reaction. Likewise, initial concentrations of the radical, R_{in} , were calculated from twice the long-time limiting absorbance after subtracting that absorbance due to the amount of phenol red which was not initially reduced. The fact that these assumptions resulted in self-consistent rate constants under a variety of conditions is indirect proof of the postulated mechanism.

A conventional method of determining second-order rate constants is to plot the reciprocal of concentration <u>vs</u> time. If a plot of this nature results in a straight line, the reaction is shown to be second order (107). The disproportionation reaction (Reaction 3c) can be rewritten as

$$2 R \rightarrow 0 + P \tag{4}$$

where \underline{R} is the radical, \underline{O} the sulfonephthalein, and \underline{P} the sulfonephthalin. This reaction can be described by the equations

$$- d[R]/dt = k[R]^2$$
(5)

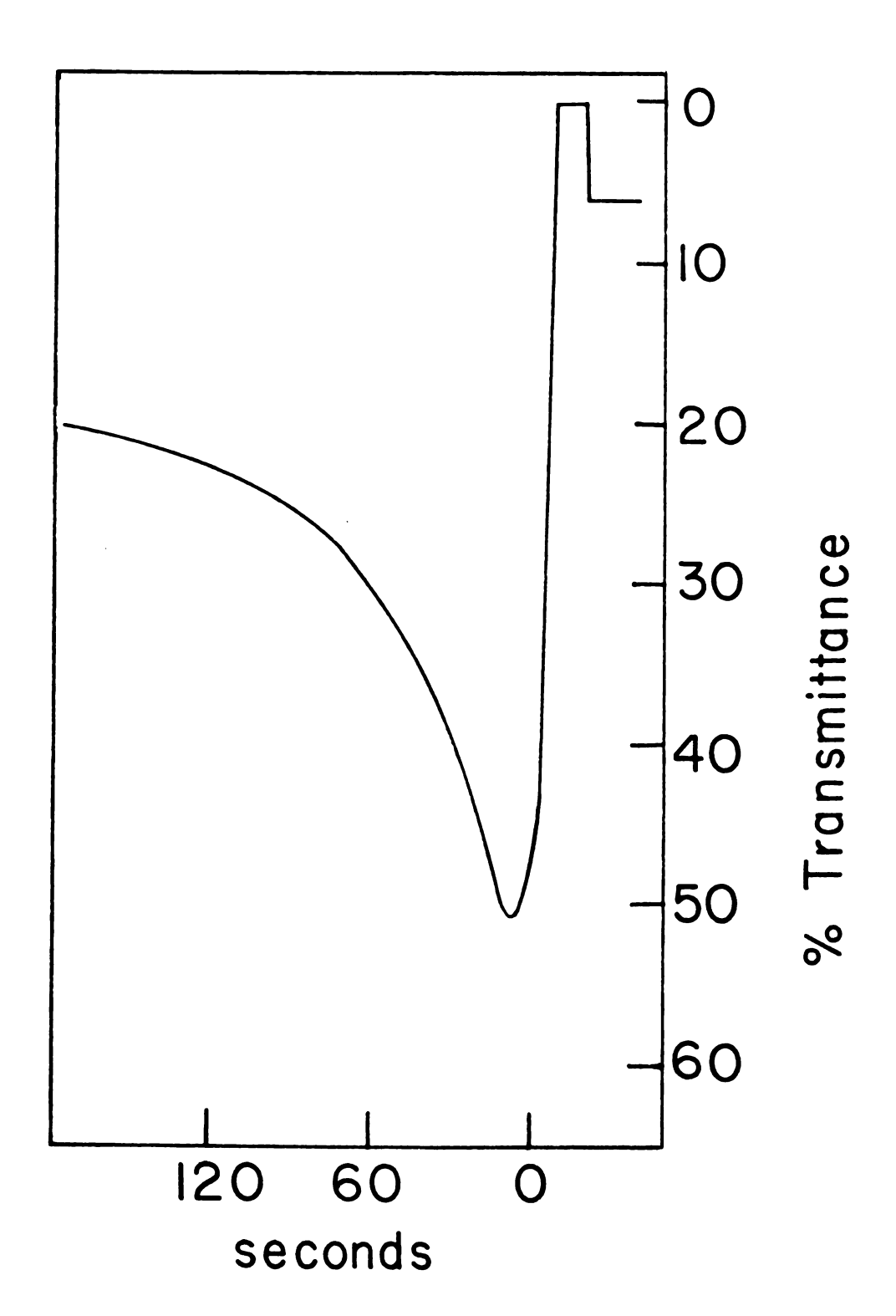
$$d[0]/dt = k[R]^2/2$$
 (6)

$$d[P]/dt = k[R]^2/2 \tag{7}$$

and, from the stoichiometry for complete disproportionation

$$[R] = [R]_{in} - 2[0]$$
 (8)

Figure 16. A typical experimental curve for reduction of phenol red with V(II), and the following generation of phenol red by disproportionation of the radical.



Equation 6 can be rearranged as follows

$$2\int_{0}^{d[0]} \frac{d[0]}{[R]^2} = k \int_{0}^{t} dt$$
 (9)

However, [R] is not directly determinable in the case of phenol red, so that Equations 8 and 9 must be combined to give

$$2\int_{0}^{[0]} \frac{d[0]}{\{[R]_{in} - 2[0]\}^{2}} = kt$$
 (10)

Integration of Equation 10 gives kt directly in terms of [0] and $[R]_{in}$, the experimentally determinable quantities.

Hence, if the concentration \underline{vs} time data are plotted according to Equation 11, the slope of this plot gives directly the second order rate constant for disproportionation.

Experiments were conducted with nine different solutions, with initial radical concentrations ranging from 3.7 to 7.7 x 10^{-5} M. A representative experiment, with the data plotted in accordance with Equation 11, is shown in Figure 17. Results of these nine experiments are summarized in Table VII, which lists the measured rate constants along with the initial radical concentrations for each experiment.

During the course of this investigation rate constants for disproportionation of phenol red in acetate buffered aqueous solutions were measured electrochemically by cyclic voltammetry with various amounts of gelatin present. The average value of all of these measurements is $3.4 \times 10^2 \, \underline{\text{M}}^{-1}\text{-sec}^{-1}$, which is (fortuitously) identical with the average value of the spectrophotometrically determined rate

Figure 17. A typical second order plot of phenol red radical \underline{vs} time.

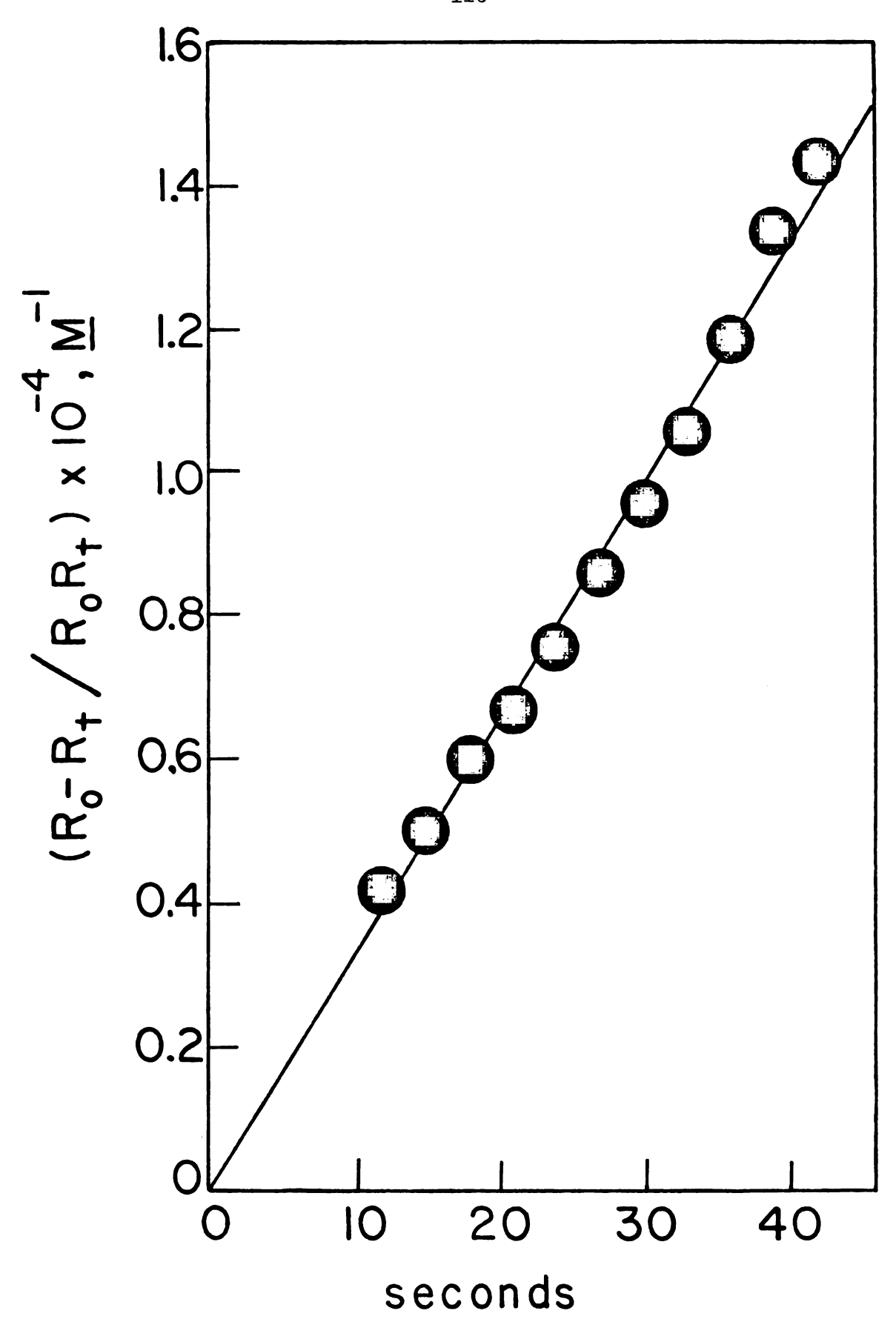


Table VII. Disproportionation Rate Constants for Phenol Red Radicals in Acetate Buffered Aqueous Solutions from Conventional Second Order Plots.

Initial Radical Concentration, $\underline{R}_{in} \times 10^{5}, \underline{M}$	Rate Constant, $\underline{k} \times 10^{-2}, \underline{M}^{-1} - \sec^{-1}$
7.7	3.2
6.4	3.3
6.2	3.4
6.0	3.4
6.0	3.4
5.9	3.6
5.0	3.3
4.9	3.5
3.7	3.5

^a Average value is 3.4 x $10^2 \, \underline{\text{M}}^{-1}$ - \sec^{-1} with a standard deviation of 3.6 %.

constant in Table VII. This excellent agreement is taken as further evidence of the correctness of the disproportionation mechanism, as well as convincing evidence of the validity of measuring homogenous rate constants with modern electrochemical techniques.

Based on the above results it is apparent that phenol red provided a convenient system for comparing electrochemically measured rate constants with those obtained by more classical means. Surprisingly, the literature contains virtually no other direct comparisons of this type, apparently because the time scale for electrochemical methods complements rather than overlaps classical approaches. Thus, previous comparisons involved an extrapolation of first order rate constants as a function of pH, dielectric constant, etc (8-12, 108, and references contained therein). The comparisons reported here for phenol red and cresol purple avoid this problem since the disproportionation reaction is second order and the time scale can be altered by simply working at different concentrations. In general, this approach was not possible until very recently, since rigorous electrochemical theory for higher than first order processes (50-52) is of very recent origin.

J <u>Electrochemical Measurement of Rate Constants</u>

Clearly several techniques could be used to measure rate constants of compounds considered in this investigation. Nevertheless, cyclic voltammetry was found to be by far the most convenient and versatile technique. For example, a rate constant was obtained for cresol purple by cyclic voltammetry in spite of the fact that this compound exhibits two conventional polarographic reduction waves of equal height so that

a rate constant could not be obtained by conventional polarography (109). Furthermore, conventional polarography requires an analysis of both reduction waves to determine the rate of the disproportionation reaction (109), whereas cyclic voltammetry requires data from only the first wave (52). This aspect of cyclic voltammetry is highly advantageous in that it permits measuring rate constants at low pH where the second reduction wave is masked by hydrogen discharge. Thus, in addition to being inherently more versatile and sensitive than conventional polarography, cyclic voltammetry is also applicable to a wider variety of solution conditions.

Briefly, the experimental procedure employed for the cyclic voltammetry of these acid-base indicators was as follows. Cyclic voltammograms were recorded for a series of scan rates, together with appropriate scan-and-hold experiments to generate the proper baseline for measurement of the anodic peak current (78). Experimental values of $\frac{1}{2}$ were then converted to values of \underline{k} C_0^* with the aid of a large scale plot of the theoretical data of Olmstead and Nicholson (52). In each case spherical parameters were determined and used to identify the proper theoretical working curve. Although generally such spherical corrections are relatively small, they are significant for most of the scan rates required in this investigation. Experiments were performed with $(\underline{E}_{\lambda} - \underline{E}_{1/2})\underline{n}$ of approximately four, subsequently corrected with the empirical equation of Olmstead and Nicholson (52). From values of $\underline{k}_2 C_0^{\pi} \tau$, \underline{k}_2 was calculated for each scan rate employed. Tables VIII through XXXVII list these cyclic voltammetric data for each of these acid-base indicators.

Table VIII. Cyclic Voltammetric Data on Cresol Purple. a,b,c,d

Scan Rate, v, mV/sec	Cathodic Peak Current, $\frac{i}{p}$, μA .	<u>i</u> c/v ^{1/2}	Peak Current Ratio, <u>i</u> a/ <u>i</u> c	Rate Constant ^e M ⁻¹ - sec ⁻¹
24.3	8.0	1.62	0.943	18.0
26.3	8.2	1.61	0.945	18.8
28.7	8.6	1.60	0.947	19.6
31.6	9.0	1.60	0.955	18.2
35.1	9.4	1.59	0.958	18.7

^a 25% (by weight) methanol-water, 0.10 \underline{M} total citrate buffer, pH 4.8, C_0^* = 5.92 $\underline{m}M$, no gelatin or Triton X-100 present.

b Diffusion coefficient, $\underline{D}_0 = 2.1 \times 10^{-6} \text{ cm}^2/\text{sec.}$

c Radius of drop, $\underline{r} = 0.44$ mm.

^d Spherical Correction Factor, $\rho \approx 80 \times 10^{-4}$.

e $\underline{\mathbf{k}}_2$ = 18.7 ± 1.7; 1.7 is three times the standard deviation of these five experiments.

121

Table IX. Cyclic Voltammetric Data on Cresol Purple. a,b,c,d

Scan Rate, v, mV/sec	Cathodic Peak Current, $\frac{i}{p}^{c}$,	$\frac{i^{c}}{p}/\underline{v}^{1/2}$	Peak Current Ratio, $\frac{i}{a}/\frac{i}{c}$	Rate Constant ^e M ⁻¹ - sec ⁻¹
27.5	9.2	1.75	0.935	25.6
33.0	9.9	1.72	0.944	26.2
38.9	10.6	1.70	0.949	27.8
44.0	11.2	1.69	0.959	25.2
50.8	12.1	1.69	0.963	25.7
58.0	12.8	1.68	0.966	26.8
66.1	13.6	1.67	0.972	25.8
75.1	14.5	1.67	0.976	25.6

^a Aqueous solution, 0.20 \underline{M} acetic acid & 0.20 \underline{M} sodium acetate, pH \simeq 4.8, C_0^* = 5.01 \underline{mM} , no gelatin or Triton X-100 present.

b Diffusion coefficient, $\underline{D}_0 = 2.7 \times 10^{-6} \text{ cm}^2/\text{sec.}$

^c Radius of drop, $\underline{r} = 0.44$ mm.

^d Spherical Correction Factor, $\rho \approx 70 \times 10^{-4}$.

e $\underline{\mathbf{k}}_2$ = 26.1 ± 2.5; 2.5 is three times the standard deviation of these eight experiments.

Table X. Cyclic Voltammetric Data on Thymol Blue. A,b,c,d

Scan Rate, $\underline{\mathbf{v}}$, $\underline{\mathbf{m}}\mathbf{V}/\mathrm{sec}$	Cathodic Peak Current, $\frac{i}{p}$,	$\frac{i^{c}}{p}/\underline{v}^{1/2}$	Peak Current Ratio, $\frac{i}{a}/\frac{i}{c}$	Rate Constant ^e M ⁻¹ - sec ⁻¹
22.6	7.6	1.61	0.910	32.2
24.4	7.9	1.60	0.918	31.0
26.4	8.2	1.60	0.921	32.2
28.8	8.5	1.58	0.929	31.0
35.2	9.3	1.57	0.936	33.9
39.6	9.9	1.57	0.944	32.6
45.3	10.4	1.55	0.947	34.6

^a 25% (by weight) methanol-water, 0.10 \underline{M} total citrate buffer, pH 4.8, C_{O}^{*} = 4.78 $\underline{m}\underline{M}$, no gelatin or Triton X-100 present.

b Diffusion coefficient, $\underline{D}_0 = 2.5 \times 10^{-6} \text{ cm}^2/\text{sec.}$

^c Radius of drop, \underline{r} = 0.44 mm.

^d Spherical Correction Factor, $\rho \approx 80 \times 10^{-4}$.

e $\underline{\mathbf{k}}_2$ = 32.5 ± 3.7; 3.7 is three times the standard deviation of these seven experiments.

123

Table XI. Cyclic Voltammetric Data on Thymol Blue. a,b,c,d

Scan Rate, v, mV/sec	Cathodic Peak Current, $\frac{i}{p}^{c}$, μA .	$\frac{i^c}{p}/v^{1/2}$	Peak Current Ratio, <u>i</u> a/ <u>i</u> c	Rate Constant ^e $ \underline{M}^{-1} - \sec^{-1} $
27.5	8.8	1.67	0.931	31.9
33.0	9.5	1.64	0.942	31.4
38.9	10.1	1.63	0.947	33.3
44.0	10.7	1.62	0.953	33.2
50.8	11.5	1.61	0.959	33.4
58.0	12.2	1.61	0.963	33.9
66.1	13.1	1.61	0.967	34.5
75.1	13.9	1.60	0.971	36.2

a 25% (by weight) methanol-water, 0.20 \underline{M} acetic acid & 0.20 \underline{M} sodium acetate, pH \simeq 4.8, C_{O}^{*} = 4.99 $\underline{m}\underline{M}$, no gelatin or Triton X-100 present.

b Diffusion coefficient, $\underline{D}_0 = 2.6 \times 10^{-6} \text{ cm}^2/\text{sec.}$

c Radius of drop, $\underline{r} = 0.44$ mm.

^d Spherical Correction Factor, $\rho \approx 80 \times 10^{-4}$.

e $\underline{\mathbf{k}}_2$ = 33.5 \pm 4.5; 4.5 is three times the standard deviation of these eight experiments.

124

Table XII. Cyclic Voltammetric Data on Bromothymol Blue. a,b,c,d

Scan Rate, v, mV/sec	Cathodic Peak Current, $\frac{i}{p}$,	$\frac{i^{c}}{p}/v^{1/2}$	Peak Current Ratio, <u>i</u> / <u>i</u> c	Rate Constant ^e $ \underline{M}^{-1} - \sec^{-1} $
24.4	3.9	0.789	0.919	66.4
26.4	4.0	0.779	0.924	65.9
28.8	4.15	0.773	0.928	67.6
31.7	4.35	0.772	0.934	67.1
35.2	4.55	0.767	0.940	67.2
39.6	4.75	0.755	0.947	65.7

a 25% (by weight) methanol-water, 0.10 \underline{M} total citrate buffer, pH 4.8, C_0^* = 2.36 $\underline{m}M$, no gelatin or Triton X-100 present.

b Diffusion coefficient, $\underline{D}_0 = 2.5 \times 10^{-6} \text{ cm}^2/\text{sec.}$

c Radius of drop, $\underline{r} = 0.44$ mm.

d Spherical Correction Factor, $\rho \approx 60 \times 10^{-4}$.

e $\underline{\mathbf{k}}_2$ = 66.7 ± 2.3; 2.3 is three times the standard deviation of these six experiments.

Table XIII. Cyclic Voltammetric Data on Bromocresol Green.a,b,c,d

Scan Rate, v, mV/sec	Cathodic Peak Current, $\frac{i}{p}^{c}$,	$\frac{i^c}{p}/v^{1/2}$	Peak Current Ratio, $\frac{i}{a}/\frac{i}{c}$	Rate Constant ^e $ \underline{M}^{-1} - \sec^{-1} $
22.6	3.4 ₅	0.726	0.920	68.8
25.4	3.6	0.714	0.930	65.8
28.8	3.8	0.708	0.934	69.3
31.7	3.9 ₅	0.702	0.937	71.7
35.2	4.1 ₅	0.699	0.946	68.0
39.6	4.4	0.699	0.950	70.8
45.3	4.7	0.697	0.957	69.4

a 25% (by weight) methanol-water, 0.10 \underline{M} total citrate buffer, pH 4.8, C_0^* = 2.08 $\underline{m}M$, no gelatin or Triton X-100 present.

b Diffusion coefficient, $\underline{D}_0 = 2.7 \times 10^{-6} \text{ cm}^2/\text{sec.}$

Radius of drop, $\underline{r} = 0.44 \text{ mm}$.

^d Spherical Correction Factor, $\rho \approx 60 \times 10^{-4}$.

e $\underline{\mathbf{k}}_2$ = 69.1 \pm 5.3; 5.3 is three times the standard deviation of these seven experiments.

Table XIV. Cyclic Voltammetric Data on Phenol Red. A,b,c,d

Scan Rate, v, mV/sec	Cathodic Peak Current, $\frac{i}{p}$, μ A.	$\frac{i^{c}_{p}}{\sqrt{v}}^{1/2}$	Peak Current Ratio, $\frac{i}{a}/\frac{i}{c}$	Rate Constant, M-1 - sec-1
61.1	5.3 ₅	0.684	0.907	149
71.3	5.7 ₅	0.681	0.917	151
85.6	6.3	0.681	0.921	169
107	6.9 ₅	0.672	0.935	171
122	7.4	0.669	0.946	162

^a 25% (by weight) methanol-water, 0.10 \underline{M} total citrate buffer, pH 2.5, C_0^* = 2.26 \underline{mM} , no gelatin or Triton X-100 present.

b Diffusion coefficient, $\underline{D}_0 = 2.2 \times 10^{-6} \text{ cm}^2/\text{sec.}$

c Radius of drop, $\underline{r} = 0.44 \text{ mm}$.

d Spherical Correction Factor, $\rho \approx 25 \times 10^{-4}$.

e $\underline{\mathbf{k}}_2$ = 160 ± 30; 30 is three times the standard deviation of these five experiments.

Table XV. Cyclic Voltammetric Data on Phenol Red. a,b,c,d

Scan Rate, v, mV/sec	Cathodic Peak Current, $\frac{i}{p}$,	$\frac{i^{c}}{p}/\underline{v}^{1/2}$	Peak Current Ratio, $\frac{i}{a}/\frac{i}{c}$	Rate Constant, \underline{M}^{-1} - \sec^{-1}
61.1	5.4	0.690	0.907	149
71.3	5.8	0.687	0.914	158
85.6	6.2	0.670	0.919	176
107	6.9	0.667	0.935	172
122	7.3 ₅	0.665	0.946	163

a 25% (by weight) methanol-water, 0.10 \underline{M} total citrate buffer, pH 2.5, C_0^* = 2.25 \underline{mM} , 0.05% gelatin added.

b Diffusion Coefficient, $\underline{D}_0 = 2.2 \times 10^{-6} \text{ cm}^2/\text{sec.}$

c Radius of drop, $\underline{r} = 0.44$ mm.

d Spherical Correction Factor, $\rho \approx 25 \times 10^{-4}$.

e $\underline{\mathbf{k}}_2$ = 164 $\overset{+}{=}$ 29; 29 is three times the standard deviation of these five experiments.

128

Table XVI. Cyclic Voltammetric Data on Phenol Red., b,c,d

Scan Rate, v, mV/sec	Cathodic Peak Current, $\frac{i}{p}^{c}$, μ A.	$\frac{i^{c}}{p}/\underline{v}^{1/2}$	Peak Current Ratio, <u>i</u> a/ <u>i</u> c	Rate Constant, \underline{M}^{-1} - \sec^{-1}
33.3	4.8	0.832	0.856	168
39.3	5.2	0.829	0.878	159
48.0	5.7	0.823	0.890	169
57.6	6.2	0.817	0.901	180
72.1	6.7	0.789	0.925	163
86.5	7.3	0.785	0.931	176
108	8.0	0.769	0.943	180
127	8.6	0.763	0.950	183

a 25% (by weight) methanol-water, 0.10 \underline{M} total citrate buffer, pH 4.8, C_0^* = 2.32 \underline{mM} , no gelatin or Triton X-100 present.

b Diffusion coeficient, $\underline{D}_0 = 2.2 \times 10^{-6}$.

c Radius of drop, \underline{r} = 0.44 mm.

^d Spherical Correction Factor, $\rho \approx 25 \times 10^{-4}$.

e $\underline{\mathbf{k}}_2$ = 172 ± 26; 26 is three times the standard deviation of these eight experiments.

Table XVII. Cyclic Voltammetric Data on Phenol Red. a,b,c,d

Scan Rate, v, mV/sec	Cathodic Peak Current, $\frac{i}{p}$, μ A.	<u>i</u> p/ <u>v</u> ^{1/2}	Peak Current Ratio, $\frac{i}{a}/\frac{i}{c}$	Rate Constant, $\underline{M}^{-1} - \sec^{-1}$
				
53.9	5.3	0.722	0.906	146
66.3	5.8	0.712	0.913	166
78.4	6.3	0.712	0.928	156
95.8	6.9	0.705	0.942	150
123	7.8	0.703	0.949	170

^a 25% (by weight) methanol-water, 0.10 \underline{M} total citrate buffer, pH 4.8, C_0^* = 2.31 \underline{mM} , 0.05% gelatin added.

b Diffusion coefficient, $\underline{D}_0 = 2.2 \times 10^{-6} \text{ cm}^2/\text{sec.}$

c Radius of drop, $\underline{r} = 0.44 \text{ mm}$.

^d Spherical Correction Factor, $\rho \approx 25 \times 10^{-4}$.

e \underline{k}_2 = 158 ± 30; 30 is three times the standard deviation of these five experiments.

130

Table XVIII. Cyclic Voltammetric Data on Phenol Red. , b, c, d

Scan Rate, v, mV/sec	Cathodic Peak Current, $\frac{i}{p}$,	$\frac{i^c}{p}/v^{1/2}$	Peak Current Ratio, $\frac{i}{a}/\frac{i}{c}$	Rate Constant, M ⁻¹ - sec ⁻¹
34.0	2.1 ₅	0.369	0.930	160
40.1	2.3	0.363	0.939	162
48.6	2.5	0.359	0.949	163
56.7	2.7	0.359	0.954	171
68.1	2.95	0.357	0.963	164

^a 25% (by weight) methanol-water, 0.10 \underline{M} total citrate buffer, pH 6.8, C_0^* = 1.10 $\underline{m}\underline{M}$, no gelatin or Triton X-100 present.

b Diffusion coefficient, $\underline{D}_0 = 2.4 \times 10^{-6} \text{ cm}^2/\text{sec.}$

^c Radius of drop, $\underline{r} = 0.44$ mm.

^d Spherical Correction Factor, $\rho \approx 50 \times 10^{-4}$.

e $\underline{\mathbf{k}}_2$ = 164 ± 12; 12 is three times the standard deviation of these five experiments.

Table XIX. Cyclic Voltammetric Data on Phenol Red. a,b,c,d

				
Scan Rate, v, mV/sec	Cathodic Peak Current, $\frac{i^{c}}{p}$, μA .	$\frac{i^c}{p}/v^{1/2}$	Peak Current Ratio, $\frac{i}{a}/\frac{i}{c}$	Rate Constant, M ⁻¹ - sec ⁻¹
39.0	7.2 ₅	1.16	0.804	288
57.2	8.5	1.13	0.850	270
69.2	9.3	1.12	0.860	292
85.8	10.2	1.10	0.882	290
107.3	11.3	1.09	0.904	288

^a Aqueous solution, 0.10 \underline{M} total citrate buffer, pH 4.8, C_0^* = 2.47 \underline{mM} , no gelatin or Triton X-100 present.

b Diffusion coefficient, $\underline{D}_0 = 4.6 \times 10^{-6} \text{ cm}^2/\text{sec.}$

^c Radius of drop, \underline{r} = 0.44 mm.

^d Spherical Correction Factor, $\rho \approx 25 \times 10^{-4}$.

 $[\]frac{e}{k_2}$ = 286 ± 16; 16 is three times the standard deviation of these five experiments.

Table XX. Cyclic Voltammetric Data on Phenol Red. a,b,c,d

				
Scan Rate, \underline{v} , mV/sec	Cathodic Peak Current, $\frac{i^{c}}{p}$,	$\frac{i^{c}}{p}/\underline{v}^{1/2}$	Peak Current Ratio, $\frac{i}{a}/\frac{i}{c}$	Rate Constant, M-1 - sec-1
39.0	7.1	1.14	0.814	257
57.2	8.4 ₅	1.11	0.856	255
69.2	9.0	1.08	0.878	254
85.8	9.9 ₅	1.07	0.884	284
107.3	11.0	1.06	0.906	280

^a Aqueous solution, 0.10 \underline{M} total citrate buffer, pH 4.8, $C_0^* = 5.46 \underline{mM}$, 0.05% gelatin added.

b Diffusion Coefficient, $\underline{D}_0 = 4.0 \times 10^{-6} \text{ cm}^2/\text{sec.}$

^c Radius of drop, \underline{r} = 0.44 mm.

^d Spherical Correction Factor, $\rho \simeq 25 \times 10^{-4}$.

 $[\]frac{e}{\underline{k}_2}$ = 266 ± 44; 44 is three times the standard deviation of these five experiments.

133
Table XXI. Cyclic Voltammetric Data on Phenol Red. a,b,c,d

Scan Rate, v, mV/sec	Cathodic Peak Current, $\frac{i^c}{p}$, μA .	$\frac{i^c}{p}/v^{1/2}$	Peak Current Ratio, $\frac{i}{a}/\frac{i}{c}$	Rate Constant, \underline{M}^{-1} - \sec^{-1}
27.5	5.7	1.09	0.772	324
33.0	6.2	1.08	0.795	323
60.0	7.5	0.97	0.853	330
73.5	8.3	0.96	0.880	323
94.4	9.0 ₅	0.93	0.895	343
118	10.1	0.93	0.916	326
144	11.1	0.92	0.923	353

^a Aqueous solution, 0.20 \underline{M} acetic acid & 0.20 \underline{M} sodium acetate, pH \simeq 4.8, C_0^* = 2.24 $\underline{m}\underline{M}$, no gelatin or Triton X-100 present.

b Diffusion coefficient, $\underline{D}_0 = 5.0 \times 10^{-6} \text{ cm}^2/\text{sec.}$

c Radius of drop, $\underline{r} = 0.44$ mm.

^d Spherical Correction Factor, $\rho \approx 30 \times 10^{-4}$.

e $\underline{\mathbf{k}}_2$ = 332 ± 35; 35 is three times the standard deviation of these seven experiments.

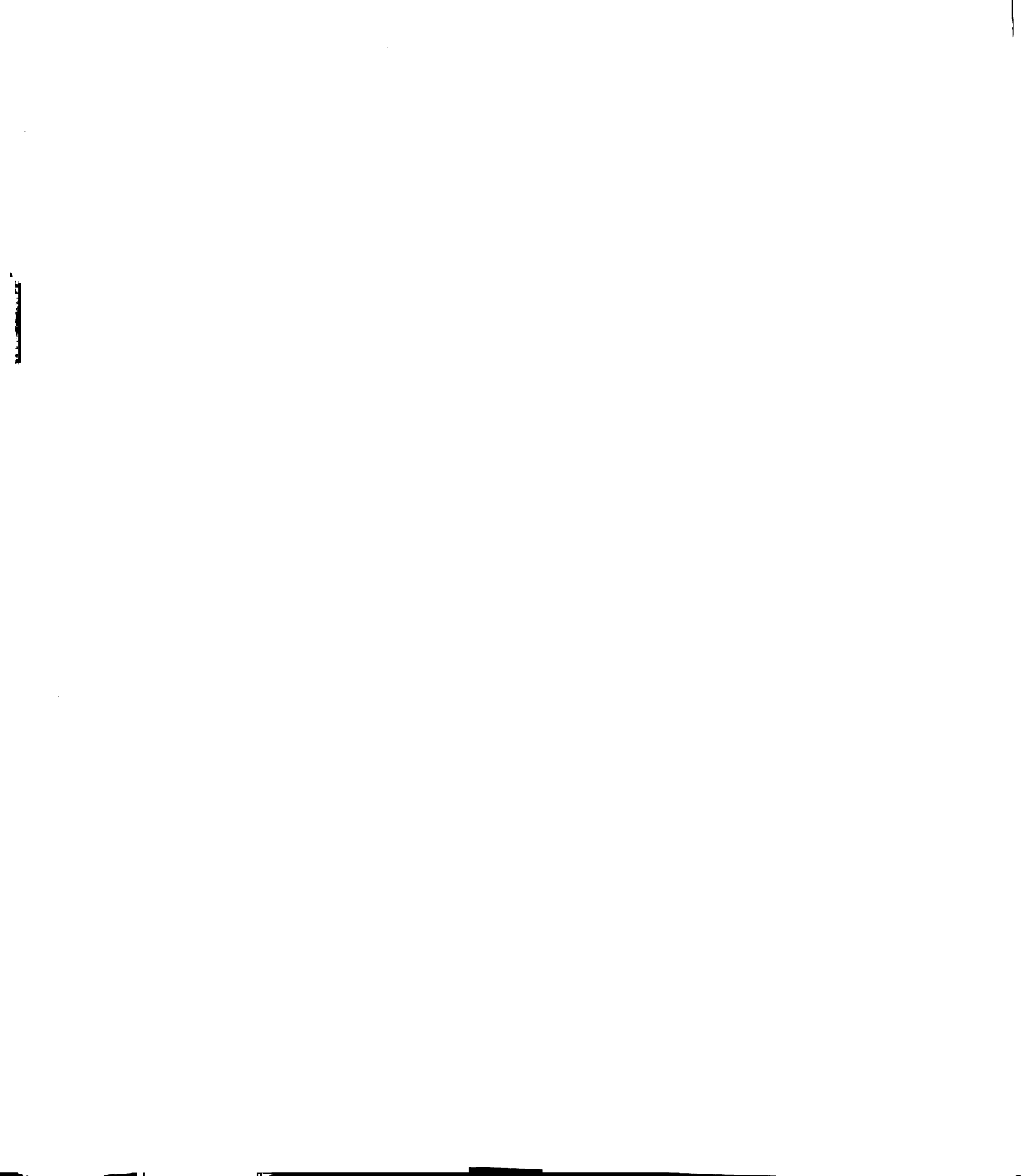


Table XXII. Cyclic Voltammetric Data on Phenol Red., b,c,d

Scan Rate, v, mV/sec	Cathodic Peak Current, $\frac{i^c}{p}$, μA .	$\frac{i^{c}_{p}/v^{1/2}}{2}$	Peak Current Ratio, <u>i</u> a/ <u>i</u> c	Rate Constant, M-1 - sec-1
37.5	5.2	0.850	0.813	345
46.9	5.7	0.837	0.839	342
57.7	6.2 ₅	0.822	0.856	355
75.0	7.0	0.807	0.879	365
93.8	7.6 ₅	0.790	0.899	364
125	8.6	0.767	0.920	366

^a Aqueous solution, 0.20 \underline{M} acetic acid & 0.20 \underline{M} sodium acetate, pH \approx 4.8, C_0^* = 1.96 $\underline{m}\underline{M}$, no gelatin or Triton X-100 present.

b Diffusion coefficient, $\underline{D}_0 = 5.0 \times 10^{-6} \text{ cm}^2/\text{sec.}$

c Radius of drop, $\underline{r} = 0.44 \text{ mm}$.

^d Spherical Correction Factor, $\rho \approx 30 \times 10^{-5}$.

 $[\]frac{e}{k_2}$ = 356 \pm 32; 32 is three times the standard deviation of these six experiments.

135

Table XXIII. Cyclic Voltammetric Data on Phenol Red. , b, c, d

Scan Rate, v, mV/sec	Cathodic Peak Current, $\frac{i}{p}$,	<u>i</u> c/v ^{1/2}	Peak Current Ratio, <u>i</u> a/ <u>i</u> c	Rate Constant, M ⁻¹ - sec ⁻¹
27.5	5.8	1.11	0.768	343
33.0	6.3 ₅	1.10	0.795	323
38.9	6.6	1.06	0.810	336
47.2	7.1	1.03	0.824	354
60.0	7.7 ₅	1.00	0.858	328
73.4	8.6	1.00	0.876	335

^a Aqueous solution, 0.20 \underline{M} acetic acid & 0.20 \underline{M} sodium acetate, pH \approx 4.8, C_0^* = 2.22 \underline{mM} , 0.017% gelatin added.

b Diffusion coefficient, $\underline{D}_0 = 4.9 \times 10^{-6} \text{ cm}^2/\text{sec.}$

^c Radius of drop, $\underline{r} = 0.44$ mm.

^d Spherical Correction Factor, $\rho \approx 30 \times 10^{-4}$.

e $\underline{\mathbf{k}}_2$ = 337 ± 33; 33 is three times the standard deviation of these six experiments.

136

Table XXIV. Cyclic Voltammetric Data on Phenol Reda, b, c, d

Scan Rate, v, mV/sec	Cathodic Peak Current, $\frac{i}{p}$, μA .	$\frac{i^c}{p}/v^{1/2}$	Peak Current Ratio, <u>i</u> / <u>i</u> c	Rate Constant, M-1 - sec-1
47.2	6.8	0.99	0.831	345
55.0	7.3	0.98	0.849	339
66.1	7.9 ₅	0.97	0.868	336
132	10.7	0.93	0.925	335
144	11.1	0.925	0.930	339
165	11.8	0.92	0.940	325

^a Aqueous solution, 0.20 \underline{M} acetic acid & 0.20 \underline{M} sodium acetate, pH \simeq 4.8, C_0^* = 2.20 $\underline{m}\underline{M}$, 0.049% gelatin added.

b Diffusion coefficient, $\underline{D}_0 = 4.9 \times 10^{-6} \text{ cm}^2/\text{sec.}$

c Radius of drop, $\underline{r} = 0.44 \text{ mm}$.

^d Spherical Correction Factor, $\rho \approx 30 \times 10^{-4}$.

 $[\]frac{\mathbf{k}}{2}$ = 336 ± 20; 20 is three times the standard deviation of these six experiments.

137

Table XXV. Cyclic Voltammetric Data on Phenol Red. A,b,c,d

Scan Rate, v, mV/sec	Cathodic Peak Current, $\frac{i}{p}$, μA .	$\frac{i^c}{p}/v^{1/2}$	Peak Current Ratio, <u>i</u> a/ <u>i</u> c	Rate Constant, \underline{M}^{-1} - \sec^{-1}
39.5	9.9	1.58	0.754	370
48.0	10.7	1.54	0.783	351
56.0	11.4	1.52	0.800	355
67.2	12.4	1.51	0.821	356
84.0	13.3	1.45	0.851	347
129	15.7	1.38	0.890	348
153	17.0	1.37	0.899	368
198	18.6	1.32	0.923	353

^a Aqueous Solution, 0.10 \underline{M} acetic acid & 0.10 \underline{M} sodium acetate, 1.0 \underline{M} KCl, pH \simeq 4.8, C_0^* = 3.04 $\underline{m}\underline{M}$, 0.020% gelatin added.



b Diffusion coefficient, $\underline{D}_0 = 4.5 \times 10^{-6} \text{ cm}^2/\text{sec.}$

c Radius of drop, $\underline{r} = 0.44$ mm.

^d Spherical Correction Factor, $\rho \approx 25 \times 10^{-4}$.

e $\underline{\mathbf{k}}_2$ = 356 ± 26; 26 is three times the standard deviation of these eight experiments.

138

Table XXVI. Cyclic Voltammetric Data on Phenol Red. a,b,c,d

Scan Rate, v, mV/sec	Cathodic Peak Current, $\frac{i}{p}$,	$\frac{i^c}{p}/v^{1/2}$	Peak Current Ratio, <u>i</u> a/ <u>i</u> c	Rate Constant, \underline{M}^{-1} - \sec^{-1}
33.6	8.9 ₅	1.54	0.737	365
39.5	9.6 ₅	1.53	0.762	351
48.0	10.4	1.50	0.782	359
56.0	10.9	1.46	0.802	353
67.2	11.7	1.43	0.829	338
129	15.6	1.38	0.888	360
153	16.3	1.32	0.908	336
177	17.3	1.30	0.920	334
198	18.2	1.29	0.925	345

^a Aqueous solution, 0.10 \underline{M} acetic acid & 0.10 \underline{M} sodium acetate, 1.0 \underline{M} KCl, pH \simeq 4.8, C_0^* = 3.00 \underline{m} M, 0.032% gelatin added.

b Diffusion coefficient, $\underline{D}_0 = 4.1 \times 10^{-6} \text{ cm}^2/\text{sec.}$

c Radius of drop, $\underline{r} = 0.44$ mm.

^d Spherical Correction Factor, $\rho \approx 25 \times 10^{-4}$.

e $\underline{\mathbf{k}}_2$ = 349 ± 34; 34 is three times the standard deviation of these nine experiments.

139

Table XXVII. Cyclic Voltammetric Data on Phenol Red., b,c,d

Scan Rate, v, mV/sec	Cathodic Peak Current, $\frac{i}{p}$,	<u>i</u> c/v ^{1/2}	Peak Current Ratio, <u>i</u> a/ <u>i</u> c	Rate Constant, \underline{M}^{-1} - \sec^{-1}
33.6	8.5	1.47	0.747	342
48.0	9.7	1.40	0.794	327
56.0	10.5	1.40	0.814	325
84.0	12.3	1.34	0.846	367
112	14.0	1.32	0.875	367
129	14.7	1.30	0.898	329
153	16.0	1.29	0.906	350
177	17.0	1.28	0.912	371
198	17.9	1.27	0.923	362

^a Aqueous solution, 0.10 \underline{M} acetic acid & 0.10 \underline{M} sodium acetate, 1.0 \underline{M} KCl, pH \approx 4.8, C_0^* = 2.96 $\underline{m}\underline{M}$, 0.45% gelatin added.

b Diffusion coefficient, $\underline{D}_0 = 3.9 \times 10^{-6} \text{ cm}^2/\text{sec.}$

c Radius of drop, r = 0.44 mm.

^d Spherical Correction Factor, $\rho \simeq 25 \times 10^{-4}$.

 $[\]frac{e}{\underline{k}_2}$ = 349 \pm 56; 56 is three times the standard deviation for these nine experiments.

140

Table XXVIII.Cyclic Voltammetric Data on Cresol Red., b, c, d

Scan Rate, v, mV/sec	Cathodic Peak Current, $\frac{c}{p}$,	$\frac{i^c}{p}/v^{1/2}$	Peak Current Ratio, <u>i</u> a/ <u>i</u> c	Rate Constant, \underline{M}^{-1} - \sec^{-1}
50.9	2.35	0.330	0.840	682
60.0	2.5	0.322	0.860	671
72.1	2.7	0.318	0.881	652
86.5	2.9	0.312	0.897	663
103	3.1	0.306	0.912	654
123	3.3	0.299	0.925	653
50.9	2.2 ₅	0.316	0.844	673
61.8	2.4 ₅	0.312	0.867	655
78.6	2.7 ₅	0.310	0.890	658

The first six experiments in this table were conducted in the presence of 0.020% gelatin, whereas the last three experiments were performed in the presence of 0.040% gelatin.

^{25% (}by weight) methanol-water, 0.10 \underline{M} total citrate buffer, pH 4.8, $C_0^* = 0.90 \ \underline{mM}$ (0.020% gelatin solution) and 0.89 \underline{mM} (0.040% gelatin solution).

Diffusion coefficient, $\underline{D}_0 = 2.7 \times 10^{-6} \text{ cm}^2/\text{sec}$ in both solutions.

Radius of drop, $\underline{r} = 0.44$ mm.

Spherical Correction Factor, $\rho \approx 16 \times 10^{-4}$.

f $\underline{\mathbf{k}}_2$ = 662 ± 33; 33 is three times the standard deviation of these nine experiments.

141

Table XXIX. Cyclic Voltammetric Data on Cresol Red., b, c, d

Scan Rate, v, mV/sec	Cathodic Peak Current, $\frac{i}{p}$,	$\frac{i^c}{p}/v^{1/2}$	Peak Current Ratio, $\frac{i}{a}/\frac{i}{c}$	Rate Constant, \underline{M}^{-1} - sec ⁻¹
101	13.5	1.34	0.657	2.11 x 10 ³
135	15.2	1.31	0.689	2.16 x 10 ³
162	16.0	1.27	0.703	2.31 x 10 ³
184	16.9	1.24	0.726	2.16 x 10 ³
213	17.8	1.22	0.732	2.37×10^3
238	18.6	1.20	0.752	2.24 x 10 ³
270	19.5	1.19	0.763	2.38×10^3

^a Aqueous solution, 0.10 \underline{M} acetic acid & 0.10 \underline{M} sodium acetate, pH \simeq 4.8, 1.0 \underline{M} KCl, C_0^* = 2.70 $\underline{m}\underline{M}$, 0.013% gelatin added.

b Diffusion coefficient, $\underline{D}_0 = 4.5 \times 10^{-6} \text{ cm}^2/\text{sec.}$

c Radius of drop, $\underline{r} = 0.44 \text{ mm}$.

^d Spherical Correction Factor, $\rho \approx 10 \times 10^{-4}$.

e $\underline{\mathbf{k}}_2$ = (2.23 ± 0.33) x 10³; 0.33 x 10³ is three times the standard deviation of these seven experiments.

142

Table XXX. Cyclic Voltammetric Data on Cresol Red., b, c, d

Scan Rate, v, mV/sec	Cathodic Peak Current, $\frac{i}{p}$,	$\frac{i^{c}}{p}/v^{1/2}$	Peak Current Ratio, $\frac{i}{a}/\frac{i}{c}$	Rate Constant, \underline{M}^{-1} - \sec^{-1}
101	13.4	1.33	0.645	2.34 x 10 ³
135	14.6	1.26	0.684	2.28 x 10 ³
162	15.8	1.24	0.701	2.33 x 10 ³
184	16.5	1.22	0.728	2.13×10^3
213	17.5	1.20	0.742	2.18×10^3
238	18.6	1.20	0.752	2.29×10^3

^a Aqueous solution, 0.10 \underline{M} acetic acid & 0.10 \underline{M} sodium acetate, pH \simeq 4.8, 1.0 \underline{M} KCl, C_0^* = 2.67 $\underline{m}\underline{M}$, 0.26% gelatin added.

b Diffusion coefficient, $\underline{D}_0 = 4.0 \times 10^{-6} \text{ cm}^2/\text{sec.}$

^c Radius of drop, $\underline{r} = 0.44$ mm.

d Spherical Correction Factor, $\rho \approx 10 \times 10^{-4}$.

e $\underline{\mathbf{k}}_2$ = (2.27 ± 0.17) x 10³; 0.17 x 10³ is three times the standard deviation of these six experiments.

143

Table XXXI. Cyclic Voltammetric Data on Cresol Red.a,b,c,d

Scan Rate, v, mV/sec	Cathodic Peak Current, $\frac{i}{p}$, μ A.	$\frac{i^c}{p}/v^{1/2}$	Peak Current Ratio, $\frac{i}{a}/\frac{i}{c}$	Rate Constant, \underline{M}^{-1} - \sec^{-1}
101	13.0	1.29	0.654	2.29 x 10 ³
135	14.2	1.22	0.690	2.24×10^3
162	15.5	1.22	0.710	2.26×10^3
184	16.2	1.19	0.730	2.19×10^3
213	17.0	1.17	0.750	2.13×10^3
238	17.7	1.15	0.760	2.19×10^3
270	18.5	1.12	0.776	2.20 x 10 ³

^a Aqueous solution, 0.10 \underline{M} acetic acid & 0.10 \underline{M} sodium acetate, pH \simeq 4.8, 1.0 \underline{M} KCl, C_0^* = 2.60 \underline{m} M, 0.051% gelatin added.

b Diffusion coefficient, $\underline{D}_0 = 3.9 \times 10^{-6} \text{ cm}^2/\text{sec.}$

c Radius of drop, $\underline{r} = 0.44$ mm.

^d Spherical Correction Factor, $\rho \approx 10 \times 10^{-4}$.

e $\underline{\mathbf{k}}_2$ = (2.22 ± 0.26) x 10³; 0.26 x 10³ is three times the standard deviation of these seven experiments.

144
Table XXXII. Cyclic Voltammetric Data on Cresol Red. , b, c, d

Scan Rate, v, mV/sec	Cathodic Peak Current, $\frac{i^{c}}{p}$, μA .	$\frac{i^c}{p}/v^{1/2}$	Peak Current Ratio, $\frac{i}{a}/\frac{i}{c}$	Rate Constant, \underline{M}^{-1} - \sec^{-1}
101	5.0 ₅	0.50	0.767	2.23 x 10 ³
135	5.6 ₅	0.495	0.805	2.17 x 10 ³
162	6.2	0.49	0.823	2.27 x 10 ³
184	6.6	0.485	0.834	2.34×10^3
213	7.0	0.48	0.857	2.18 x 10 ³
238	7.4	0.48	0.865	2.27 x 10 ³
270	7.9 ₅	0.48	0.880	2.20×10^3

^a Aqueous solution, 0.10 \underline{M} acetic acid & 0.10 \underline{M} sodium acetate, pH \simeq 4.8, 1.0 \underline{M} KCl, C_0^* = 1.04 $\underline{m}\underline{M}$, 0.051% gelatin added.

b Diffusion coefficient, $\underline{D}_0 = 3.9 \times 10^{-6} \text{ cm}^2/\text{sec.}$

c Radius of drop, $\underline{r} = 0.44$ mm.

^d Spherical Correction Factor, $\rho \approx 10 \times 10^{-4}$.

e $\underline{\mathbf{k}}_2$ = (2.24 ± 0.18) x 10³; 0.18 x 10³ is three times the standard deviation of these seven experiments.

145

Table XXXIII. Cyclic Voltammetric Data on Bromophenol Red. a,b,c,d

Scan Rate, v, mV/sec	Cathodic Peak Current, $\frac{i}{p}$,	$\frac{i^c}{p}/v^{1/2}$	Peak Current Ratio, <u>i</u> / <u>i</u> c	Rate Constant, \underline{M}^{-1} - \sec^{-1}
50.1	7.4	1.05	0.705	9.7 x 10 ²
60.8	8.0	1.03	0.725	9.9 x 10 ²
73.4	8.6	1.00	0.744	10.3×10^2
88.7	9.3 ₅	0.99	0.770	10.0 x 10 ²
106	10.2	0.99	0.784	10.7 x 10 ²

^a 25% (by weight) methanol-water, 0.10 \underline{M} total citrate buffer, pH 4.8, $C_0^* = 1.98 \ \underline{mM}$, 0.010% gelatin added.

b Diffusion coefficient, $\underline{D}_0 = 4.7 \times 10^{-6} \text{ cm}^2/\text{sec.}$

^c Radius of drop, $\underline{r} = 0.44$ mm.

^d Spherical Correction Factor, $\rho \approx 8 \times 10^{-4}$.

e $\underline{\mathbf{k}}_2$ = (1.01 ± 0.10) x 10³; 0.10 x 10³ is three times the standard deviation of these five experiments.

Table XXXIV. Cyclic Voltammetric Data on Bromophenol Red. A,b,c,d

Scan Rate, v, mV/sec	Cathodic Peak Current, $\frac{i}{p}$,	$\frac{i^c}{p}/v^{1/2}$	Peak Current Ratio, $\frac{i}{a}/\frac{i}{c}$	Rate Constant, \underline{M}^{-1} - sec $^{-1}$
50.1	7.2	1.02	0.701	9.9 x 10 ²
60.8	7.8 ₅	1.01	0.726	9.9 x 10 ²
73.4	8.5	0.99	0.753	9.6 x 10 ²
88.7	9.3	0.99	0.769	10.2 x 10 ²
106	10.1	0.98	0.788	10.5×10^2

^a 25% (by weight) methanol-water, 0.10 \underline{M} total citrate buffer, pH 4.8, C_0^* = 1.96 $\underline{m}M$, 0.020% gelatin added.

b Diffusion coefficient, $\underline{D}_0 = 4.4 \times 10^{-6} \text{ cm}^2/\text{sec.}$

^c Radius of drop, $\underline{r} = 0.44$ mm.

^d Spherical Correction Factor, $\rho \approx 8 \times 10^{-4}$.

e $\underline{\mathbf{k}}_2$ = (1.00 ± 0.10) x 10³; 0.10 x 10³ is three times the standard deviation of these five experiments.

147

Table XXXV. Cyclic Voltammetric Data on Bromophenol Red., b, c, d

Scan Rate, v, mV/sec	Cathodic Peak Current, $\frac{i}{p}$,	$\frac{i^c}{p}/v^{1/2}$	Peak Current Ratio, <u>i</u> / <u>i</u> c	Rate Constant, \underline{M}^{-1} - \sec^{-1}
50.1	7.3	1.03	0.698	10.3 x 10 ²
60.8	8.0	1.03	0.725	10.1 x 10 ²
73.4	8.6 ₅	1.01	0.751	9.9 x 10 ²
88.7	9.3	0.99	0.771	10.2 x 10 ²
106	10.0	0.97	0.790	10.6 x 10 ²

^a 25% (by weight) methanol-water, 0.10 \underline{M} total citrate buffer, pH 4.8, C_0^* = 1.92 $\underline{m}M$, 0.040% gelatin added.

b Diffusion coefficient, $\underline{D}_0 = 3.9 \times 10^{-6} \text{ cm}^2/\text{sec.}$

^c Radius of drop, $\underline{r} = 0.44$ mm.

^d Spherical Correction Factor, $\rho \approx 8 \times 10^{-4}$.

e $\underline{\mathbf{k}}_2$ = (1.02 ± .07) x 10³; 0.07 x 10³ is three times the standard deviation of these five experiments.

148

Table XXXVI. Cyclic Voltammetric Data on Chlorophenol Red., b, c, d

Scan Rate, v, mV/sec	Cathodic Peak Current, $\frac{i}{p}$, μ A.	$\frac{i^c}{p}/v^{1/2}$	Peak Current Ratio, <u>i</u> / <u>i</u> c	Rate Constant, \underline{M}^{-1} - sec $^{-1}$
35.9	3.4	0.57	0.647	10.0 x 10 ²
43.1	3.6 ₅	0.56	0.671	9.7 x 10 ²
50.7	3.9	0.55	0.686	10.2 x 10 ²
. 59•9	4.2	0.54	0.708	10.1 x 10 ²
71.9	4.55	0.54	0.720	11.1 x 10 ²
86.2	4.85	0.52	0.742	11.3 x 10 ²
103	5.2 ₅	0.52	0.767	11.1 x 10 ²
123	5.65	0.51	0.788	11.3 x 10 ²

^a 25% (by weight) methanol-water, 0.10 \underline{M} total citrate buffer, pH 4.8, C_0^* = 1.96, no gelatin or Triton X-100 present.

b Diffusion coefficient, $\underline{D}_0 = 1.9 \times 10^{-6} \text{ cm}^2/\text{sec.}$

c Radius of drop, \underline{r} = 0.44 mm.

^d Spherical Correction Factor, $\rho \approx 6 \times 10^{-4}$.

e $\underline{\mathbf{k}}_2$ = (1.06 ± 0.20) x 10³; 0.20 x 10³ is three times the standard deviation of these eight experiments.

149
Table XXXVII. Cyclic Voltammetric Data on Bromocresol Purple. a,b,c,d

Scan Rate, v, V/sec	Cathodic Peak Current, $\frac{i^{c}}{p}$, μA .	$\frac{i^c}{p}/v^{1/2}$	Peak Current Ratio, $\frac{i}{a}/\frac{i}{c}$	Rate Constant, f
0.53	13.8	18.9		
0.70	15.3	18.3		
1.05	18.5	18.0		
2.11	25.8	17.8		
3.01	30.5	17.6		
10.5	56.0	17.3		
17.1	71.0	17.2	0.63	1.9 x 10 ⁵
19.5	71.0	16.1	0.64	2.0 ₅ x 10 ⁵
23.3	75.0	15.6	0.67	2.0 x 10 ⁵
27.3	80.0	15.3	0.69	2.1 x 10 ⁵
31.1	85.0	15.2	0.72	1.9 ₅ x 10 ⁵

^a 25% (by weight) methanol-water, 0.10 \underline{M} total citrate buffer, pH 4.8, C_0^* = 0.77 $\underline{m}\underline{M}$, no gelatin or Triton X-100 present.

b Diffusion coefficient, $\underline{D}_0 = 2.4 \times 10^{-6} \text{ cm}^2/\text{sec.}$

^c Radius of drop, $\underline{r} = 0.44$ mm.

d No spherical correction factor used.

e $\underline{\mathbf{k}}_2$ = (2.0 ± 0.2) x 10⁵; 0.2 x 10⁵ is three times the standard deviation of these calculated rate constants.

f No rate constants obtainable below a scan rate of about 15 V/sec.

K Effects of Maximum Suppressors

Although Senne and Marple did not comment specifically on the fact, all their experiments were performed in the presence of Triton X-100. Some of the polarograms recorded for this thesis investigation exhibited maxima and phenomena indicative of adsorption and/or stirring. To some extent such phenomena appeared to depend on the molecular structure of the compound investigated, for example sometimes being greater for phenol red than cresol purple. More surprisingly, such phenomena also depended on the purity of the compound under investigation. For example, Figure 18 shows a cyclic voltammogram for a stockroom sample of phenol red whereas Figure 19 shows a cyclic voltammogram for a purified sample. Moreover, conventional polarograms also exhibited these dramatic differences. For example, Figure 20 shows a conventional polarogram for the same stockroom sample of phenol red whereas Figure 21 shows a conventional polarogram for a purified sample. These interesting results were not investigated further since it was found that reliable data could be obtained by working with pure compounds. Nevertheless, it was observed that Triton X-100 and gelatin both qualitatively suppressed this anomolous behavior, and therefore these systems presented the possibility of evaluating the effect of maximum suppressors On kinetic measurements.

In an earlier investigation (108) on azobenzene it was found that gelatin suppressed adsorption without interferring with kinetic measurements. Since from a pragmatic viewpoint the use of a "gelatin" electrode is much simpler than for example using rigorous theory <u>vis</u> a <u>vis</u> Wopshall and Shain (34-36), it seemed useful to test the generality of previous conclusions obtained from azobenzene studies. Phenol red is an ideal

•		
•		

Figure 18. Cyclic voltammogram on unpurified sample of phenol red in the absence of gelatin.

Aqueous solution

 C_{O}^{*} = 3.10 \underline{mM} phenol red

0.20 \underline{M} acetic acid

0.20 \underline{M} sodium acetate

Scan rate = 67 mV/sec

Rate constant unobtainable

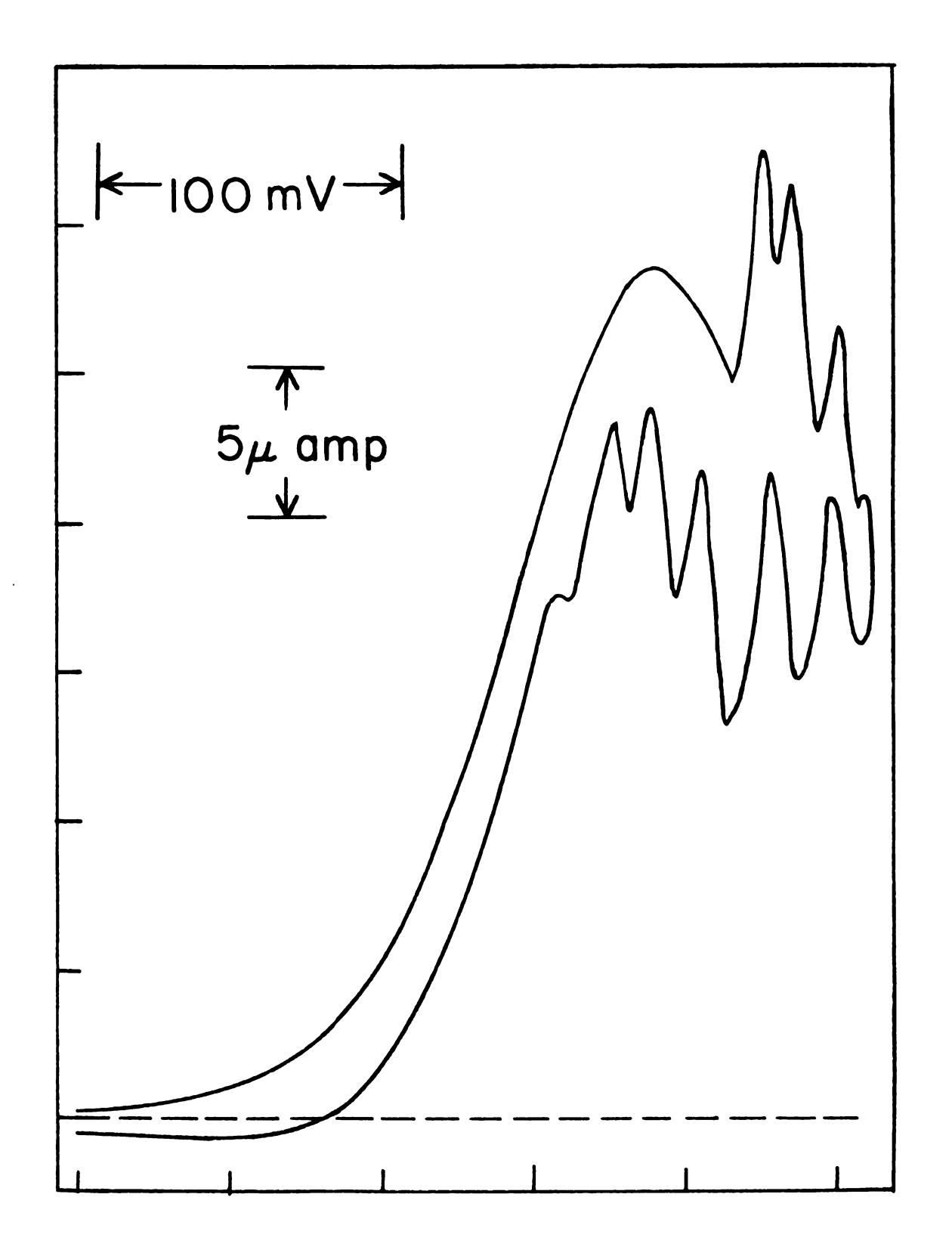


Figure 19. Cyclic voltammogram on purified sample of phenol red in the absence of gelatin.

Aqueous solution

 $C_0 = 2.2^{\text{t}} \text{ mM} \text{ phenol red}$

0.20 M acetic acid

0.20 M sodium acetate

Scan rate = 73 mV/sec

Rate constant = 3.4 x $10^2 \, \underline{\text{M}}$ -1 - sec -1

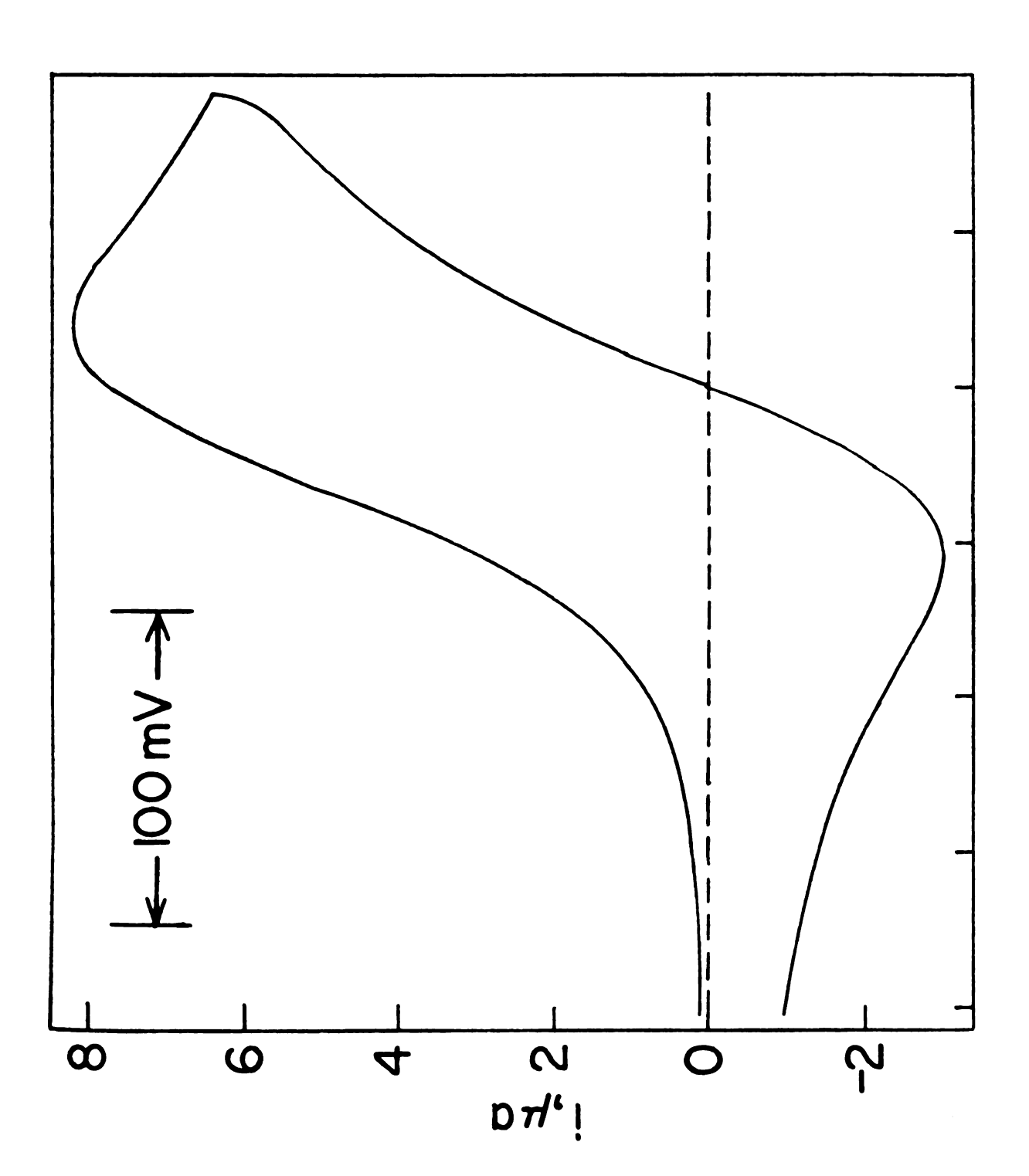


Figure 20. Conventional polarogram on unpurified sample of

phenol red in the absence of gelatin.

Aqueous solution

c₀ = 0.60 mM

0.20 M acetic acid

 $0.20\ \underline{M}\ \text{sodium}\ \text{acetate}$

Hg column height = 54 cm.

 $m^{2/3}$ _t1/6 = 1.12

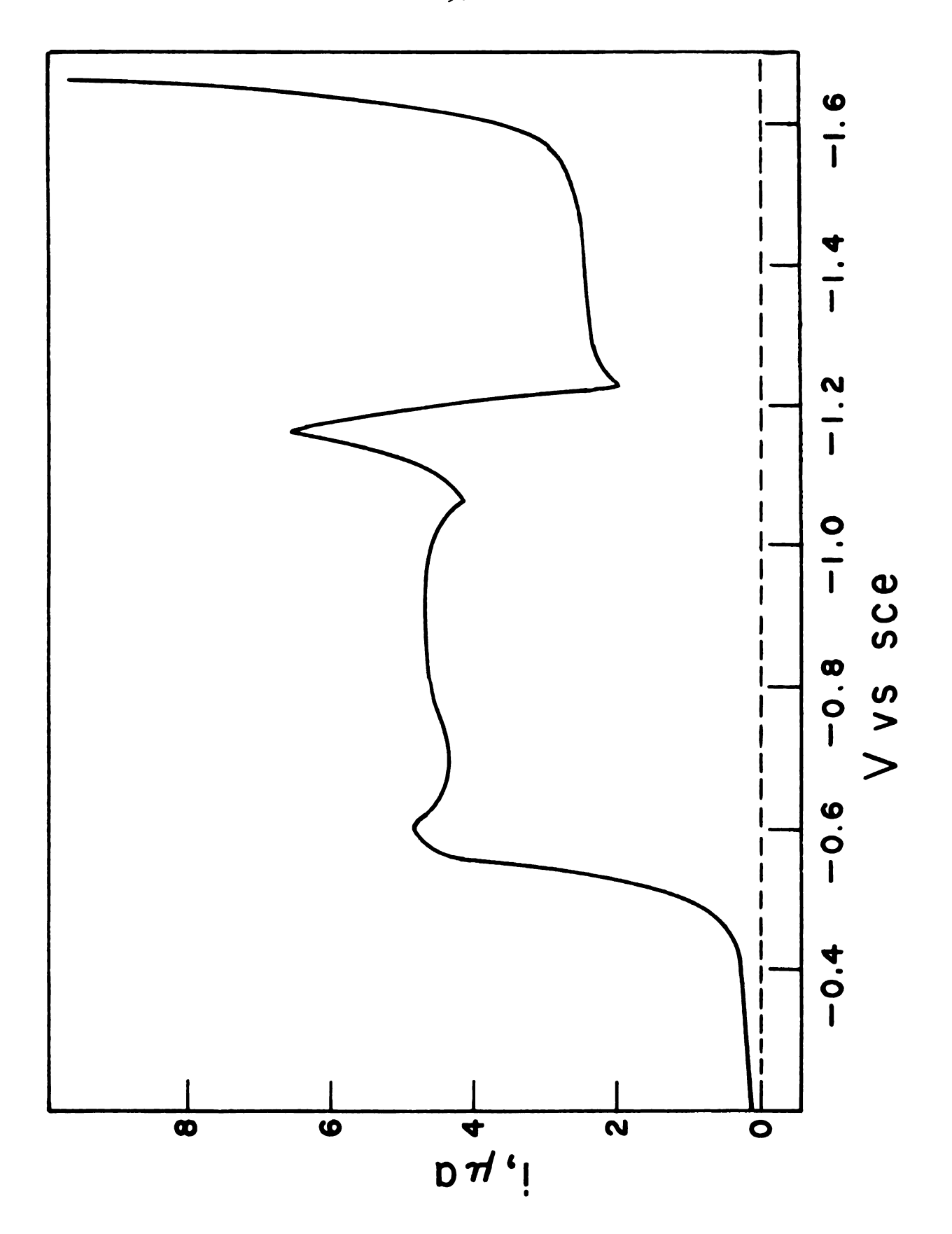


Figure 21. Conventional polarogram on purified sample of

phenol red in the absence of gelatin.

Aqueous solution

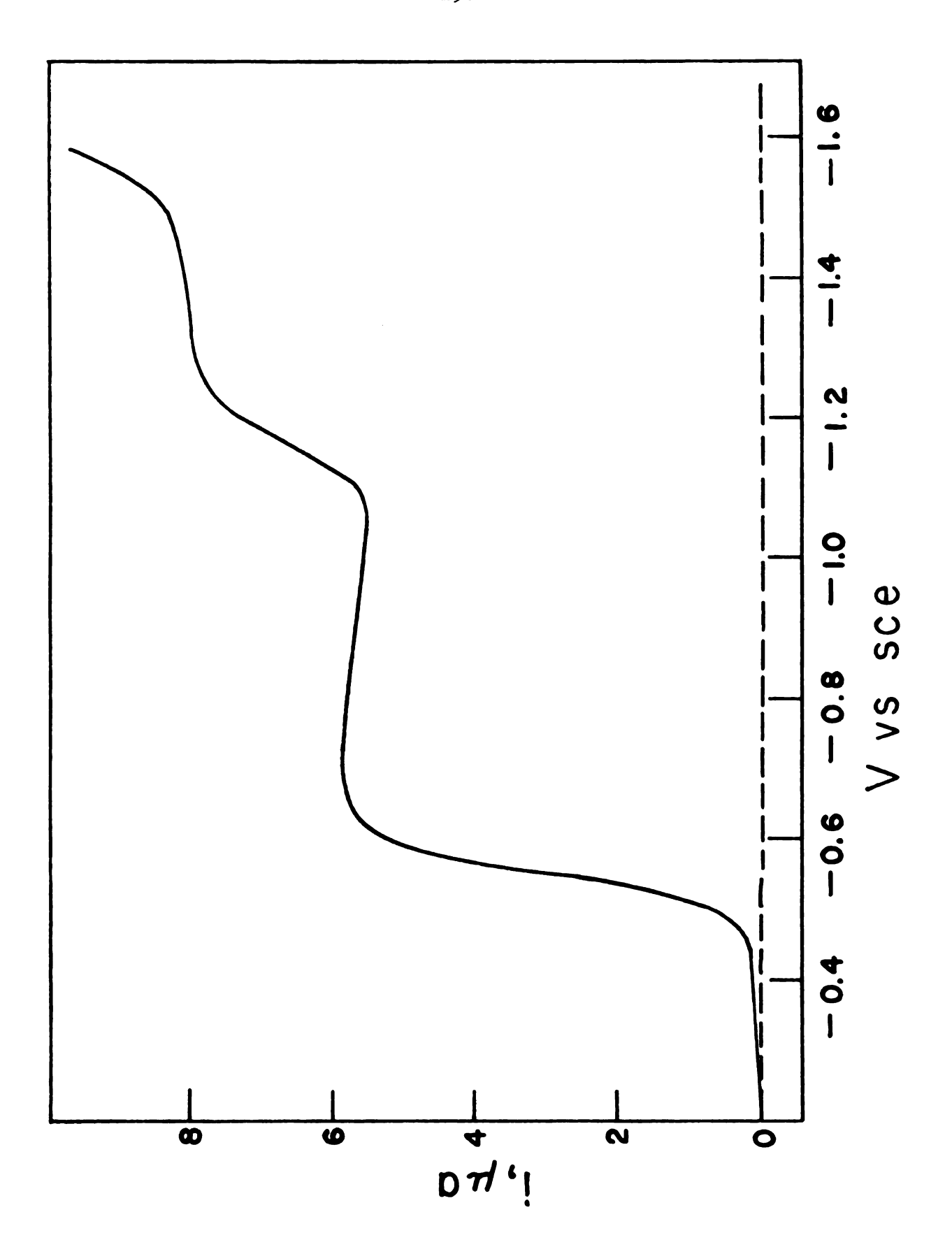
 $c_0 = 2.24 \, \text{mM}$

0.20 M acetic acid

0.20 \underline{M} sodium acetate

Hg column height = 54 cm.

 $m^{2/3}t^{1/6} = 1.12$



s; be

us

th

ca

pl

WO:

ti

cor

tr

abo

ree men

cre

sys Vid

<u>cer</u>

Was rati

gela able

stan

depe

end]

be made in the absence of gelatin as well as on samples which provided useful polarograms only in the presence of gelatin. Moreover, for this system the correct rate constant was presumably known.

Measurements were performed on both purified and unpurified samples of phenol red with various concentrations of gelatin. In every case the systems behaved as would be expected for the disproportionation reaction, with no other complications (presumably the value of \underline{k}_{S} would be altered, but for scan rates employed in this study electron transfer for the first wave remained Nernstian). In addition, rate constants measured from cyclic voltammograms in the manner described above were within experimental error of the value that was obtained by independent spectrophotometric measurements (3.4 x $10^2 \, \underline{\text{M}}^{-1}$ - \sec^{-1}), regardless of gelatin concentration. Typical results from such experiments on phenol red, along with results from similar experiments on cresol red, are summarized in Table XXXVIII. Thus, at least for these systems, use of gelatin is an expedient and acceptable approach, provided, of course, that the interest is not in the adsorption phenomenon per se, or in details of the heterogenous electron transfer reaction.

The effect of Triton X-100 as a maximum suppressor for phenol red was also investigated since Senne and Marple employed Triton X-100 rather than gelatin. Qualitatively, the effects of Triton X-100 and gelatin were found to be the same. However, Triton X-100 is unacceptable for quantitative measurements. For, example, apparent rate constants measured with cyclic voltammetry in the presence of Triton X-100 depended on the concentration of Triton X-100 as well as on scan rate and phenol red concentration. Typical results are shown in Figure 22

Table XXXVIII. Effect of Gelatin on Disproportionation Rate Constants by Cyclic Voltammetry for Radicals of Cresol Red and Phenol Red in Aqueous Solution.

Compound	C _O , <u>mM</u>	Gelatin, %	$\underline{k}_2^b, \underline{M}^{-1} - \sec^{-1}$
Cresol red ^C	2.74	0	unobtainable
	2.70	0.013	2.2 ₃ x 10 ³
	2.67	0.026	$2.2_7 \times 10^3$
	2.60	0.051	$2.2_2 \times 10^3$
	1.04	0.051	$2.2_{4} \times 10^{3}$
Phenol $\mathtt{red}^{ ext{d}}$	3.10	0	unobtainable
	3.04	0.020	3.5 ₆ x 10 ²
	3.00	0.032	3.4 ₉ x 10 ²
	2.96	0.045	3.4 ₉ x 10 ²
Phenol red ^e	2.24	0	$3.4_{4} \times 10^{2}$
	2.22	0.017	3.3 ₇ x 10 ²
	2.20	0.049	3.3 ₆ x 10 ²
Phenol red ^f	2.47	0	2.8 ₆ x 10 ²
	2.46	0.050	2.6 ₅ x 10 ²

Cyclic voltammetric data for these compounds are given in Tables VIII-XXXVII.

 $^{^{\}rm b}$ Rate constants to within $^{\rm \pm}$ 10% of stated values.

^c Cresol red, unpurified, 1.0 \underline{M} KCl, 0.10 \underline{M} acetic acid, 0.10 \underline{M} sodium acetate, pH = 4.8.

^d Phenol red, unpurified, 1.0 \underline{M} KCl, 0.10 \underline{M} acetic acid, 0.10 \underline{M} sodium acetate, pH = 4.8.

^e Phenol red, purified, 0.20 \underline{M} acetic acid, 0.20 \underline{M} sodium acetate, essentially same solution conditions as in spectrophotometric study, see Table VII.

f Phenol red, purified, 0.10 M total citrate buffer, pH = 4.8.

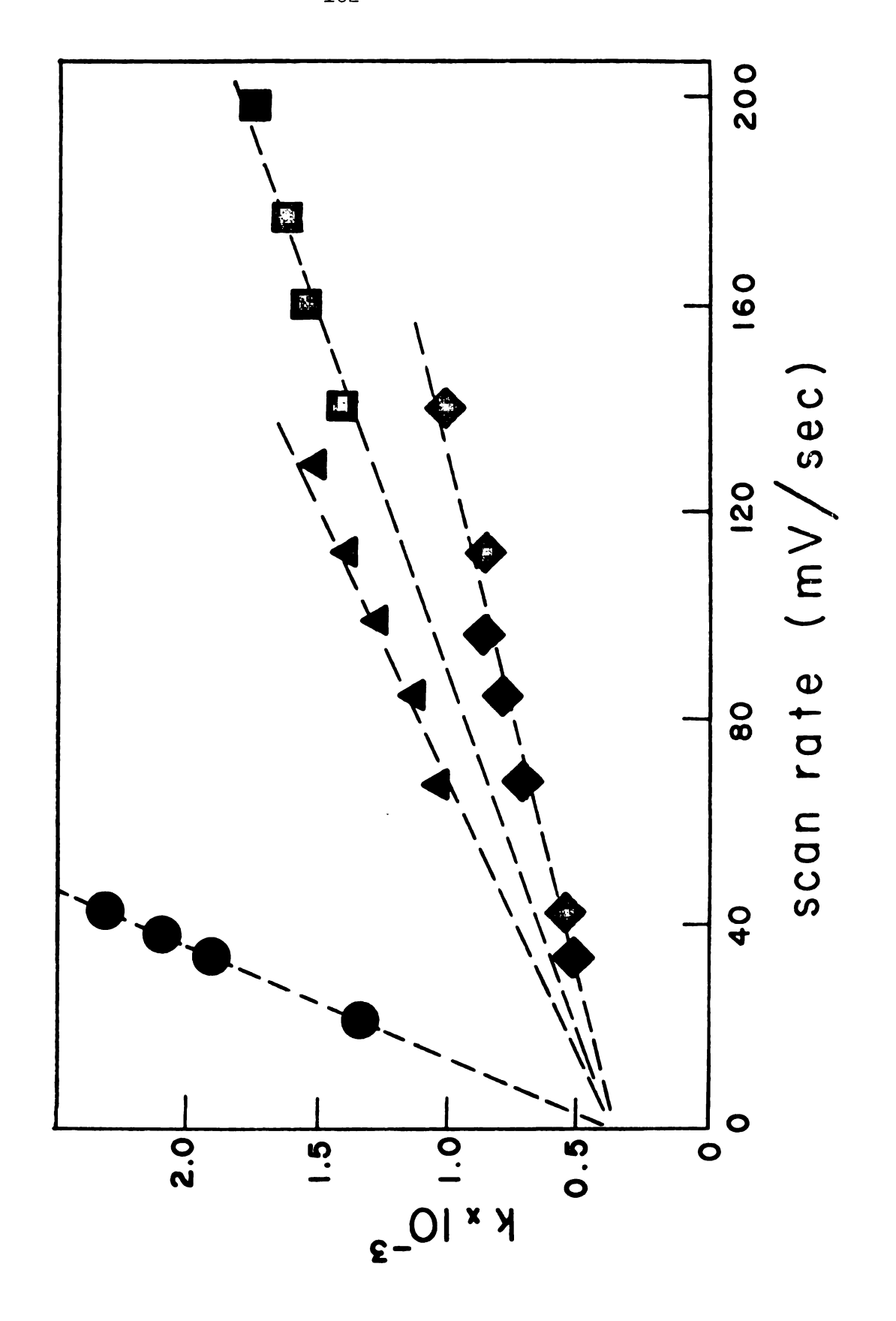
Figure 22. Variation of apparent rate constant^{a,b} with scan rate and phenol red concentration in the presence

of 0.014% Triton X-100.

 $C_0 = 0.49 \text{ mM}$ $C_0 = 1.33 \text{ mM}$ $C_0 = 1.51 \text{ mM}$ $C_0 = 3.03 \text{ mM}$

a Rate constants for disproportionation of phenol red radical as measured by cyclic voltammetry.

 $^{\rm b}$ 1.0 $\underline{\rm M}$ KCl, 0.10 $\underline{\rm M}$ acetic acid, and 0.10 $\underline{\rm M}$ sodium acetate in strictly aqueous solution.



where apparent rate constants are plotted <u>vs</u> scan rate for several bulk concentrations of phenol red. These data are reminiscent of data reported by Wopshall and Shain (36) for azobenzene. In fact, these authors suggested using plots like Figure 22 to obtain homogenous rate constants for systems showing weak adsorption; the value of <u>k</u> extrapolated to zero scan rate is ostensibly the correct <u>k</u>. Interestingly, the data of Figure 22 all extrapolate to a common rate constant close to the correct value for phenol red. This fact suggests that Triton X-100 suppresses adsorption enough to eliminate obvious anomalies, but that some residual adsorption still remains. Unfortunately, this explanation is not correct, since it was found that apparent rate constants measured in the presence of both gelatin and Triton X-100 simultaneously are still a function of Triton X-100 concentration. Obviously, one has to be careful in using empirical approaches, such as "gelatin" electrodes, in electrochemical kinetics.

L Considerations of Kinetic Effects

Because of solubility limitations, experiments were generally conducted in 25% (by weight) methanol-water solutions containing a total $0.10~\underline{M}$ citrate buffer at a measured pH. For example, these conditions apply to the data in Table V. However, experiments were also conducted on a few of these compounds in strictly aqueous solutions. These experiments show that the dielectric constant of the medium has a significant effect on the rate of disproportionation, as can be seen by comparing the rate constants in Tables V and XXXVIII. For example, with both solutions containing a total $0.10~\underline{M}$ citrate buffer at pH 4.8, the rate of disproportionation of phenol red radical is about 70% faster in the

str

sti

cor.

tai of

pht

proj thi

the

of atom

ster

negs the

act:

phth the

that

111)

reac

теdi

sulf

reac

Thus

strictly aqueous solution than in the 25% methanol-water mixture.

The sulfonephthalein acid-base indicators can be viewed as substituted triphenylmethyl compounds, with one of the phenyl moieties containing a sulfonate group, and the other two phenyl moieties containing a wide variety of possible substituents. Thus, explanations of differences in the relative rates of disproportionation of sulfone-phthalein radicals require a consideration of many factors.

The influence of the sulfonate group on the relative rates of disproportionation is probably minimal since all of these radicals have this group located at an identical position in the molecule. However, the sulfonate group may play an important role in the kinetics of all of these radicals; for example, its proximity to the central carbon atom where the free electron is presumably localized may result in a steric effect. Furthermore, the sulfonate group obviously carries a negative charge, and therefore as increase in rate with an increase in the dielectric constant of the medium would be expected for these reactions(107). This dielectric effect is observed for these sulfonephthalein radicals, and may be due to this reason. On the other hand, the observed dielectric effect also can be explained on another basis that is consistent with the proposed meshanism. Thus, Kirkwood (110, 111) has shown that if the activated complex is more polar than the reactants (as presumably would be the case if the products are ions), the rate of the reaction increases with the dielectric constant of the medium. This theory may be applicable to the disproportionation of Sulfonephthalein radicals since, except for the sulfonate group, the reactants are radicals whereas the products are ions (Reaction 3c). Thus, there are at least two possible explanations for the increased

disproportionation rates of these radicals with increased dielectric constant.

The first four compounds in Table V all exhibit relatively low rates of disproportionation, and have a methyl group <u>ortho</u> to the central carbon atom. The other six compounds in Table V have a proton instead of a methyl group in this position, and show significantly higher rates of disproportionation. These relative rates suggest that the methyl group causes steric hindrance at the central carbon atom. This behavior appears reasonable since, with the free electron localized on the central carbon atom, this position of the molecule would appear to be a reactive site for at least one of the partners in Reaction 3c.

Another effect of structure on the rate of disproportionation is that radicals having either alkyl or halo groups meta to the carbon atom that directly joins the central carbon atom exhibit significantly higher rates than analogous compounds with protons at these positions. A possible reason for this behavior is that alkyl groups are electron-releasing, and as such, may promote alternative (to the central carbon atom) reactive sites on the radicals. On the other hand, halo groups, being electrophilic, may attract a portion of the charge of the free electron that is presumably localized on the central carbon atom.

Hence, halo groups may partially delocalize this free electron into the rings, and therefore also promote alternative reactive sites on the radical. In other words, both electron-releasing and electron-donating groups may promote alternative reactive sites on these radicals. This behavior even holds for the four radicals that possess methyl groups which sterically hinder the reaction.

•

5;

ŝ

LITERATURE CITED

- 1. Heyrovsky, J., Chem.Listy, 16, 256 (1922).
- 2. Heyrovsky, J., Phil. Mag., <u>45</u>, 303 (1923).
- 3. Heyrovsky, J., and Shikata, M., Rec. Trav. Chim., 44, 496 (1925).
- 4. Bard, A. J., Ed., "Electroanalytical Chemistry," Vol. 1., Marcel Dekker, Inc., New York, N.Y., 1966.
- 5. Bard, A. J., Ed., "Electroanalytical Chemistry," Vol. 2., Marcel Dekker, Inc., New York, N.Y., 1967.
- 6. Bard, A. J., Ed., "Electroanalytical Chemistry," Vol. 3., Marcel Dekker, Inc., New York, N.Y., 1967.
- 7. Bard, A. J., Ed., "Electroanalytical Chemistry," Vol. 4., Marcel Dekker, Inc., New York, N.Y., 1969.
- 8. Nicholson, R. S., Anal. Chem., 42, 130R (1970).
- 9. Hume, D. N., Anal. Chem., 40, 174R (1968).
- 10. Reinmuth, W. H., Anal. Chem., 40, 185R (1968).
- 11. Hume, D. N., Anal. Chem., 38, 261R (1966).
- 12. Reinmuth, W. H., Anal. Chem., <u>38</u>, 270R (1966).
- 13. Matheson, L. A., and Nichols, N., Trans. Electrochem. Soc., <u>73</u>, 193 (1938).
- 14. Randles, J. E. B., Trans. Faraday Soc., 44, 327 (1948).
- 15. Sevcik, A., Collect. Czech. Chem. Commun., <u>13</u>, 349 (1948).
- 16. Delahay, P. J., J. Amer. Chem. Soc., <u>75</u>, 1190 (1953).
- 17. Nicholson, M. M., J. Amer. Chem. Soc., <u>76</u>, 2539 (1954).
- 18. Frankenthal, R. P., and Shain, I., J. Amer. Chem. Soc., <u>78</u>, 2969 (1956).
- **19.** Reinmuth, W. H., J. Amer. Chem. Soc., <u>79</u>, 6358 (1957).
- 20. DeMars, R. D., and Shain, I., J. Amer. Chem. Soc., <u>81</u>, 2654 (1959).
- 21. Gokhshtein, A. Y., and Gokhshtein, Y. P., Dokl. Akad. Nauk SSSR, 131, 601 (1960).
- 22. Reinmuth, W. H., Anal. Chem., <u>33</u>, 1793 (1961).

- 23. Reinmuth, W. H., Anal. Chem., <u>33</u>, 185 (1961).
- 24. Nicholson, R. S., and Shain, I., Anal. Chem., 36, 706 (1964).
- 25. Olmstead, M. L., and Nicholson, R. S., Anal. Chem., <u>38</u>, 150 (1966).
- 26. Matsuda, H., and Ayabe, Y., Z. Electrochem., 59, 494 (1955).
- 27. Nicholson, R. S., Anal. Chem., 37, 1351 (1965).
- 28. Gokhshtein, Y. P., and Gokhshtein, A. Y., Dokl. Akad. Nauk SSSR, 128, 985 (1959).
- 29. Gokhshtein, Y. P., and Gokhshtein, A. Y., in "Advances in Polarography," Longmuir, I. S., ed., Vol. II., Pergamon Press, New York, N.Y., 1960, p. 465.
- 30. Polcyn, D. S., and Shain, I., Anal. Chem., 38, 370 (1966).
- 31. Polcyn, D. S., and Shain, I., Anal. Chem., 38, 376 (1966).
- 32. Berzins, T., and Delahay, P., J. Amer. Chem. Soc., 75, 555 (1953).
- 33. Nicholson, M. M., J. Amer. Chem. Soc., 79, 7 (1957).
- 34. Wopschall, R. H., and Shain, I., Anal. Chem., 39, 1514 (1967).
- 35. Wopschall, R. H., and Shain, I., Anal. Chem., 39, 1527 (1967).
- 36. Wopschall, R. H., and Shain, I., Anal. Chem., <u>39</u>, 1535 (1967).
- 37. Hulbert, M. H., and Shain, I., Anal. Chem., 42, 162 (1970).
- 38. Saveant, J. M., and Vianello, E., in "Advances in Polarography," Longmuir, I. S., ed., Vol.I., Pergamon Press, New York, N.Y., 1960, p. 367.
- 39. Saveant, J. M., and Vianello, E., Electrochim. Acta, <u>10</u>, 905 (1965).
- 40. Saveant, J. M., and Vianello, E., Electrochim. Acta, 8, 905 (1963).
- 41. Saveant, J. M., and Vianello, E., Compt. Rend., <u>256</u>, 2597 (1963).
- 42. Nicholson, R. S., and Shain, I., Anal. Chem., <u>37</u>, 178 (1965).
- 43. Nicholson, R. S., and Shain, I., Anal. Chem., <u>37</u>, 190 (1965).
- 44. Olmstead, M. L., and Nicholson, R. S., J. Electroanal. Chem., $\underline{14}$, 133 (1967).
- 45. Schuman, M. S., Anal. Chem., <u>41</u>, 142 (1969).
- 46. Schuman, M. S., Anal. Chem., <u>42</u>, 521 (1970).

- 47. Saveant, J. M., and Vianello, E., Electrochim. Acta, 12, 1545 (1967).
- 48. Nicholson, R. S., Anal. Chem., 37, 667 (1965).
- 49. Kudirka, P. J., M. S. Thesis, Michigan State University, East Lansing, Michigan, 1968.
- 50. Olmstead, M. L., Ph. D. Thesis, Michigan State University, East Lansing, Michigan, 1968.
- 51. Olmstead, M. L., Hamilton, R. G., and Nicholson, R. S., Anal. Chem., 41, 260 (1969).
- 52. Olmstead, M. L., and Nicholson, R. S., Anal. Chem., 41, 862 (1969).
- 53. Vlcek, A., in "Progress in Inorganic Chemistry," Zuman, P., ed., Vol. 5., Interscience, New York, N.Y., 1963, p. 211.
- 54. Delahay, P., "New Instrumental Methods in Electrochemistry," Interscience, New York, N.Y., 1954.
- 55. Schwarz, W. M., and Shain, I., J. Phys. Chem., <u>69</u>, 30 (1965).
- 56. Wawzonek, S., and Duty, R. C., J. Electrochem. Soc., 108, 1135 (1961).
- 57. Duty, R. C., Ph. D. Thesis, State University of Iowa, Ames, Iowa, 1961.
- 58. Wawzonek, S., and Wagenknecht, J. H., J. Electrochem. Soc., <u>110</u>, 420 (1963).
- 59. Senne, J. K., and Marple, L. W., Anal. Chem., $\frac{42}{1970}$, 1147 (1970).
- 60. Von Stackelberg, M., and Strache, W., Z. Electrochem., <u>53</u>, 118 (1949).
- 61. Kolthoff, I. M., Lee, T. S., Stocesova, D., and Parry, E. P., Anal. Chem., 22, 521 (1950)
- 62. Ehlers, V. B., and Sease, J. W., Anal. Chem., 31, 16 (1959).
- 63. Hush, N. S., and Oldham, K. B., J. Electroanal. Chem., 6, 34 (1963).
- 64. Fukui, K., Morokuma, K., Kato, H., and Yonezawa, T., Bull. Chem. Soc. Japan, 36, 217 (1963).
- 65. Wawzonek, S., Duty, R. C., and Wagenknecht, J. H., J. Electrochem. Soc., 111, 74 (1964).
- 66. Parkanyi, C., and Zahradnik, R., Coll. Czech. Chem. Comm., <u>30</u>, 353 (1965).
- 67. Hussey, W. W., and Diefenderfer, A. J., J. Amer. Chem. Soc., <u>89</u>, 5359 (1967).

- 68. Fry, A. J., and Moore, R. H., J. Org. Chem., 33, 1283 (1968).
- 69. Sease, J. W., Burton, F. G., and Nickol, S. L., J. Amer. Chem. Soc., 90, 2595 (1968).
- 70. Caldwell, R. A., and Hacobian, S., Aust. J. Chem., 21, 1403 (1968).
- 71. Ulery, H. E., J. Electrochem. Soc., 116, 1201 (1969).
- 72. Caldwell, R. A., and Hacobian, S., Aust. J. Chem., <u>21</u>, 1 (1968).
- 73. Matsui, Y., Kawakodo, R., and Dato, Y., Bull. Chem. Soc. Japan, $\underline{41}$, 2913 (1968).
- 74. Lawless, J., and Hawley, M. D., J. Electroanal. Chem., <u>21</u>, 365 (1969).
- 75. Butin, K. P., Stanko, V. I., Belokoneva, N. A., Anorova, G. A., Klimova, T. V., and Beletskaya, I. P., Dokl. Akad. Nauk SSSR, 188, 819 (1969).
- 76. Mairanovskii, S. G., Barashkova, N. V., and Vol'kenshtein, Y. B., Elektrokhimiya, <u>1</u>, 60 (1965).
- 77. Brown, E. R., McCord, T. G., Smith, D. E., and DeFord, D. D., Anal. Chem., <u>38</u>, 1119 (1966).
- 78. Underkofler, W. L., and Shain, I., Anal. Chem., 35, 1778 (1963).
- 79. Bard, A. J., and Solon, E., Anal. Chem., 34, 1181 (1962).
- 80. Ross, J. W., DeMars, R. D., and Shain, I., Anal. Chem., <u>28</u>, 1768 (1956).
- 81. Beckwith, P., and Crouch, S. R. (to be published).
- 82. O'Donnell, J. F., Ayres, J. T., and Mann, C. K., Anal. Chem., <u>37</u>, 1161 (1965).
- 83. O'Donnell, J. F., Ph. D. Thesis, Florida State University, Tallahassee, Florida, 1966.
- 84. Orndorff, W. R., and Sherwood, F. W., J. Amer. Chem. Soc., <u>45</u>, 486 (1923).
- 85. Lundquist, J. T., and Nicholson, R. S. (unpublished results).
- 86. Kirmse, W., Angew. Chem. Internat. Edit., $\underline{4}$, 1 (1965).
- 87. Nefedov, O. M., and Manakov, M. N., Angew. Chem. Internat. Edit., 5, 1021 (1966).
- 88. Köbrich, G., Angew. Chem. Internat. Edit., <u>6</u>, 41 (1967).

- 89. Bethell, D., in "Advances in Physical Organic Chemistry," Gold, V., ed., Vol. VII., Academic Press, New York, N.Y., 1969, pp. 153-209.
- 90. Moss, R. A., Chem. Eng. News, June 16, 1969, pp. 60-68.
- 91. Moss, R. A., Chem. Eng. News, June 30, 1969, pp. 50-58.
- 92. Hine, J., and Dowell, A. M., J. Amer. Chem. Soc., 76, 2688 (1954).
- 93. Hine, J., and Burske, N. W., J. Amer. Chem. Soc., 78, 3337 (1956).
- 94. Hine, J., Burske, N. W., Hine, M., and Langford, P. B., J. Amer. Chem. Soc., 79, 1406 (1957).
- 95. Hine, J., and Porter, J. J., J. Amer. Chem. Soc., 79, 5493 (1957).
- 96. Hine, J., and Langford, P. B., J. Amer. Chem. Soc., <u>79</u>, 5497 (1957).
- 97. Hine, J., and Ehrenson, S. J., J. Amer. Chem. Soc., <u>80</u>, 824 (1958).
- 98. Moss, R. A., and Mamantov, A., Tetrahedron Lett., 30, 3425 (1968).
- 99. Nefedov, O. M., and Shafran, R. N., Izv. AN SSSR, Ser. Khim., 538 (1965).
- 100. Meites, L., "Polarographic Techniques," 2nd ed., Interscience, New York, N.Y., 1965.
- 101. Gilchrist, T. L., and Rees, C. W., "Carbenes, Nitrenes, and Arynes," Appleton-Century-Crofts, New York, N.Y., 1969, p 48.
- 102. Sternberg, H. W., Markby, R. E., Wender, I., and Mohilner, D. M., J. Electrochem. Soc., 113, 1060 (1966).
- 103. Gilchrist, T. L., and Rees, C. W., "Carbenes, Nitrenes, and Arynes," Appleton-Century-Crofts, New York, N.Y., 1969, p 109.
- 104. Hoffmann, R. W., "Dehydrobenzene and Cycloalkynes," Academic Press, New York, N.Y., 1967, pp 44-45.
- 105. Bates, R. G., "Determination of pH," J. Wiley & Sons, New York, N.Y., 1964, pp 131-141.
- 106. Kolthoff, I. M., and Lingane, J. J., "Polarography," Vol. 1., Interscience, New York, N.Y., 1952, pp 268-294.
- 107. Benson, S. W., "The Foundations of Chemical Kinetics," McGraw-Hill, New York, N.Y., 1960.
- 108. Lundquist, J. T., and Nicholson, R. S., J. Electroanal. Chem., $\underline{16}$, 445 (1968).

- 109. Orleman, E. F., and Kern, D. M. H., J. Amer. Chem. Soc., <u>75</u>, 3058 (1953).
- 110. Kirkwood, J. G., J. Chem. Phys., 2, 351 (1934).
- lll. Frost, A. A., and Pearson, R. G., "Kinetics and Mechanism," 2nd ed., J. Wiley & Sons, New York, N.Y., 1961, Chapter 7.

